In-Depth Characterization of Somatic and Germ Cell Mutagenic Response to Procarbazine Hydrochloride by Novel Error Corrected Sequencing

By

Annette Dodge

Thesis submitted in partial fulfillment of requirements for the degree of

Master of Science

In

Biology

With a Specialization in

Environment and Chemical Toxicology

University of Ottawa,

Ottawa, ON

ABSTRACT

Assessment of chemical mutagenicity is essential to protecting human health from genetic disease. Current assays are limited in their ability to provide mechanistic insight into the endogenous and exogenous processes involved in mutagenesis. Duplex Sequencing (DS), a novel error-corrected sequencing technology, overcomes many of the limitations faced by conventional mutagenicity assays. DS could be used to eliminate reliance on standalone reporter assays and provide mechanistic information alongside mutation frequency (MF) data. Furthermore, customizable panels enable assessment of the endogenous genomic features that drive mutagenesis. However, the performance of DS must be thoroughly assessed before it can be routinely implemented for standard testing. The objectives of this study were to demonstrate the potential of DS as a robust *in vivo* mutagenicity test and to explore its rich data to gain a better understanding of spontaneous and chemically-induced mutagenicity in somatic and germ cells. We used DS to study spontaneous and procarbazine (PRC)-induced mutations in the bone marrow (BM) and germ cells of MutaMouse males across a panel of 20 diverse genomic targets. Mice were exposed to 0, 6.25, 12.5, or 25 mg/kg-bw/day for 28 days by oral gavage and tissues were sampled at least 28 days post-exposure. Results were compared with those obtained using the conventional *lacZ* viral plaque assay on the same samples. DS detected significant increases in MF and distinct spectra consistent with the known mutagenic mechanisms of PRC in both tissues. Mouse PRC doses at which significant effects were observed are in range with those used for chemotherapy, suggesting that similar effects may be observed in human patients. This supports the contribution of PRC towards secondary cancers following treatment. DS results were comparable to those obtained using the gold-standard *lacZ* TGR assay, with DS showing greater sensitivity to detect smaller changes in MF. Analysis of mutation spectra and the genomic features that drive the mutational response revealed intrinsic differences between BM and germ cells that may underlie differences in endogenous mutagenic mechanisms and/or DNA repair pathways. The results suggest that germ cells may have intrinsic mechanisms to reduce mutation burden relative to somatic cells. While historically analysis of germ cell mutagenicity has been neglected in favour of somatic cells, our work supports the independent assessment of germ cell mutagenicity during regulatory testing. Finally, we conducted power analyses to inform the optimal DS study designs for the two tissues. We found that low intra-group variability within BM samples allows a reduction in sample size to three animals per group whilst still maintaining 80% power to detect an effect. In contrast, the relatively high intra-group variability and low background MF in germ cells suggests a minimum of eight animals per group to detect an effect.

Overall, our results support the use of DS as a mutagenicity test and highlight many of the advantages it holds over conventional assays. Moreover, our study reveals the potential for mutagenic effects in PRC-treated cancer patients. Further work to test DS with more chemicals and across a wider range of tissues is recommended for future implementation as a mutagenicity test.

ACKNOWLEDGMENTS

I would like to express my deepest gratitude to the following people for their invaluable support and contributions throughout the completion of this thesis.

First and foremost, I am immensely grateful to my two supervisors, Dr. Carole Yauk and Dr. Francesco Marchetti, for their guidance, expertise, and unwavering support. Their insights and feedback have been instrumental in shaping the direction and quality of this research. Under their guidance I have enhanced my scientific communication skills, improved my critical thinking, and grown in my career. It was challenging to start my Master's degree in the middle of a pandemic, but with kindness and endless consideration, Dr. Yauk and Dr. Marchetti made the past couple years truly wonderful. Thank you both for everything, I would not have been able to get to where I am today without your help.

I would like to extend my appreciation to my committee members, Dr. Alex Wong and Dr. Kin Chan, as well as Dr. Gilda Stefanelli who is serving as my thesis examiner. I am thankful for their valuable input and constructive criticism. Their expertise and thoughtful suggestions have significantly enriched the contents of this thesis.

I am indebted to the faculty members of the Department of Biology at the University of Ottawa and Carleton University for their dedication to teaching and fostering a stimulating academic environment. Their commitment to excellence has inspired and challenged me throughout my studies. Furthermore, I would like to acknowledge the support and resources provided by the University of Ottawa. The access to library facilities, research databases, and technical assistance has been instrumental in conducting this study.

I would like to express my sincere gratitude to my colleagues at Health Canada, without whom this work would not have been possible. I am particularly indebted to Danielle LeBlanc and Gu Zhou for their time and effort spent training me in the lab. You both made the lab into a very welcoming environment, and I will forever be grateful for the many hours you lent in teaching me new skills. On the bioinformatics team, I would like to thank Andrew Williams for his help with my statistical analyses and for his patience in answering my seemingly endless amounts of questions. I would also like to give a special thanks to Dr. Matthew Meier, not only for his invaluable help with bioinformatics, but also for introducing me to Dr. Yauk and getting me started on this incredible journey. Finally, I want to extend

thanks to my colleagues at Twinstrand Biosciences for their contributions to my manuscripts and for their help with the sequencing data.

A big thank you to all my fellow graduate students. To Anne-Marie Fortin, Elizabeth Huliganga, and Tatiana Kozbenko, who all warmly welcomed me into their ranks as fellow Master's students; thank you for sharing your experiences with me and helping me navigate graduate studies. To Eunnara Cho, Geronimo Parodi-Matteo, David Shuster, and Emmanuelle Monniez; it was great to get to work with you and thank you for making the lab such a lively place! Good luck with all your projects! To David Eickmeyer, our amazing lab technician, thank you for all your help with administration and maintaining the lab. Finally, to Madison Stewart and Elena Esina, I am truly happy to have gotten the time to work with you. I can't wait to see you both progress through your own Masters, I know you will accomplish amazing things!

Finally, I want to express my deepest gratitude to my friends and family for their unconditional love, encouragement, and unwavering belief in my abilities. Their constant support and sacrifices have been the foundation of my academic pursuits. Thank you, to all my friends who listened to me complain and kept me laughing throughout my most stressful times; to my sweet cat Cinder, who always kept me company during long hours studying; to my loving grandmother who always expressed interest in my research; and to my brothers for always having my back. But most of all, I want to thank my parents. Your endless love and support have kept me afloat during all the ups and downs these past two years. For all the care you've taken of me over the years, this thesis is dedicated to you.

In conclusion, this thesis represents the culmination of the contributions and support from a multitude of people. Each one has played an integral role in my academic and personal growth, and I am forever grateful for their unwavering support.

Contents

LIST OF TABLES

Chapter Two

Chapter Three

LIST OF FIGURES

Chapter One

Chapter Two

Chapter Three

LIST OF ABBREVIATIONS

BaP	Benzo[a]pyrene
BM	Bone Marrow
BMD	Benchmark Dose
BMR	Benchmark Response
bp	Base pairs
bw	Body weight
chr	chromosome
CI	Confidence Interval
COSMIC	Catalogue of Somatic Mutations in Cancer
DCS	Duplex Consensus Sequence
DS	Duplex Sequencing
ecNGS	Error-Corrected Next Generation Sequencing
ENU	N-ethyl-N-nitrosourea
FC	Fold-Change
GLM	Generalized Linear Model
GLMM	Generalised Linear Mixed Model
HPRT	Hypoxanthine phosphoribosyl transferase
IARC	International Agency for Research on Cancer
Indel	Insertions and deletions
MDES	Minimum Detectable Effect Size
MF	Mutation Frequency
MF_{Max}	Maximum Mutation Frequency
MF_{Min}	Minimum Mutation Frequency
MNV	Multi-nucleotide Variant

NGS	Next-Generation Sequencing
NSERC	Natural Sciences and Engineering Research Council of Canada
OECD	Organisation for Economic Co-operation and Development
PBS	Phosphate-buffered Saline
PCR	Polymerase Chain Reaction
Pfu	Plaque-forming unit
P-gal	phenyl β-d-galactopyranoside
PRC	Procarbazine Hydrochloride
SBS	Single-Base Substitutions
SEM	Standard Error of the Mean
SNV	Single-Nucleotide Variant
SRA	Sequence Read Archives
SSCSs	Single Strand Consensus sequence
SV	Structural Variant
TCR	Transcription-Coupled Repair
TG	Test Guideline
TGR assay	Transgenic Rodent Mutation Reporter Gene assay
UCSC	University of California Santa Cruz
UMI	Unique Molecular Identifier
VC	Vehicle Control
VCF	Variant Call File

STATEMENT OF CONTRIBUTION

Chapter 2: **Duplex Sequencing Provides Detailed Characterization of Mutation Frequencies and Spectra in the Bone Marrow of MutaMouse Males Exposed to Procarbazine Hydrochloride**

This chapter in press in Archives of Toxicology in May 2023.

Authors:

Annette E. Dodge[1,2], Danielle P.M. LeBlanc[1], Gu Zhou[1], Andrew Williams[1], Matthew J. Meier[1], Phu Van[3], Fang Yin Lo[3], Charles C. Valentine[3], Jesse J. Salk[3], Carole L. Yauk[2,4], Francesco Marchetti[1,4]

Affiliations:

[1]Environmental Health Science and Research Bureau, Health Canada, Ottawa, Ontario, Canada
[2]Department of Biology, University of Ottawa, Ottawa, Ontario, Canada
[3]TwinStrand Biosciences Inc. Seattle, Washington, USA
[4]Department of Biology, Carleton University, Ottawa, Ontario, Canada

Study Concept and Design……Annette Dodge
Carole L. Yauk
Francesco Marchetti

Laboratory Work…….... Danielle P.M. LeBlanc
Gu Zhou

Library Preparation and Bioinformatic Processing…….. Phu Van
Fang Yin Lo
Charles C. Valentine

Data Analysis……Annette Dodge
Andrew Williams
Matthew J. Meier

Manuscript Preparation …….. Annette Dodge
Carole L. Yauk
Francesco Marchetti
Jesse J. Salk

Chapter 3: **Duplex Sequencing Reveals Dose-Dependent Increases in Mutation Frequency and a Unique Spectrum in Procarbazine-Exposed Male Mouse Germ Cells**

Authors:

Annette E. Dodge[1,2], Danielle P.M. LeBlanc[2], Gu Zhou[2], Andrew Williams[2], Elena Esina[1], Matthew J. Meier[2], Charles C. Valentine[3], Jesse J. Salk[3], Carole L. Yauk[1,4], Francesco Marchetti[2,4]

Affiliations:

[1]Department of Biology, University of Ottawa, Ottawa, Ontario, Canada
[2]Environmental Health Science and Research Bureau, Health Canada, Ottawa, Ontario, Canada
[3]TwinStrand Biosciences Inc. Seattle, Washington, USA
[4]Department of Biology, Carleton University, Ottawa, Ontario, Canada

Study Concept and Design……Annette Dodge
Carole L. Yauk
Francesco Marchetti

Laboratory Work…….. Annette Dodge
Danielle P.M. LeBlanc
Gu Zhou

Bioinformatics and Data Analysis……Annette Dodge
Andrew Williams
Elena Esina
Matthew J. Meier
Clint C. Valentine

Manuscript Preparation …….. Annette Dodge
Carole L. Yauk
Francesco Marchetti
Jesse J. Salk

CHAPTER ONE

INTRODUCTION

ANNETTE DODGE

1.1 The Importance of Genotoxicity Testing

The integrity of the DNA molecule is crucial for the proper functioning of all units of life, from cells, tissues, and organs to populations. Genetic toxicology is the study of how chemical or physical agents affect the genome. Specifically, genotoxicity refers to the ability of harmful substances to cause DNA damage, mutations, and chromosomal changes in cells. Exposure to genotoxic chemicals can induce adverse effects on genetic components via a variety of mechanisms that may translate into genetic diseases. These effects are variable and depend on the affected gene and tissue. In somatic cells, the most severe consequence of genetic toxicity is the development of cancer (Jackson et al., 2018). There is also evidence that genetic damage is implicated in a broad spectrum of other diseases, including metabolic imbalances, immune dysfunction, musculoskeletal disorders, endocrine disorders, and many others (Erickson, 2003; Godschalk et al., 2020). In germ cells (the sperm and egg), genetic damage can translate into birth defects or heritable diseases that may be propagated to future generations. Understanding the risk posed by substances to the DNA is essential for protecting the genome and preventing disease (Marchetti et al., 2020).

Genotoxicity testing is used to identify substances that can cause permanent genetic alterations in somatic or germ cells (Organization for Economic Co-operation and Development (OECD), 2017). Government authorities, such as Health Canada, use this information to identify the hazards and risks posed by commercial and environmental products to human health. They can then develop regulatory policies to limit the exposure of Canadian citizens to these harmful substances. There are generally three major endpoints considered in regulatory genetic toxicology testing: 1) mutagenicity; inherited changes in the DNA sequence including point mutations or small deletions/insertions, 2) clastogenicity; structural chromosome changes, and 3) aneugenicity; the occurrence of an abnormal number of chromosomes in a haploid set (Eastmond et al., 2009). Every aspect of genotoxicity testing is crucial for protecting the genome from adverse genetic effects that may translate into serious genetic diseases.

1.2 Mutagenicity Testing

Mutagenicity assays were introduced into regulatory testing in the 1950s and continue to be developed for more effective and efficient testing (Wassom, 1989). Historically, as more chemicals were used in therapeutics, food processing, and other industries, assessment of mutagenic ability was recognized as critical to the protection of human health (Auerbach, 1960). Initially, the main priority was

identifying agents that cause mutations in germ cells. However, in 1970s Ames, (1973) demonstrated a strong correlation between bacterial mutagenicity and carcinogenicity. The focus of mutagenicity assessment quickly shifted from germ cells to somatic cells and the correlation with cancer. Subsequent development of current testing assays made it easy to detect somatic cell mutagens with short term assays. In contrast, there lacked efficient and sensitive novel methods for detecting mutagenic effects in germ cells (Ren et al., 2017). Thus, germ cell mutagenesis was often neglected as research on cancer predictivity was driven forward. Yet, more studies are now attempting to return to the root of mutagenicity testing and improve our ability to detect germ cell mutagens (Demarini, 2012; Marchetti et al., 2020). Today, mutagenicity is used to encapsulate both the risk of cancer and germ cell driven heritable disease.

Mutations that confer a proliferative advantage within somatic cells may promote clonal expansion, potentially initiating the development of a neoplasm (Hassanpour & Dehghani, 2017; Jackson et al., 2018). Today, it is well established that mutations contribute to the development of cancer (Basu, 2018; McCann et al., 1975). Mutagenicity assays are routinely used to screen chemicals for potential oncogenic hazards prior to the more time-intensive and costly rodent cancer bioassays. However, these assays focus only on hazard identification and very rarely provide information on the mechanism behind mutation induction (Salk & Kennedy, 2020). Recently, there has been a shift away from this qualitative paradigm, towards quantitative toxicological approaches centred on using mutagenicity endpoints for risk assessment. There has been much work towards refining dose-response modelling approaches to establish points of departure for potency comparisons to advance this paradigm change (Heflich et al. 2020). More emphasis is also being placed on understanding the mechanisms leading to mutagenic outcomes. For example, the analysis of specific patterns of mutation subtypes can inform on mutagenic mechanisms and be linked to mutation patterns observed in human cancers (Valentine et al., 2020). This provides insight into human relevance of the observed effects and can be used to determine which next steps may be necessary after a positive mutagenicity assay. The development of methods that provide more detailed information on mutagenic mechanism will allow us to better link specific exposures with the development of cancers, and potentially help us understand the basis of other genetic diseases as well.

1.3 Germ Cell Mutagenesis

Germ cell mutations remain an endpoint of regulatory concern. Although germ cell mutations are rare at an individual level, they can have a profound impact on a population level. First, a single mutation in germ cells can produce an offspring that contains that mutation in every cell of its body; thus, the chances of the mutation to affect the health of that individual is much larger than for somatic mutations. In a recent study, it was estimated 3.5-5.9% of the global population are affected by some rare disease, 71.9% of which have a genetic origin (Nguengang Wakap et al., 2019). This equates to roughly 300 million people worldwide who suffer from a rare genetic disease. Second, even a relatively small increase in germ cell mutation rate can translate to millions of *de novo* mutations transmitted through the generations. For example, within the 700 genes linked with intellectual disability, it was estimated that a modest 25% increase in mutations by tobacco smoke would result in an extra 1.9 million loss of function mutations worldwide per generation. This translates to 500,000 children affected by autosomal dominant mutations who would display a disease phenotype (Beal et al., 2017).

While there is abundant evidence that many agents induce inherited changes in the offspring of exposed animals, obtaining definite data in humans is more difficult (Demarini, 2012; Marchetti et al., 2020; Yauk et al., 2015). Efforts to characterise human germline mutagens must be improved to protect our population from disease.

Historically, regulatory authorities assumed that decisions based on evidence of chemical mutagenicity in somatic cells, such as the bone marrow or liver, will by default protect the germline. However, there are quantitative differences between the induction of mutations within somatic cells and germ cells. There are several examples of germ cells showing adverse effects to mutagen exposure at doses that do not elicit adverse effects within somatic cells. For example, N-Hydroxymethylacrylamide induced dominant lethal mutations in the germ cells of male mice but showed no effect for the micronucleus assay in erythrocytes of the same mice (Witt et al., 2003). Additionally, side stream smoke induced tandem repeats in sperm at doses that did not induce micronuclei in the reticulocytes and erythrocytes of the blood and bone marrow of exposed mice (Marchetti et al., 2011). There are several unique factors that distinguish germ cell from somatic cell mutagenesis. In addition to metabolic differences, and differences in proliferation rate, the process of meiosis provides opportunities to affect nucleotide composition (Arbel-Eden & Simchen, 2019) and post-meiotic haploid germ cells cannot rely on sister chromatids as templates for homology-based repair mechanisms (Baarends et al., 2001).

Additionally, male germ cells will progressively lose DNA repair capacity throughout spermatogenesis, which could lead to the accumulation of DNA damage in maturing sperm, thus increasing the risk for mutagenesis in the embryo (Marchetti & Wyrobek, 2008; Olsen et al., 2005). Therefore, it is important to measure mutation induction in both somatic and germ cells when considering the potential hazards and risks posed by a chemical.

1.4 Current Practices in Mutagenicity Assessment

The current conventional tests for mutagenicity testing begin *in vitro* with the bacterial mutation (Ames) assay (OECD 471, 2020) and cell line assays such as HPRT (hypoxanthine phosphorybosyl transferase) gene mutation assay (OECD 476, 2016). While highly effective, *in vitro* assays have several limitations that make them imperfect surrogates for human toxicology. Differences in metabolic activation, a small number of cell types, and continuous cellular proliferation that can lead to jackpot clonal mutations make it difficult to extrapolate *in vitro* results to humans. Therefore, if positive results are obtained for *in vitro* assays, *in vivo* mutagenicity assessment is often required (Eastmond et al., 2009; Health Canada, 2016).

1.4.1 Limitations of Standard in vivo *Mutagenicity Assays*

Current *in vivo* mutagenicity assays rely on mutation detection using selectable phenotypes. The most widely used test is the transgenic rodent mutation reporter assay (the TGR assay, OECD 488, 2022), which quantifies mutations in a reporter gene following a multi step transfer of DNA from mutagen-exposed rodent into bacteria. Mutations in the reporter gene cause a distinct bacterial phenotype under selective conditions, allowing the quantification of a ratio of mutant cells to the number of cells in the absence of selection (Gingerich et al., 2014; Lambert et al., 2005). However, this assay, and others based on reporter genes, has several critical limitations. First, selectable markers often require unique strains of animals, thus are limited to only a few common model organisms, and cannot be integrated with other standard toxicity tests. The *Pig-a* mutation assay (Olsen et al., 2017) is an exception wherein mutation of the reporter gene causes a phenotypic change in the animal's blood cells. However, this assay cannot be applied to other tissues. Second, most assays measure mutation induction in only a single exogenous reporter gene that does not accurately represent the diverse structure and function of the mammalian genome. Many genomic features are thought to modulate differential sensitivity to chemical mutagens (Hodgkinson & Eyre-Walker, 2011; Makova & Hardison, 2015); these cannot be assessed when relying on

a single reporter (Salk & Kennedy, 2020). Third, the vast majority of the existing mutagenicity tests yield little mechanistic data. For instance, characterization of the mutation spectra using the TGR assay is impractical given the need to laboriously pick and independently sequence many viral plaques (Beal et al., 2020). Finally, selection-based assays are limited to the detection of functional mutations that cause a phenotypic change. Thus, silent mutations will not be counted. Despite their importance for genotoxicity testing over the last decades, selection-based assays like the TGR assay do not support the current shift towards quantitative mutagenicity testing for risk assessment.

1.5 The Application of Next-generation Sequencing Technologies for Mutagenicity Assessment

Over the past 2 decades, advances in Next-Generation Sequencing (NGS) technology have revolutionized many fields of biology, including evolutionary biology, genetics, and cancer biology. NGS is capable of sequencing entire genomes and thus presents a potential alternative to selection-based assays that would allow the screening of many loci, in any cell type, and in wild-type animal strains. However, NGS methods have very high technical error rates (~1×10^{-3} per nucleotide), that are orders of magnitude higher than typical endogenous per-nucleotide mutation frequencies (< 1×10^{-7}) (Kennedy et al., 2014; Lynch, 2010). Due to the random nature of mutation induction, genetic toxicology assessment requires the ability to detect ultra-low frequency mutations in a large population of non-mutant DNA molecules. Thus, for *de novo* mutation detection, standard NGS methods must be improved to reduce the error rate (Salk & Kennedy, 2020).

1.5.1 Duplex Sequencing

Duplex sequencing (DS) is an error-corrected NGS methodology that greatly improves the accuracy of mutation detection (Schmitt et al., 2012). Error rate is reduced by labelling each strand of the fragmented DNA molecule with its own unique molecular identifier so that, following amplification, reads from both DNA strands may be assembled and grouped (Figure 1.1). A single-strand consensus sequence (SSCS) is created by comparing reads bearing the same tag. Any variant that does not occur on every read is eliminated as an error. SSCSs are compared to their complementary strand and any variant that does not occur on both SSCSs are eliminated as an error. By relying on the double strandedness of DNA for error correction, DS increases the sensitivity to detect true mutations. Error-correction makes DS more than 10,000 times more accurate than standard NGS (Kennedy et al., 2014). We believe error-

corrected sequencing technologies will reshape the way we conduct mutagenicity testing and allow us to overcome many of the limitations faced with traditional assays.

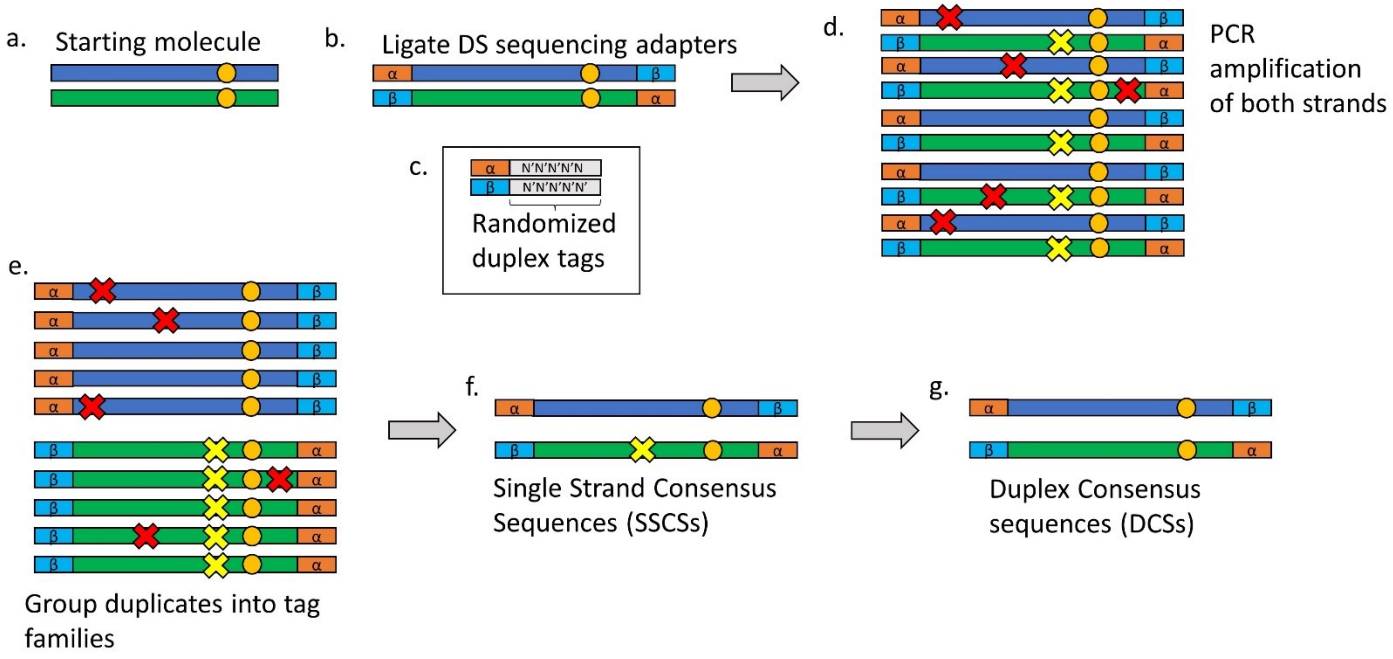

Figure 1.1 Overview of Duplex Sequencing. (a) Depiction of the sample DNA molecule with one true mutation (yellow circle). (b) Ligation of the adapters to both ends of the sample DNA. (c) Schematic of a Duplex Sequencing adapter, showing the random double-stranded tag and the invariant spacer sequence. (d) PCR amplification of each strand of a DNA duplex results in two distinct, yet complementary, PCR products. (e) Reads sharing unique tag sequences are grouped together in tag families. Variants are of three types: true mutations (yellow circle), sequencing errors (red X), and first-round PCR errors (yellow X). (f) Comparing each read in a tag family creates a SSCS. SSCSs remove sequencing errors, but not first-round PCR errors. (g). Comparison of the SSCSs from the paired families with tags αβ and βα creates a DCS. DCSs eliminate first-round PCR errors. True mutations are scored only if they are present at the same position in all reads of a tag family and on both strands of the DNA. The figure is adapted from Kennedy et al., 2013.

1.5.2 The Application of Duplex Sequencing for Mutagenicity Testing and Risk Assessment

DS is effective at measuring increases in MF in mouse somatic tissues following exposure to established environmental mutagens including benzo[a]pyrene (BaP) (LeBlanc et al., 2022), aflatoxin (Chawanthayatham et al., 2017), N-ethyl-N-nitrosourea (ENU) and urethane (Valentine et al., 2020). DS makes use of custom mutagenesis panels comprised of multiple targeted regions that span a broad range of genomic features including location, GC content, trinucleotide abundances, and genic status (LeBlanc et al., 2022). The ability to query large portions of the mammalian genome for chemically induced mutations is a major advantage of DS over traditional assays that enables us to explore how different genomic features might affect mutation susceptibility. Recent work in mouse bone marrow has shown significant differences in the magnitude of the response across loci following exposure to BaP (LeBlanc et al., 2022). Another study found similar variations in chemically-induced mutation susceptibility amongst five genes within mouse bone marrow, liver, lung, spleen, and blood (Valentine et al., 2020). By querying loci with various genomic features, we can hypothesize on the factors that influence mutagenesis.

Many endogenous factors are thought to modulate chemical mutagenicity, including transcription status, genomic region, sequence context, chromatin state, and others. The recognition and repair of DNA damage occurs more quickly in actively transcribed regions of the genome compared to non transcribed regions. This transcription-coupled repair (TCR) contributes to decreased risk of mutagenesis within transcribed regions (Hanawalt & Spivak, 2008; Xia et al., 2020). Additionally, the packaging of DNA into chromatin can hinder the access of repair proteins and affect the efficiency of repair. Adar et al. (2016) showed that repair of UV-induced DNA damage in human skin fibroblasts occurred preferentially in active and open chromatin states, while heterochromatic regions were repaired more slowly. This occurred for both transcription-coupled and general excision repair. Thus, there appears to be increased risk of mutagenesis in heterochromatin compared to euchromatin (Makova & Hardison, 2015). The customizable panel of endogenous genomic loci utilized by DS allow us to explore the effects of various genomic factors on chemical mutagenicity.

The relative frequency of the different mutation subtypes (ie, the specific base substitution subtypes, insertions, deletions, and multi-nucleotide variants) reflects the mechanism of the mutagen. For instance, BaP mutagenesis is characterized by G>T transversions, a consequence of bulky adduct formation at the N2 of guanine (Beal et al., 2015; Denissenko et al., 1996; LeBlanc et al., 2022).

Alternatively, the alkylating agent ENU produces primarily A>T or A>G mutations resulting from inefficient repair of O-alkyl damage on guanine and thymine residues (Kucab et al., 2019). Local sequence context also strongly influences the frequency of a given type of mutation (Michaelson et al., 2012; Sung et al., 2015). Analysis of the trinucleotide spectrum induced by a chemical is not practical using traditional mutagenesis assays. Small reporters do not represent whole-genome nucleotide distribution and could thus bias the spectrum (Kennedy et al., 2014). Furthermore, these assays produce relatively small numbers of mutations, often rendering the spectrum analysis underpowered. In contrast, DS uses a panel of targets that better reflects the whole-genome nucleotide composition and produces much higher amounts of sequencing data. DS has since provided highly detailed mutation spectra for various established mutagens including BaP (LeBlanc et al., 2022), aflatoxin (Chawanthayatham et al., 2017b), ENU and urethane (Valentine et al., 2020). Overall, because DS is a sequencing-based approach it readily produces the data needed for mutation spectrum analysis to enhance risk assessment.

One of the main priorities of mutagenicity testing is identifying the potential for human carcinogenesis. However, linking exposure to human cancer is exceedingly complex and requires abundant epidemiological data. Epidemiological studies are often confounded by exposure to other mutagens and by the natural accumulation of mutations through ageing. Recently, large-scale sequencing of cancer samples (Cancer Genome Atlas and others) paired with the development of new statistical methods have introduced cancer mutational signatures (Alexandrov et al., 2013). Mutational signatures are recurring patterns of sequence-context-dependent mutation types observed in cancer samples with similar aetiologies. Non-negative matrix factorization is used to computationally parse out constituent mutational processes from the sum of mutations accumulated throughout the tumour's lifetime. This work has since reported many signatures associated with specific cancer types or mutational processes (COSMIC v.3.3, June 2022). It is possible to link these cancer signatures with the trinucleotide spectra of specific mutagens extracted by DS (Chawanthayatham et al., 2017; LeBlanc et al., 2022; Valentine et al., 2020). For instance, BaP, the main carcinogenic agent found in cigarette smoke, produces a mutation spectrum that is highly similar to mutational signatures observed in human lung cancers (LeBlanc et al., 2022; Valentine et al., 2020). These signature analyses can thus provide empirical evidence for the contribution of environmental mutagens to the mutation spectrum observed in human cancers. Developing tools that can link exposures to human cancer development will have a profound impact on clinical medicine and public health.

1.5.3 Considerations for the Implementation of Duplex Sequencing as a Regulatory Test

Before DS can be used as a regulatory test for chemical mutagenicity assessment, more work is needed to assess the performance of DS across a range of chemicals with differing modes of action and potencies. So far, DS has only been tested on well-established mutagens, most of which are highly potent such as BaP and ENU (LeBlanc et al., 2022; Valentine et al., 2020). Thus, the sensitivity of DS to assess less potent mutagens must be established. An additional consideration is the response of the various genomic targets within the DS panel. As mentioned previously, the DS targets tend to differ in mutagenesis susceptibility. We must characterise how the different targets respond to different chemicals and potencies to consider how we can account for the variability in target susceptibility during regulatory decision making. As such, more work testing DS with different chemicals is required. The work covered in this thesis aims to evaluate the use of DS for measuring chemically induced mutations. Our goal is to help establish DS as an effective methodology for assessing chemical mutagenicity in both somatic and germ cells. We will use DS to study the effects of a mutagenic compound, procarbazine (PRC), on rodent tissues and directly compare the results to those obtained by using the TGR assay performed on the same rodents.

DS must also be tested on a variety of tissues before it can be accepted as a mutagenicity assay. Currently, DS has been tested on various somatic tissues, including bone marrow (LeBlanc et al., 2022), liver (Chawanthayatham et al., 2017), lung, spleen, and blood (Valentine et al., 2020). While these tissues are incredibly important for regulatory purposes, DS has not yet been tested in germ cells. As mentioned, identifying and protecting citizens from germ cell mutagens is one of the founding objectives of mutagenicity testing. Assessing the performance of DS for testing germ cell mutagenicity will be necessary for it to be utilized as a mutagenicity test. Furthermore, the abundant mechanistic information, alongside the susceptibility of the different DS loci will better allow us to study the unique mutagenic mechanisms that may exist within germ cells compared to somatic cells. This work will assess the mutagenicity of PRC within mouse bone marrow and male germ cells harvested from the seminiferous tubules. We will thus be able to compare the effects of the chemical between the two tissues to assess differences between germ and somatic cells.

1.6 Model Chemical; Procarbazine Hydrochloride

PRC is a hydrazine derivative frequently used in combination with other anti-neoplastic agents to treat Hodgkin's lymphoma and several other human cancers (Andrieu et al., 2016). While effective, PRC has been associated with the development of secondary cancers following treatment including acute non-lymphocytic leukemia and non-Hodgkin's lymphoma (Henry-Amar, 1992; IARC, 1981; Kaldor et al., 1988). There is clear evidence that PRC is an effective *in vivo* clastogen, inducing micronuclei in hematopoietic cells (Phonethepswath et al., 2013; Suzuki et al., 1999). PRC shows mutagenic ability within mouse bone marrow, blood, lung, spleen, and testis, though these effects are observed at higher doses than its clastogenic effects (Beal et al., 2020; Revollo et al., 2017; Suzuki et al., 1999). We predict that PRC will be a less potent mutagen than those that have been tested previously with DS, allowing us to assess the sensitivity of the assay. Furthermore, the molecular mechanism by which PRC induces mutations is not thoroughly understood. Experiments have been undertaken to sequence PRC-induced mutants detected by the *lacZ* (Beal et al., 2020) and *Pig-a* (Revollo et al., 2017) assays. However, as mentioned previously, such reporter gene-specific assays are poorly suited to characterising the mutation spectra in the detail necessary for in depth mechanistic analyses. DS will allow us to investigate the mutagenic mechanism of PRC in greater depth than has been previously possible. Furthermore, comparisons with cancer mutational signatures will help us understand PRC's role in the development of cancers following treatment. For these reasons, PRC is an ideal chemical to test the applicability of DS in mutagenicity testing.

1.7 Thesis Objectives

There are two overarching goals for this study:

1. To demonstrate the potential of DS as a robust *in vivo* mutagenicity test that could replace the TGR assay as the next "gold standard" in research and regulatory applications.
2. To explore the rich data provided by DS to gain a better understanding of spontaneous and PRC-induced mutagenicity in somatic and germ cells.

The four specific objectives for my thesis are:

1. **Evaluate the performance of DS for effective assessment of *in vivo* spontaneous and induced mutations in bone marrow and male germ cells following exposure to PRC.** DS was used to analyse MF in the bone marrow and germ cells of MutaMouse males exposed to PRC alongside vehicle controls. MF determined by DS was compared to mutant frequency obtained using the TGR assay on the same samples. Dose-response modelling was applied to compare the response between tissues.

2. **Assess genomic features that drive mutational response and determine whether they differ between bone marrow and germ cells**. The twenty 2.4kb genomic targets were sequenced with DS for each animal. Mutation frequencies in the targets were compared and the influence of transcription status, chromatin state, sequence context, and other factors was investigated in both tissues. This work informs the features that drive mutational response to genotoxic agents and potential differences in these between somatic and germ cells.

3. **Use bioinformatics approaches to characterize mutagenic mechanisms and determine the mutational signature of PRC in bone marrow and germ cells of MutaMouse males**. Mutation subtypes detected by DS were compared between control and PRC-treated groups, as well as between germ and bone marrow cells. Advanced bioinformatics analyses were used to identify COSMIC SBS signatures that most closely resemble the PRC mutational spectra and whether these differ between somatic tissues and germ cells.

4. **Explore optimal DS study designs for assessing mutagenicity by modeling sample size and sequencing data yield within mouse bone marrow and germ cells**. A power analysis was conducted to determine if sample size and the total duplex bases sequenced per animal may be

reduced without compromising the quality of the data obtained. These analyses were based on the observed parameters of our exposure studies in each tissue, including background mutation frequency and sample variance.

Overall, this project supports the uptake of DS as a modernized mutagenicity testing methodology that can improve our ability to assess the potential dangers of chemicals efficiently and effectively. Its application will undoubtedly impact regulatory decision-making aimed at the prevention of genetic diseases, including cancer, for Canadian citizens in the future.

1.8 References

Adar, S., Hu, J., Lieb, J. D., & Sancar, A. (2016). Genome-wide kinetics of DNA excision repair in relation to chromatin state and mutagenesis [Article]. *Proceedings of the National Academy of Sciences - PNAS*, *113*(15), E2124–E2133. https://doi.org/10.1073/pnas.1603388113

Alexandrov, L. B., Nik-Zainal, S., Wedge, D. C., Campbell, P. J., & Stratton, M. R. (2013). Deciphering signatures of mutational processes operative in human cancer. *Cell Reports*, *3*(1), 246–259. https://doi.org/10.1016/J.CELREP.2012.12.008

Ames, B. N. (1973). Carcinogens are Mutagens: Their Detection and Classification [Article]. *Environmental Health Perspectives*, *6*, 115–118. https://doi.org/10.1289/ehp.7306115

Andrieu, J. M., Ifrah, N., Payen, C., Fermanian, J., Coscas, Y., & Flandrin, G. (2016). Increased risk of secondary acute nonlymphocytic leukemia after extended-field radiation therapy combined with MOPP chemotherapy for Hodgkin's disease. *Https://Doi.Org/10.1200/JCO.1990.8.7.1148*, *8*(7), 1148–1154. https://doi.org/10.1200/JCO.1990.8.7.1148

Arbel-Eden, A., & Simchen, G. (2019). Elevated Mutagenicity in Meiosis and Its Mechanism [Article]. *BioEssays*, *41*(4), e1800235-n/a. https://doi.org/10.1002/bies.201800235

Auerbach, C. (1960). Chemical mutagenesis in animals. *Abh Deutsch Akad Wiss Berlin Klin Med*, *1*, 1–12.

Baarends, W., van der Laan, R., & Grootegoed, J. (2001). DNA repair mechanisms and gametogenesis [Article]. *Reproduction (Cambridge, England)*, *121*(1), 31–39. https://doi.org/10.1530/rep.0.1210031

Basu, A. (2018). DNA Damage, Mutagenesis and Cancer. *International Journal of Molecular Sciences*, *19*(4), 970. https://doi.org/10.3390/ijms19040970

Beal, M. A., Gagné, R., Williams, A., Marchetti, F., & Yauk, C. L. (2015). Characterizing Benzo[a]pyrene-induced lacZ mutation spectrum in transgenic mice using next-generation sequencing. *BMC Genomics*, *16*(1). https://doi.org/10.1186/S12864-015-2004-4

Beal, M. A., Meier, M. J., LeBlanc, D. P., Maurice, C., O'Brien, J. M., Yauk, C. L., & Marchetti, F. (2020). Chemically induced mutations in a MutaMouse reporter gene inform mechanisms underlying human cancer mutational signatures. *Communications Biology*, *3*(1). https://doi.org/10.1038/S42003-020-01174-Y

Beal, M. A., Yauk, C. L., & Marchetti, F. (2017). From sperm to offspring: Assessing the heritable genetic consequences of paternal smoking and potential public health impacts. *Mutation Research/Reviews in Mutation Research*, *773*, 26–50. https://doi.org/10.1016/J.MRREV.2017.04.001

Chawanthayatham, S., Valentine, C. C., Fedeles, B. I., Fox, E. J., Loeb, L. A., Levine, S. S., Slocum, S. L., Wogan, G. N., Croy, R. G., & Essigmann, J. M. (2017a). Mutational spectra of aflatoxin B_1 in vivo establish biomarkers of exposure for human hepatocellular carcinoma [Article]. *Proceedings of the National Academy of Sciences - PNAS*, *114*(15), E3101–E3109. https://doi.org/10.1073/pnas.1700759114

Chawanthayatham, S., Valentine, C. C., Fedeles, B. I., Fox, E. J., Loeb, L. A., Levine, S. S., Slocum, S. L., Wogan, G. N., Croy, R. G., & Essigmann, J. M. (2017b). Mutational spectra of aflatoxin B1 in vivo establish biomarkers of exposure for human hepatocellular carcinoma. *Proceedings of the National Academy of Sciences of the United States of America*, *114*(15), E3101–E3109. https://doi.org/10.1073/PNAS.1700759114

Chawanthayatham, S., Valentine, C. C., Fedeles, B. I., Fox, E. J., Loeb, L. A., Levine, S. S., Slocum, S. L., Wogan, G. N., Croy, R. G., & Essigmann, J. M. (2017c). Mutational spectra of aflatoxin B1 in vivo establish biomarkers of exposure for human hepatocellular carcinoma. *Proceedings of the National*

Academy of Sciences of the United States of America, *114*(15), E3101–E3109. https://doi.org/10.1073/PNAS.1700759114/-/DCSUPPLEMENTAL/PNAS.201700759SI.PDF

Demarini, D. M. (2012). Declaring the existence of human germ-cell mutagens. *Environmental and Molecular Mutagenesis*, *53*(3), 166–172. https://doi.org/10.1002/EM.21685

Denissenko, M. F., Pao, A., Tang, M., & Pfeifer, G. P. (1996). Preferential Formation of Benzo[a]pyrene Adducts at Lung Cancer Mutational Hotspots in P53 [Article]. *Science (American Association for the Advancement of Science)*, *274*(5286), 430–432. https://doi.org/10.1126/science.274.5286.430

Eastmond, D. A., Hartwig, A., Anderson, D., Anwar, W. A., Cimino, M. C., Dobrev, I., Douglas, G. R., Nohmi, T., Phillips, D. H., & Vickers, C. (2009). Mutagenicity testing for chemical risk assessment: update of the WHO/IPCS Harmonized Scheme [Article]. *Mutagenesis*, *24*(4), 341–349. https://doi.org/10.1093/mutage/gep014

Erickson, R. P. (2003). Somatic gene mutation and human disease other than cancer. *Mutation Research/Reviews in Mutation Research*, *543*(2), 125–136. https://doi.org/10.1016/S1383-5742(03)00010-3

Gingerich, J. D., Soper, L., Lemieux, C. L., Marchetti, F., & Douglas, G. R. (2014). *Transgenic Rodent Gene Mutation Assay in Somatic Tissues*. 305–321. https://doi.org/10.1007/978-1-4939-1068-7_18

Godschalk, R. W. L., Yauk, C. L., van Benthem, J., Douglas, G. R., & Marchetti, F. (2020). In utero Exposure to Genotoxicants Leading to Genetic Mosaicism: An Overlooked Window of Susceptibility in Genetic Toxicology Testing? *Environmental and Molecular Mutagenesis*, *61*(1), 55–65. https://doi.org/10.1002/EM.22347

Hanawalt, P. C., & Spivak, G. (2008). Transcription-coupled DNA repair: two decades of progress and surprises [Article]. *Nature Reviews. Molecular Cell Biology*, *9*(12), 958–970. https://doi.org/10.1038/nrm2549

Hassanpour, S. H., & Dehghani, M. (2017). Review of cancer from perspective of molecular. *Journal of Cancer Research and Practice*, *4*(4), 127–129. https://doi.org/10.1016/J.JCRPR.2017.07.001

Health Canada. (2016). Guidance on Genotoxicity Testing and Data Interpretation for Pharmaceuticals Intended for Human Use. *ICH Topic S2(R1).* .

Henry-Amar, M. (1992). Second cancer after the treatment for Hodgkin's disease: a report from the International Database on Hodgkin's Disease [Article]. *Annals of Oncology*, *3*(suppl-4), S117–S128. https://doi.org/10.1093/annonc/3.suppl_4.S117

Hodgkinson, A., & Eyre-Walker, A. (2011). Variation in the mutation rate across mammalian genomes. *Nature Reviews. Genetics*, *12*(11), 756–766. https://doi.org/10.1038/NRG3098

IARC. (1981). Evaluations of the Carcinogenic Risk of Chemicals o Humans; Some Antineoplastic and Immunosuppressive Agents. *International Agency for Research on Cancer. WHO*, *26*, 311–340.

Jackson, M., Marks, L., May, G. H. W., & Wilson, J. B. (2018). The genetic basis of disease. In *Essays in Biochemistry* (Vol. 62, Issue 5, pp. 643–723). Portland Press Ltd. https://doi.org/10.1042/EBC20170053

Kaldor, J. M., Day, N. E., & Hemminki, K. (1988). Quantifying the carcinogenicity of antineoplastic drugs [Article]. *European Journal of Cancer & Clinical Oncology*, *24*(4), 703–711. https://doi.org/10.1016/0277-5379(88)90302-1

Kennedy, S. R., Schmitt, M. W., Fox, E. J., Kohrn, B. F., Salk, J. J., Ahn, E. H., Prindle, M. J., Kuong, K. J., Shen, J. C., Risques, R. A., & Loeb, L. A. (2014). Detecting ultralow-frequency mutations by Duplex Sequencing. *Nature Protocols*, *9*(11), 2586–2606. https://doi.org/10.1038/NPROT.2014.170

Kucab, J. E., Zou, X., Morganella, S., Joel, M., Nanda, A. S., Nagy, E., Gomez, C., Degasperi, A., Harris, R., Jackson, S. P., Arlt, V. M., Phillips, D. H., & Nik-Zainal, S. (2019). A Compendium of Mutational Signatures of Environmental Agents. *Cell*, *177*(4), 821-836.e16. https://doi.org/10.1016/J.CELL.2019.03.001

Lambert, I. B., Singer, T. M., Boucher, S. E., & Douglas, G. R. (2005). Detailed review of transgenic rodent mutation assays. *Mutation Research*, *590*(1–3), 1–280. https://doi.org/10.1016/J.MRREV.2005.04.002

LeBlanc, D. P. M., Meier, M., Lo, F. Y., Schmidt, E., Valentine, C., Williams, A., Salk, J. J., Yauk, C. L., & Marchetti, F. (2022). Duplex sequencing identifies genomic features that determine susceptibility to benzo(a)pyrene-induced in vivo mutations. *BMC Genomics*, *23*(1). https://doi.org/10.1186/S12864-022-08752-W

Lynch, M. (2010). Rate, molecular spectrum, and consequences of human mutation [Article]. *Proceedings of the National Academy of Sciences - PNAS*, *107*(3), 961–968. https://doi.org/10.1073/pnas.0912629107

Makova, K. D., & Hardison, R. C. (2015). The effects of chromatin organization on variation in mutation rates in the genome. *Nature Reviews. Genetics*, *16*(4), 213. https://doi.org/10.1038/NRG3890

Marchetti, F., Douglas, G. R., & Yauk, C. L. (2020). A Return to the Origin of the EMGS: Rejuvenating the Quest for Human Germ Cell Mutagens and Determining the Risk to Future Generations. *Environmental and Molecular Mutagenesis*, *61*(1), 42–54. https://doi.org/10.1002/EM.22327

Marchetti, F., Rowan-Carroll, A., Williams, A., Polyzos, A., Berndt-Weis, M. L., & Yauk, C. L. (2011). Sidestream tobacco smoke is a male germ cell mutagen. *Proceedings of the National Academy of Sciences of the United States of America*, *108*(31), 12811–12814. https://doi.org/10.1073/PNAS.1106896108/ASSET/44FF636A-C271-4F00-937E-3534B52DD8C4/ASSETS/GRAPHIC/PNAS.1106896108FIG01.JPEG

Marchetti, F., & Wyrobek, A. J. (2008). DNA repair decline during mouse spermiogenesis results in the accumulation of heritable DNA damage [Article]. *DNA Repair*, *7*(4), 572–581. https://doi.org/10.1016/j.dnarep.2007.12.011

McCann, J., Choi, E., Yamasaki, E., & Ames, B. N. (1975). Detection of Carcinogens as Mutagens in the Salmonella/Microsome Test: Assay of 300 Chemicals [Article]. *Proceedings of the National Academy of Sciences - PNAS*, *72*(12), 5135–5139. https://doi.org/10.1073/pnas.72.12.5135

Michaelson, J. J., Shi, Y., Gujral, M., Zheng, H., Malhotra, D., Jin, X., Jian, M., Liu, G., Greer, D., Bhandari, A., Wu, W., Corominas, R., Peoples, Á., Koren, A., Gore, A., Kang, S., Lin, G. N., Estabillo, J., Gadomski, T., … Sebat, J. (2012). Whole-genome sequencing in autism identifies hot spots for de novo germline mutation. *Cell*, *151*(7), 1431–1442. https://doi.org/10.1016/J.CELL.2012.11.019

Nguengang Wakap, S., Lambert, D. M., Olry, A., Rodwell, C., Gueydan, C., Lanneau, V., Murphy, D., le Cam, Y., & Rath, A. (2019). Estimating cumulative point prevalence of rare diseases: analysis of the Orphanet database. *European Journal of Human Genetics 2019 28:2*, *28*(2), 165–173. https://doi.org/10.1038/s41431-019-0508-0

OECD 471. (2020). *Test No. 471: Bacterial Reverse Mutation Test*. OECD. https://doi.org/10.1787/9789264071247-en

OECD 476. (2016). *Test No. 476: In Vitro Mammalian Cell Gene Mutation Tests using the Hprt and xprt genes*. OECD. https://doi.org/10.1787/9789264264809-en

OECD 488. (2022). *Test No. 488: Transgenic Rodent Somatic and Germ Cell Gene Mutation Assays*. OECD. https://doi.org/10.1787/9789264203907-en

Olsen, A., Dertinger, S. D., Krüger, C. T., Eide, D. M., Instanes, C., Brunborg, G., Hartwig, A., & Graupner, A. (2017). The Pig-a Gene Mutation Assay in Mice and Human Cells: A Review [Article]. *Basic & Clinical Pharmacology & Toxicology*, *121*(S3), 78–92. https://doi.org/10.1111/bcpt.12806

Olsen, A.-K., Lindeman, B., Wiger, R., Duale, N., & Brunborg, G. (2005). How do male germ cells handle DNA damage? [Article]. *Toxicology and Applied Pharmacology*, *207*(2), 521–531. https://doi.org/10.1016/j.taap.2005.01.060

Overview on genetic toxicology TGs. (2017). OECD. https://doi.org/10.1787/9789264274761-en

Phonethepswath, S., Avlasevich, S. L., Torous, D. K., Mereness, J., Bemis, J. C., MacGregor, J. T., & Dertinger, S. D. (2013). Flow cytometric analysis of Pig-a gene mutation and chromosomal damage induced by procarbazine hydrochloride in CD-1 mice [Article]. *Environmental and Molecular Mutagenesis*, *54*(4), 294–298. https://doi.org/10.1002/em.21758

Ren, N., Atyah, M., Chen, W.-Y., & Zhou, C.-H. (2017). The various aspects of genetic and epigenetic toxicology: testing methods and clinical applications. *J Transl Med*, *15*, 110. https://doi.org/10.1186/s12967-017-1218-4

Revollo, J., Bhalli, J. A., Tebbe, C., Noteboom, J., Thomas, D., McKinzie, P., Felton, N., Pearce, M. G., & Dobrovolsky, V. N. (2017). Spectrum of Pig-a mutations in T lymphocytes of rats treated with procarbazine. *Mutagenesis*, *32*(6), 571–579. https://doi.org/10.1093/MUTAGE/GEX032

Salk, J. J., & Kennedy, S. R. (2020). Next-Generation Genotoxicology: Using Modern Sequencing Technologies to Assess Somatic Mutagenesis and Cancer Risk. *Environmental and Molecular Mutagenesis*, *61*(1), 135–151. https://doi.org/10.1002/EM.22342

Schmitt, M. W., Kennedy, S. R., Salk, J. J., Fox, E. J., Hiatt, J. B., & Loeb, L. A. (2012). Detection of ultra-rare mutations by next-generation sequencing. *Proceedings of the National Academy of Sciences of the United States of America*, *109*(36), 14508–14513. https://doi.org/10.1073/PNAS.1208715109/-/DCSUPPLEMENTAL/PNAS.201208715SI.PDF

Sung, W., Ackerman, M. S., Gout, J.-F., Miller, S. F., Williams, E., Foster, P. L., & Lynch, M. (2015). Asymmetric context-dependent mutation patterns revealed through mutation-accumulation experiments [Article]. *Molecular Biology and Evolution*, *32*(7), 1672–1683. https://doi.org/10.1093/molbev/msv055

Suzuki, T., Uno, Y., Idehara, K., Baba, T., Maniwa, J., Ohkouchi, A., Wang, X., Hayashi, M., Sofuni, T., Tsuruoka, M., Miyajima, H., & Kondo, K. (1999). Procarbazine genotoxicity in the MutaMouse; strong clastogenicity and organ-specific induction of lacZ mutations. *Mutation Research*, *444*(2), 269–281. https://doi.org/10.1016/S1383-5718(99)00060-1

Valentine, C. C., Young, R. R., Fielden, M. R., Kulkarni, R., Williams, L. N., Li, T., Minocherhomji, S., & Salk, J. J. (2020). Direct quantification of in vivo mutagenesis and carcinogenesis using duplex sequencing. *Proceedings of the National Academy of Sciences of the United States of America*, *117*(52), 33414–33425. https://doi.org/10.1073/PNAS.2013724117/-/DCSUPPLEMENTAL

Wassom, J. S. (1989). Origins of genetic toxicology and the environmental Mutagen Society. *Environmental and Molecular Mutagenesis*, *14*(S16), 1–6. https://doi.org/10.1002/EM.2850140603

Witt, K. L., Hughes, L. A., Burka, L. T., McFee, A. F., Mathews, J. M., Black, S. L., & Bishop, J. B. (2003). Mouse bone marrow micronucleus test results do not predict the germ cell mutagenicity of N-hydroxymethylacrylamide in the mouse dominant lethal assay. *Environmental and Molecular Mutagenesis*, *41*(2), 111–120. https://doi.org/10.1002/EM.10139

Xia, B., Yan, Y., Baron, M., Wagner, F., Barkley, D., Chiodin, M., Kim, S. Y., Keefe, D. L., Alukal, J. P., Boeke, J. D., & Yanai, I. (2020). Widespread Transcriptional Scanning in the Testis Modulates Gene Evolution Rates. *Cell*, *180*(2), 248-262.e21. https://doi.org/10.1016/J.CELL.2019.12.015

Yauk, C. L., Aardema, M. J., Benthem, J. van, Bishop, J. B., Dearfield, K. L., DeMarini, D. M., Dubrova, Y. E., Honma, M., Lupski, J. R., Marchetti, F., Meistrich, M. L., Pacchierotti, F., Stewart, J., Waters, M. D., & Douglas, G. R. (2015). Approaches for identifying germ cell mutagens: Report of the 2013 IWGT workshop on germ cell assays [Article]. *Mutation Research. Genetic Toxicology and Environmental Mutagenesis*, *783*, 36–54. https://doi.org/10.1016/j.mrgentox.2015.01.008

CHAPTER TWO

DATA CHAPTER

ANNETTE DODGE

This thesis section is a version of the following article:

Dodge, A.E., LeBlanc, P.M., Zhou, G., Williams, A., Meier, M.J., Van, P., Lo, F.Y., Valentine, C.C., Salk, J.J., Yauk, C.L., Marchetti, F. (2023) Duplex Sequencing Provides Detailed Characterization of Mutation Frequencies and Spectra in the Bone Marrow of MutaMouse Males Exposed to Procarbazine Hydrochloride. *Archives of Toxicology.* Post-print.

Duplex Sequencing Provides Detailed Characterization of Mutation Frequencies and Spectra in the Bone Marrow of MutaMouse Males Exposed to Procarbazine Hydrochloride

Annette E. Dodge[1,2], Danielle P.M. LeBlanc[1], Gu Zhou[1], Andrew Williams[1], Matthew J. Meier[1], Phu Van[3], Fang Yin Lo[3], Charles C. Valentine[3], Jesse J. Salk[3], Carole L. Yauk[2,4], Francesco Marchetti[1,4]

[1]Environmental Health Science and Research Bureau, Health Canada, Ottawa, Ontario, Canada

[2]Department of Biology, University of Ottawa, Ottawa, Ontario, Canada

[3]TwinStrand Biosciences Inc. Seattle, Washington, USA

[4]Department of Biology, Carleton University, Ottawa, Ontario, Canada

Journal: Archives of Toxicology

2.1 ABSTRACT

Mutagenicity testing is an essential component of health safety assessment. Duplex Sequencing (DS), an emerging high-accuracy DNA sequencing technology, may provide substantial advantages over conventional mutagenicity assays. DS could be used to eliminate reliance on standalone reporter assays and provide mechanistic information alongside mutation frequency (MF) data. However, the performance of DS must be thoroughly assessed before it can be routinely implemented for standard testing. We used DS to study spontaneous and procarbazine (PRC)-induced mutations in the bone marrow (BM) of MutaMouse males across a panel of 20 diverse genomic targets. Mice were exposed to 0, 6.25, 12.5, or 25 mg/kg-bw/day for 28 days by oral gavage and BM sampled 42 days post-exposure. Results were compared with those obtained using the conventional *lacZ* viral plaque assay on the same samples. DS detected significant increases in mutation frequencies and changes to mutation spectra at all PRC doses. Low intra-group variability within DS samples allowed for detection of increases at lower doses than the *lacZ* assay. While the *lacZ* assay initially yielded a higher fold-change in mutant frequency than DS, inclusion of clonal mutations in DS mutation frequencies reduced this discrepancy. Power analyses suggested that three animals per dose group and 500 million duplex base pairs per sample is sufficient to detect a 1.5-fold increase in mutations with >80% power. Overall, we demonstrate several advantages of DS over classical mutagenicity assays and provide data to support efforts to identify optimal study designs for the application of DS as a regulatory test.

Keywords: Error-corrected sequencing; ecNGS; genetic toxicology; duplex sequencing; mutagenesis; transgenic rodent assay.

2.2 INTRODUCTION

Somatic mutations are a hallmark of cancer and exposure to mutagenic substances is associated with an increased risk of carcinogenesis (Jackson et al., 2018). Thus, testing the ability of chemicals to induce genotoxic effects is required prior to regulatory approval and a battery of internationally standardized assays is available for this purpose. There is also growing recognition that mutations in themselves represent an adverse effect that should be considered in regulatory decision-making (Heflich et al 2020). Assays with available Organization for Economic Co-operation Development (OECD) test guidelines are routinely employed as the gold standards to assess in vitro and in vivo mutagenicity (OECD 470, 471, 488)

In vivo mutagenesis assays, such as the transgenic rodent (TGR) gene mutation assay (OECD, 2022), provide an important early indication of oncogenic risk; these assays are used to screen for potential hazard prior to the more time-intensive and costly rodent cancer bioassays. However, these assays have significant limitations. First, the TGR assay uses unique strains of animals that prevents integration with other standard toxicity tests. Second, the TGR plaque-based assay measures mutation induction in a single exogenous reporter gene that does not accurately represent the diverse structure and function of the mammalian genome. Many genomic features are thought to modulate differential sensitivity to chemical mutagens (Hodgkinson & Eyre-Walker, 2011; Makova & Hardison, 2015); these cannot be assessed when relying on a single reporter (Salk and Kennedy, 2020). Third, the TGR assay, like many other existing mutagenicity tests, yields little mechanistic data. The pattern of mutation types induced by a chemical can provide clues to the mechanism behind the chemical's mutagenic effect; with the TGR assay this is impractical given the need to laboriously pick and independently sequence many viral plaques (Beal et al., 2020). Novel methodologies that can interrogate a broad selection of genomic targets and concurrently enumerate the spectrum of mutations across a diversity of genomic regions would provide mechanistic understanding of a chemical's mutagenic effect for better prediction of human cancer risk.

Duplex Sequencing (DS) is an error-corrected next-generation sequencing (ecNGS) technology that detects ultra-rare mutations using a customizable panel targeting a portion of the endogenous genome (Kennedy et al., 2014). Recent work has demonstrated that DS is effective at measuring increases in mutations frequencies (MF) in mouse somatic tissues following exposure to established environmental mutagens including benzo[a]pyrene (BaP) (LeBlanc et al., 2022), aflatoxin

(Chawanthayatham et al., 2017), N-ethyl-N-nitrosourea (ENU) and urethane (Valentine et al., 2020). In addition to being able to precisely quantify spontaneous and induced MF across diverse genomic contexts, chromatin states and functional domains, DS provides complementary mechanistic information in the form of detailed mutation spectral data (Salk & Kennedy, 2020) that can be linked to mechanism-associated mutational signatures extracted from genome sequences of human cancers (Alexandrov et al., 2020) or cloned *ex vivo* treated cells (Kucab et al., 2019). For instance, BaP, the main carcinogenic agent found in cigarette smoke, produces a mutation spectrum that is highly similar to mutational signatures observed in human lung cancers (Nik-Zainal et al 2016; Kucab et al 2019; LeBlanc et al 2022). These signature analyses provide empirical evidence for the contribution of environmental mutagens to the mutation spectrum observed in human cancers. Given these features, it is conceivable that ecNGS may contribute to reducing reliance on, or even eliminating the need for, TGR and other mutation reporter assays.

Before DS can be used as a regulatory test for chemical mutagenicity assessment, more work is needed to compare its performance to standard assays across a range of chemicals with differing modes of action and potency. Here, we test the performance of DS compared to the TGR assay following exposure of mice to procarbazine hydrochloride (PRC), an anti-neoplastic agent that is classified as a Class 2A probable carcinogen by the International Agency for Research on Cancer (IARC Working Group, 1981). PRC is an SN1-type methylating agent known to induce mutations in mouse somatic cells (Maurice et al., 2019; Revollo et al., 2017; Suzuki et al., 1999). We measured mutations in the bone marrow (BM) of MutaMouse males exposed to PRC using the DS mouse mutagenesis panel comprised of twenty 2.4 kb targeted regions (Mouse Mutagenesis Kit, TwinStrand Biosciences Inc., Seattle WA, USA), chosen as a balanced representation of the entire genome with respect to location, GC content, trinucleotide abundances and genic status (LeBlanc et al., 2022). Our overall aim is to demonstrate the potential of DS as a robust *in vivo* mutagenicity test that could replace the TGR assay as the next "gold standard" in research and regulatory applications.

The objectives of this study are to: 1) use DS to study the dose-response of mutation induction by PRC in MutaMouse BM; 2) characterize regional variability in spontaneous and PRC-induced MF across the panel of 20 DS loci; 3) assess the concordance of DS with the *lacZ* TGR assay; 4) compare the mutation spectrum measured by DS to that measured by sequencing mutant *lacZ* plaques; and 5) explore optimal DS study designs for assessing mutagenicity by modeling sample size and sequencing data yield.

2.3 METHODS

2.3.1 Animal Exposure and Tissue Collection

All animal handling, exposures and tissue collection were approved by the Health Canada Ottawa Animal Care Committee and followed the Canadian Council on Animal Care guidelines. All MutaMouse animals used in this study were a random subset of those included in a previous TGR study investigating the effects of sampling time on mutant frequencies (Marchetti et al., 2021). Adult MutaMouse males, 8-10 weeks of age at the beginning of the exposure were exposed by oral gavage to 6.25, 12.5, or 25 mg/kg-bw/day PRC (CAS 366-70-1; Sigma-Aldrich, Oakville, ON Canada) or phosphate-buffered saline without calcium and magnesium (PBS; Corning cellgro, Manassas, VA, USA) as vehicle control (VC) for 28 consecutive days. Six mice for each treatment group, and three mice for VC were euthanized 42 days after the final dose. Three control mice sampled 70 days after the final dosing were added to achieve a matched control group of six animals. At euthanasia, BM was collected from the femurs, flash frozen, and stored at -80°C. BM was selected as the tissue to study because it is commonly used in regulatory mutagenicity testing and is a known target for PRC (Marchetti et al., 2021; Souliotis et al., 1994).

*2.3.2 Transgenic Rodent Gene Mutation Assay (*lacZ *assay)*

The *lacZ* TGR assay was performed as per the Organization for Economic Co-operation and Development (OECD) TG 488 (2022). Genomic DNA was isolated from one femur using phenol/chloroform extraction (Gingerich et al., 2014). The quantity and purity of DNA were assessed using a NanoDrop spectrophotometer (Thermo Scientific Canada, Ottawa, Canada). λgt10 phage vectors in genomic DNA were excised using commercial packaging extract kits (Agilent Technology, Santa Clara, CA, USA), according to the manufacturer's instructions. Transgene mutant frequency was determined using the phenyl β-d-galactopyranoside (P-gal)–positive selection assay (Lambert et al., 2005). A minimum number of 125,000 plaque-forming units (pfu) were counted per sample. Mutant frequency (phenotypically selectable mutants per *lacZ* locus) was expressed as the ratio of mutant plaques to total pfu.

2.3.3 DNA Extraction and Library Preparation for Duplex Sequencing

DNA from the second femur was extracted using the Qiagen DNeasy blood and tissue kit, as described in the Qiagen User Manual (Cat. # 69504, Qiagen, Hilden, Germany). DNA quality was assessed using an Agilent Tapestation to ensure a DNA Integrity Number greater than 7.0. DNA was prepared for sequencing as described previously (Valentine et al., 2020) by TwinStrand Biosciences (Seattle, WA, USA). Briefly, 500 ng of DNA was ultrasonically sheared to a mean fragment size of approximately 300 base pairs (bp). The DNA was then end-polished, A-tailed and ligated to DuplexSeq™ Adapters (TwinStrand Biosciences, Seattle WA, USA).

The DS Mouse Mutagenesis panel has one target on each autosome, except for chromosome 1 which has two targets. Nine of the targets are located within genic regions and 11 within intergenic regions (Supp. Table 2.1). DS targets were classified as genic or intergenic based on gene intersection information obtained from the gene database GENCODE, the Mouse gene set, version M25 (Frankish et al., 2019). The chosen targets are presumed to be selectively neutral, with none of the targeted regions having known roles in cancer either in mice or human orthologs. The panel was chosen for optimal performance in hybrid capture and contains no significant pseudogenes or repetitive elements that could potentially confound alignment or variant calling. Panel trinucleotide composition shows a strong correlation with that of the whole genome (mm10; Supp. Figure 2.1). Target chromatin status and %GC content were determined using the University of California Santa Cruz (UCSC) Mouse Genome Browser, reference genome mm10 (Kent et al., 2002). Descriptions of the 20 targets are provided in Supp. Table 2.1. The panel was captured using 120mer biotinylated oligo probes (Integrated DNA Technologies, Coalville, IA, USA).

Prepared libraries were sequenced on a NovaSeq 6000 (Illumina, San Diego CA, USA). An average of 400 million raw reads were sequenced per sample yielding an average of 16,000-fold coverage of the targeted loci. All samples met a targeted 500 million duplex bases and 10,000X sequencing depth. The sequencing FASTQ files used in the current study are made available in the Sequence Read Archives (SRA) BioProject ID PRJNA909196. Per-library FASTQ files were analyzed using the DS TwinStrand DuplexSeq Mutagenesis App v3.4.2 (TwinStrand Biosciences, Seattle WA, USA) as functionally described in Valentine et al. (2020). This App produced sequencing summary metrics, mutagenesis metrics including mutation frequency (MF) and base substitution spectra, and a variant call file (VCF) per library. Briefly, the DuplexSeq Mutagenesis App involves extracting unique molecular identifier (UMI) sequences,

correcting UMI sequences, raw read alignment, grouping reads by their UMI and strand defining element, quality trimming, error-correction of read groups by duplex consensus calling, consensus post-processing, re-alignment, and variant calling. Importantly, the DuplexSeq Mutagenesis App does not include variants with a variant allele fraction >0.01 in mutagenesis metrics because highly clonal variants were considered germline polymorphisms and unlikely to be somatic in origin. Post-processing handled outside the DuplexSeq Mutagenesis App, but at TwinStrand Biosciences, involved calculating mutation frequency per-target instead of just panel-wide.

Mutations that occurred more than once in a single sample were considered under two opposing assumptions: 1) all identical mutations represent the clonal expansion of a single mutational event; or 2) all identical mutations occurred as independent mutational events, possibly due to local genomic features that render it more susceptible to mutation. Making the former assumption and counting multi-read mutations as a single mutation in the MF calculation guards against over-estimating mutant frequency that could otherwise be artificially increased by clonal expansion. This calculation is the *minimum* mutation frequency (MF_{Min}) that could explain the data. Alternatively, counting all identical mutations independently guards against the possibility of undercounting true independent mutations. This calculation is the *maximum* mutation frequency (MF_{Max}) that could explain the observed data. Since it is rarely possible to be certain which of these two assumptions apply to any given mutation (and it could be a mixture of both), here, we consider both alternatives. It is also worth noting that clonal expansion of adverse mutations can lead to genetic disease and thus such events warrant consideration.

2.3.4 Mutation Data Interpretation and Statistical Analysis

First, mutation induction was measured as mutant frequencies (phenotypically scorable mutants per *lacZ* locus) for the TGR *lacZ* assay and as MF_{Min} or MF_{Max} (represented as mutations per bp) for DS using the entire mouse mutagenesis panel. Estimated frequencies by dose were obtained for both assays using generalized linear models (GLM) in the R software with the quasibinomial distribution. Pairwise comparisons were conducted using the doBy R library (Højsgaard & Halekoh, 2018) and these estimates were then back-transformed. Here, the delta method was employed to approximate the back-transformed standard errors (standard error of the mean; SEM) of the estimated MF. A Holm-Sidak correction was applied to adjust p-values for multiple comparisons for both MF_{Min} and MF_{Max}. Next, we estimated MFs for each 2.4 kb target using generalized linear mixed models (GLMM) with a binomial error distribution in the R software. Pairwise comparisons based on dose and location relative to genes

were conducted using the doBY R library as described above. The MF_{Min} and MF_{Max} response for each target was then compared individually against the TGR lacZ assay.

The mutation spectra data generated by DS was evaluated by considering first only the mutated base and then by extending the analyses to include the flanking bases. To determine which mutation substitution types differed between control and treated groups, a modified contingency table approach was used as described by (Piegorsch & Bailer, 1994). Pairwise comparisons as described above were used to determine which mutation types were significantly increased from VC. Subsequently, we generated a 96-trinucleotide mutation spectrum and used cosine similarity to determine the Catalogue of Somatic Mutations in Cancer (COSMIC) single base substitutions (SBS) signatures (Alexandrov et al., 2020) that most closely resembled the PRC mutation spectra, using the MutationalPatterns package in R (Manders et al., 2022).

2.3.5 Benchmark Dose Comparison of lacZ *and DS Results*

Benchmark dose (BMD) modeling was conducted using the PROAST web application (version 70.1, https://rivm.nl/en/proast) to mathematically model the PRC dose-response curves for both assays. The BMD estimated in our study represents a dose that produces a 50% increase (i.e., the benchmark response; BMR) in *lacZ* mutant frequency, MF_{Min} or MF_{Max}; this BMR was selected based on previous recommendations for genotoxicity assessment (White et al., 2020). The BMD is a measure of the potency of a chemical, with a lower BMD indicating a more potent mutagen. To estimate the BMD, different mathematical models (Hill, exponential, reverse exponential, and lognormal) were applied to fit the dose-response data. The Akaike Information Criterion was used to select the model with the best fit. 95% confidence intervals based on model averaging were generated from 200 bootstrap runs and were used to statistically evaluate the differences between BMDs derived with DS versus the *lacZ* assay, and across genomic loci.

2.3.6 Power Analysis on DS Study Design

We performed a power analysis to determine the minimum sample size and total number of duplex base pairs needed to observe a significant increase in MF using DS. First, we used a binomial distribution to randomly generate control samples based on parameters from our experiment. Hypothetical mutation counts were generated based on the observed average MF_{Min} from our VC group (1.31×10^{-7} mutations per bp) and the average total number of bases sequenced per animal (depth; 7.98

x 10^8 bp). Over-dispersion was incorporated assuming a normal distribution with mean zero and standard deviation taken from the sample variance. A sample variance of 0.062 was estimated from the standard-deviation obtained from the GLMM used for per target dose-response analysis. We randomly generated a treatment group using the experimental parameters and a selected fold-increase. Next, we used a GLM to calculate the significance of the fold-change in MF between control and treated samples, as described above, and calculated the power of that analysis under the set conditions. Finally, the bisection method was used to estimate the minimum detectable effect size (MDES) of the simulated experiment yielding a power of 80% and a $p < 0.05$. We varied the sample size to calculate the power and MDES of the various conditions. Finally, we investigated the effect of sample variance and total duplex bases on our power results. We increased sample variance from 0.06 to 0.1 to roughly double our observed value and varied the total number of duplex bases. We then calculated the total number of duplex bases required to detect a 1.5-fold increase in MF with 80% power under each of the various simulated conditions.

2.4 RESULTS

2.4.1 lacZ *Mutant Frequency*

LacZ assay mutant frequency was measured by dividing the number of identified mutant plaques by the total number of plaques counted. On average, 14, 21, 51, and 100 mutants were counted for VC, 6.25, 12.5, and 25 mg/kg-bw/day PRC, respectively (Supp. Figure 2.2). PRC induced a significant increase in mutant frequency (x 10^{-5}) relative to VC in the middle and high dose groups from 7.33 ± 1.76 mutations per *lacZ* locus (± SEM) in the VC to 24.9 ± 3.07 and 46.7 ± 4.14 at the middle and high PRC doses, respectively. No statistically significant increase was observed at the low PRC dose (Table 2.1). There was substantial inter-individual variation within the *lacZ* data, as indicated by the large SEM for the average mutant frequency of each dose group. These results are highly comparable to those reported by Marchetti et al. (2021) for the same animals.

Table 2.1. Mean mutant frequency estimates and corresponding pairwise comparisons between dose groups for the *lacZ* assay obtained using a GLM.

Dose (mg/kg-bw/day)	Mutant frequency ± SEM (x 10^{-5})	Fold Changes (± SEM)	p-value*
0	7.3 ± 1.76	--	
6.25	12.7 ± 2.48	1.74 ± 0.54	8.84×10^{-2}
12.5	24.9 ± 3.07	3.39 ± 0.91	**4.05×10^{-4}**
25	46.7 ± 4.14	6.37 ± 1.63	**1.54×10^{-6}**

*Bold font indicates p-value < 0.05

2.4.2 DS Mutation Frequency

DS reads were distributed relatively evenly across the 20 targets in the 24 samples (Supp. Figure 2.3). Sequencing yielded an average of approximately 800 million duplex base pairs per sample for a total of about 20 billion duplex bases across the cohort. All samples met a minimum target of 500 million duplex bases per sample.

MF was calculated by dividing the number of identified mutants by the total number of bases sequenced per sample. Mutations include single nucleotide variants (SNVs), insertions and deletions (indels), and multi-nucleotide variants (MNVs). Under the conservative MF_{Min} assumption, 104, 136, 157, and 256 unique mutations on average were identified in mice treated with VC, 6.25, 12.5, and 25 mg/kg-bw/day PRC, respectively, with minimal inter-individual variability within each dose group (Figure 2.1, Supp. Table 2.2). Within the VC, there was no significant difference in $MF_{Min,}$ nor in the proportion of mutation subtypes, between animals sampled after 42 days and animals sampled after 70 days. PRC induced a significant dose-dependent increase in MF_{Min} relative to VC in all PRC dose groups, from $1.31 \times 10^{-7} \pm 7.47 \times 10^{-9}$ mutations per bp in the control to $3.22 \times 10^{-7} \pm 11.7 \times 10^{-9}$ in the high dose group. A 1.3-, 1.6-, and a 2.5- fold increase in MF_{Min} relative to VC was induced in 6.25, 12.5, and 25 mg/kg-bw/day dose groups, respectively (Table 2.2).

Table 2.2. Mean mutation frequency (MF_{Min}) estimates and corresponding pairwise comparisons between dose groups for DS obtained using a GLM.

Dose (mg/kg-bw/day)	MF ± SEM (x 10^{-7})	Fold Change from VC (± SEM)	p. value*
0	1.31 ± 0.07	--	--
6.25	1.65 ± 0.08	1.26 ± 0.10	**6.03×10^{-3}**
12.5	2.03 ± 0.09	1.55 ± 0.11	**1.65×10^{-5}**
25	3.22 ± 0.12	2.46 ± 0.16	**6.57×10^{-11}**

*Bold font indicates p-value < 0.05

To assess the impact of counting all mutations independently, we performed the same analyses using the MF_{Max} assumption. We identified an additional 50, 198, 351, and 770 mutations for VC, 6.25, 12.5, and 25 mg/kg-bw/day PRC, respectively. PRC induced a significant dose-dependent increase in MF_{Max} (Table 2.3, $p < 0.01$) in all groups relative to VC from $1.41 \times 10^{-7} \pm 8.38 \times 10^{-9}$ mutations per bp (± SEM) in the control to $4.82 \times 10^{-7} \pm 15.5 \times 10^{-9}$ in the high dose group (Figure 2.1). A 1.5-, 2.0-, and a 3.4-fold increase in MF_{Max} relative to VC was induced in 6.25, 12.5, and 25 mg/kg-bw/day PRC dose groups, respectively. The MF_{Max} for the middle and high dose groups were significantly higher than to the MF_{Min} for those dose groups ($p < 0.01$). Inter-individual variability did not meaningfully differ between the MF_{Min} and MF_{Max} assumptions.

Table 2.3. Mean mutation frequency (MF_{Max}) estimates and corresponding pairwise comparisons between dose groups for DS obtained using a GLM.

Dose (mg/kg-bw/day)	MF ± SEM (x 10^{-7})	Fold Change from VC (± SEM)	p-value*
0	1.41 ± 0.08	--	--
6.25	2.05 ± 0.10	1.45 ± 0.11	**9.51×10^{-5}**
12.5	2.78 ± 0.12	1.97 ±0.14	**1.16×10^{-8}**
25	4.82 ± 0.16	3.42 ± 0.23	**6.48×10^{-14}**

*bold font indicates p-value < 0.05

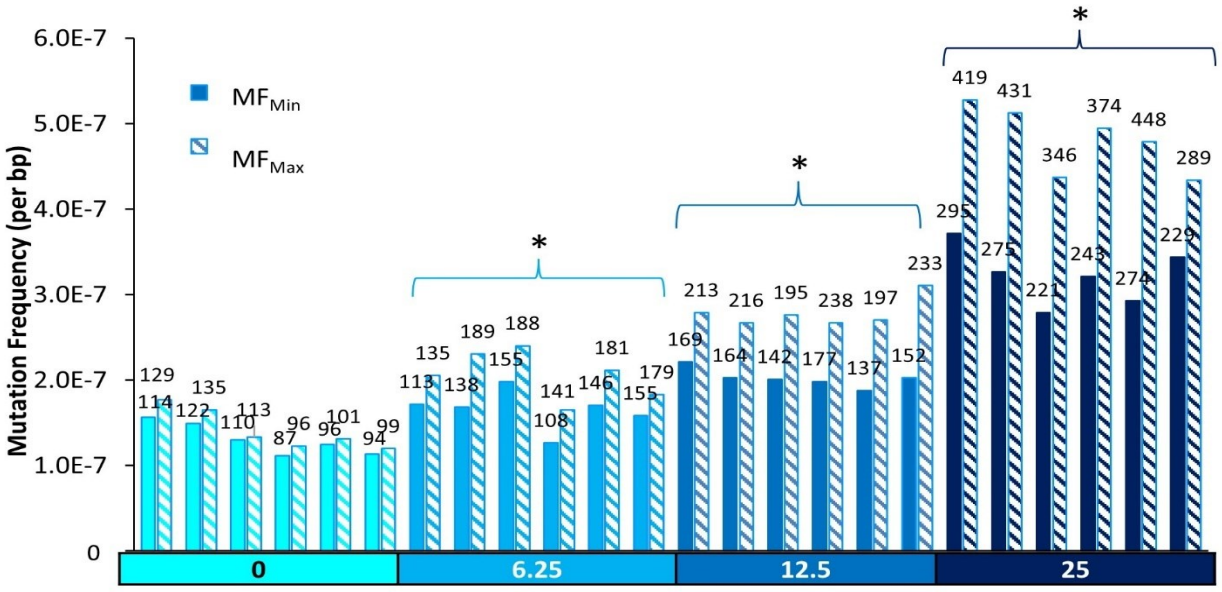

Figure 2.1. Duplex Sequencing mutation frequencies (MF) in the bone marrow of MutaMouse males at various doses of PRC. Bars represent the MF (mutations per bp) for each animal using MF_{Min} or MF_{Max}. Data labels indicate total mutation count per animal. X-axis indicates PRC dose group (mg/kg-bw/day). Asterisks indicate a significant difference ($p < 0.05$ relative to the control in the average MF across animals).

2.4.3 DS Mutation Frequency by Target

Next, we analyzed mutation induction across the 20 genomic targets using the MF_{Min} assumption. The background MF_{Min} differed by 2.8-fold across the targets, with the highest MF_{Min} observed for the second target on chromosome 1 (chr1.2: 2.41 x 10^{-7}) and the lowest MF_{Min} on chromosome 10 (0.858 x 10^{-7}). When ranking the MF across targets within the VC, we observe that the highest and lowest responding targets are similar to those in a previous study (LeBlanc et al., 2022). This reproducibility indicates a robust number of mutations within the control group. PRC induced a significant increase in MF_{Min} relative to VC in 14 of the 20 targets at the high PRC dose (Figure 2.2). At the middle PRC dose, only the target on chromosome 17 had a significant increase in MF_{Min}. No target had a significant increase in MF_{Min} compared to VC at the low dose. We observed a maximum 2.5-fold difference between the target with the highest MF_{Min} at the high PRC dose (chromosome 17; 5.21 x 10^{-7}) and the target with the lowest MF_{Min} at the high dose (chromosome 13; 2.13 x 10^{-7}). Similarly, we observed a 2.7- and 2.6- fold change between the targets with the highest and lowest MF_{Min} for the middle and low PRC doses, respectively. The targets with the highest MF_{Min} were on chromosome 17 for the high and middle PRC doses, and on the second target on chromosome 1 (i.e., chr1.2) for the VC and

low PRC dose. Three of the five targets with the lowest background MF_{Min}, those on chromosomes 3, 5 and 13, were also among the five targets with the lowest MF_{Min} at the high PRC dose, suggesting these targets may be less sensitive to mutation induction. Finally, responsiveness to PRC varied between targets. The fold-increase from VC at the high dose group for chr17 was 3x higher than the target with the lowest fold-increase, chr1.2 (Figure 2.3). Thus, susceptibility to mutation induction varies by genomic locus.

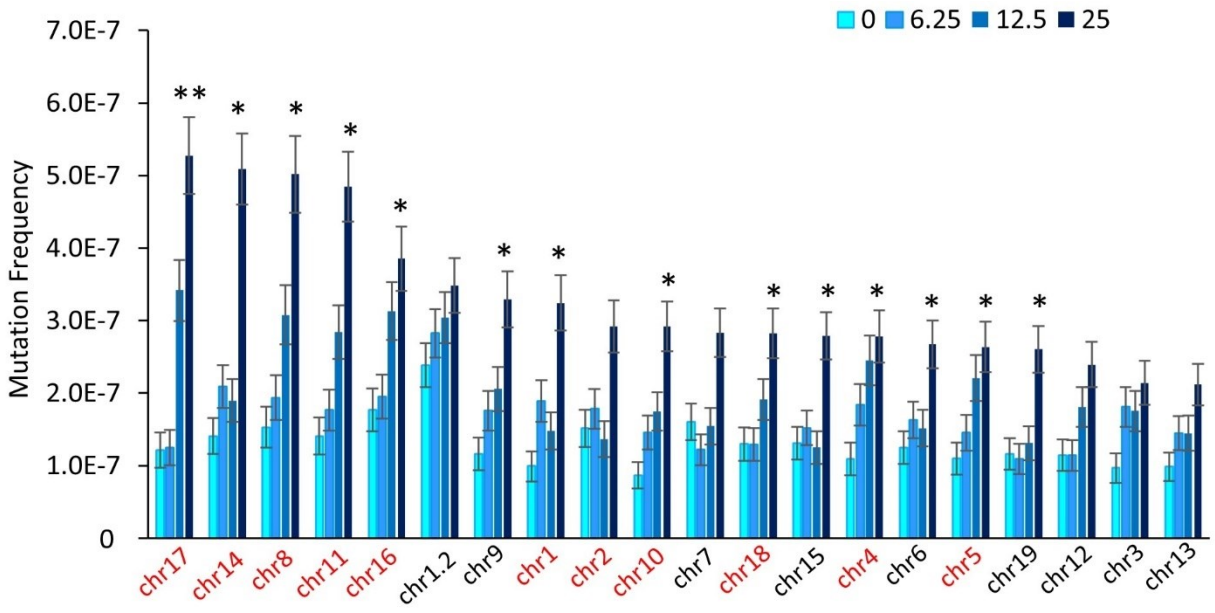

Figure 2.2. Spontaneous and PRC-induced MF by Duplex Sequencing target ordered from highest MF_{Min} in the high PRC dose group to the lowest. Data are mean MF ± SEM mutations per bp, for each target (n = 6), separated by dose (mg/kg-bw/day). Intergenic targets are labelled in red and genic targets are in black. Asterisks indicate a significant increase in the high PRC dose relative to the controls. The double asterisk indicates a significant increase in the high and middle PRC doses relative to controls. (Generalized linear mixed model, $p < 0.05$).

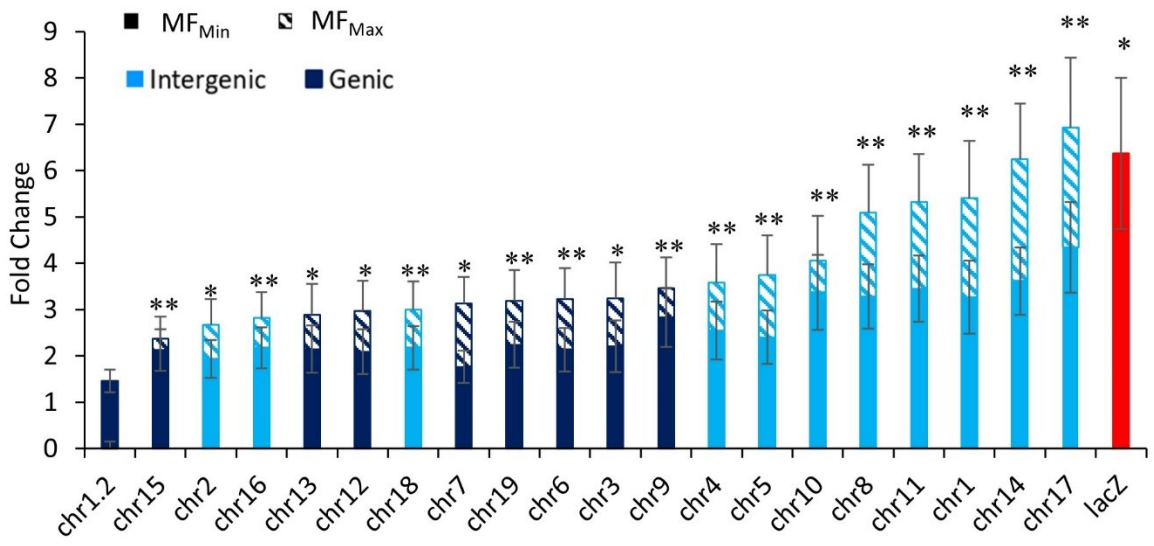

Figure 2.3. Fold change in MF between PRC high-dose group and VC for the 20 Duplex Sequencing targets as well as for the *lacZ* gene (red bar). Estimated using a general linear mixed model. DS targets are listed along the X-axis. Errors bars are SEM. Asterisks indicate the fold change was a significant increase in MF from VC for MF_{Max}. Double asterisks indicate significance for both MF_{Max} and MF_{Min}. The targets chr17, chr14, chr1, chr11, chr8, and chr10 were within range of the lacZ fold change.

We observed that genomic targets in intergenic regions tended to have a higher susceptibility to PRC than targets in genic regions, which, if expressed, can be subjected to transcription-coupled repair (TCR). The five targets with the highest MF_{Min} at the high PRC dose were all located in intergenic regions, while 4/5 targets with the lowest MF_{Min} were genic (Figure 2.2). Overall, a combined analysis of intergenic targets showed a significantly higher mean MF_{Min} than the combined genic targets in the middle and high PRC dose groups by 1.3 and 1.4-fold respectively ($p < 0.001$) (Supp. Figure 2.4). These results did not change when using MF_{Max}. Furthermore, intergenic targets showed a significant increase in MF_{Min} and MF_{Max} at all PRC doses compared to the VC, whereas the genic targets showed a significant increase only at the high dose for MF_{Min} and the middle and high dose for MF_{Max}. Conversely, the mean background MF_{Min} observed in intergenic targets (1.26×10^{-7}) was not significantly different from the mean background MF_{Min} in genic targets (1.28×10^{-7}). These results were not changed when using MF_{Max}.

2.4.4 DS and TGR concordance

To assess DS concordance with the TGR assay, we compared the DS MF_{Min} to the *lacZ* mutant frequency in the same samples. There was a significant positive correlation between the induced DS

MF_{Min} and *lacZ* mutant frequencies (Figure 2.4; Pearson's correlation; r = 0.85, p = 6.19 x 10^{-7}), with *lacZ* displaying more inter-individual variability. The correlation increased further when we used MF_{Max} (Pearson's correlation; r = 0.87, p = 2.88 x 10^{-8}), although the magnitude of the response to PRC was still higher in the *lacZ* assay (Table 2.1, Table 2.2, Table 2.3). The *lacZ* fold changes relative to control for each dose group were greater by an average of 2-fold than DS MF_{Min} and 1.5-fold compared with DS MF_{Max}.

We then assessed the concordance of MF of individual DS targets with the *lacZ* assay for the two PRC doses that significantly increased *lacZ* mutations. The fold-change in MF between VC and the PRC dose groups was estimated for each target, using either the MF_{Min} or MF_{Max} DS data (Figure 2.3). Using MF_{Min}, the target on chromosome 17 (4.34 ± 0.98-fold-increase) was the only one within range of the fold-change observed using the *lacZ* assay (6.37 ± 1.63). Conversely, using MF_{Max}, we observed six targets whose fold-increase in MF falls within the *lacZ* assay range, namely the targets on chromosome 17, 14, 1, 11, 8, and 10. These six targets were all intergenic. Similar trends were observed at the middle PRC dose, where four and 10 targets were within range of the *lacZ* fold-change (3.39 ± 0.91) when MF_{Min} and MF_{Max} values were used, respectively. Of these, all targets except for the one on chromosome 3 were intergenic (Supp. Figure 2.5). Thus, the data show intergenic targets generated fold changes in MF that more closely approximated *lacZ* assay results than genic targets.

Finally, we examined DS and *lacZ* concordance using BMD modelling to identify the dose at which a 50% increase in MF occurred above background. The BMD for the *lacZ* assay was 3.7 mg/kg-bw/day (95% CI of 1.6-6.6 mg/kg-bw/day), which was significantly lower than the BMD of 11.1 mg/kg-bw/day (95% CI of 8.7-13.8 mg/kg-bw/day) obtained using DS MF_{Min} (Figure 2.5A). However, using MF_{Max} produced a BMD of 8.4 mg/kg-bw/day (95% CI of 6.5-10.4 mg/kg-bw/day), which overlaps with the CI of the *lacZ* assay. Thus, quantitative concordance of DS with the *lacZ* assay improves when MF_{Max} are used. We also produced BMDs for each of the 20 DS targets individually calculated as MF_{Max} (Figure 2.5B) and compared these to the *lacZ* BMD. Every target had CIs that overlapped with the *lacZ* CI, except for targets on chromosomes 7, 15, and 19, which were significantly higher. Chr 1.2 failed to produce a BMD due to its weak dose-response and high mutation background frequency. Overall, BMD concordance between the assays improved when MF_{Max} was used.

A

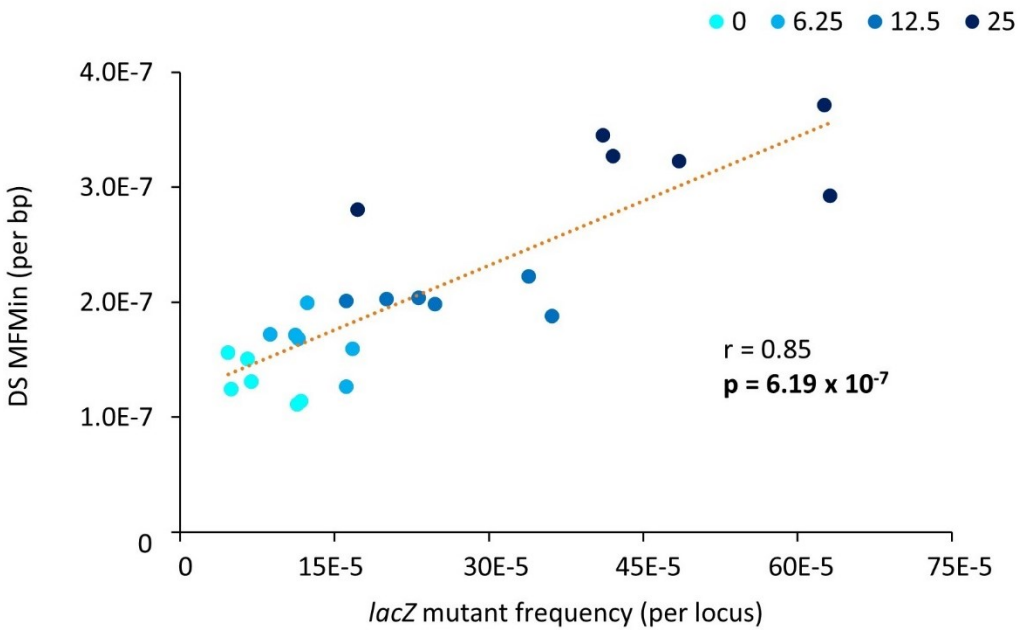

B

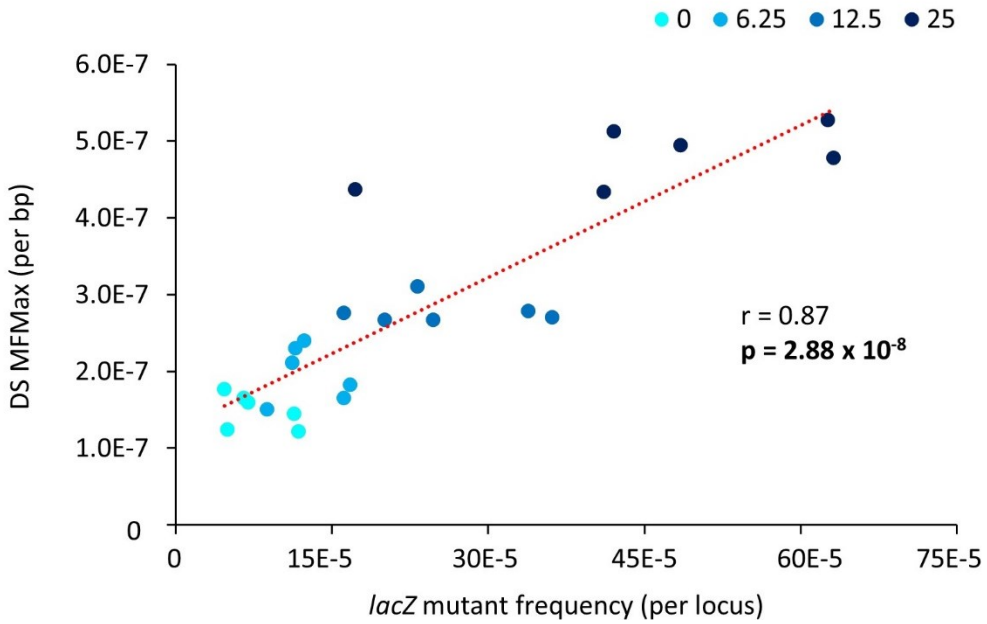

Figure 2.4. **Pearson's correlation analysis between *lacZ* mutant frequency and Duplex Sequencing** using MF_{Min} (**A**) or MF_{Max} (**B**) for MutaMouse males exposed to different doses (different shades of blue) of PRC (in mg/kg-bw/day). Data are presented as the individual MFs for each animal.

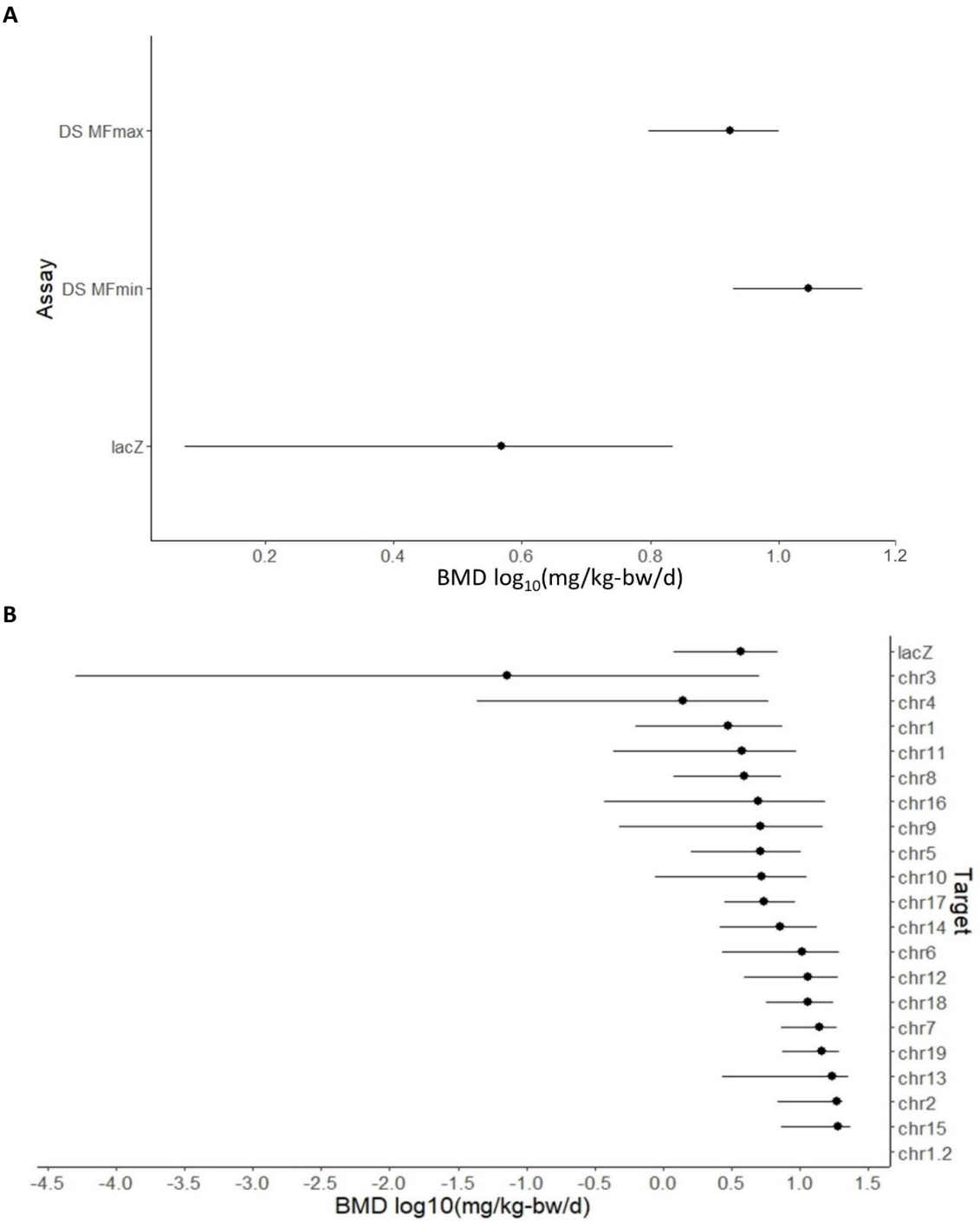

Figure 2.5. 95% confidence intervals (CI) based on BMD model averaging analyses. (**A**) $\log_{10}$ BMD for a 50% increase of *lacZ* mutant frequency and the Duplex Sequencing MF, using either MF_{Min} or MF_{Max}. (**B**) $\log_{10}$ BMD of *lacZ* mutant frequency and Duplex Sequencing MF_{Max} for each genomic target. DS targets are organized from smallest BMD to highest. Target chr1.2 failed to produce a BMD due to poor dose response.

2.4.5 Mutation Spectrum

Both the spontaneous and PRC-induced mutation spectra (MF_{Min}) consisted primarily of SNVs, followed by small deletions, then MNVs, and lastly, small insertions (Figure 2.6). Pairwise comparison of DS mutation data revealed that the overall mutation spectra were significantly different from each other at all PRC doses (modified contingency table; $p < 0.05$). PRC primarily induced T:A>C:G and C:G>T:A transitions accounting for 29% and 28% of total mutations at the high dose, followed by T:A>A:T transversions (13%) and T:A>G:C transversions (4%). This differed from the background mutation spectrum, which consisted primarily of C:G>G:C transversions (33%), C:G>A:T transversions (33%), and C:G>T:A transitions (17%). We observed significant dose-dependent increases in T:A>C:G transitions in all three dose groups compared with VC; T:A>A:T transversions were significantly increased at the middle and high PRC dose compared with VC; and T:A>G:C transversions and C:G>T:A transitions were increased at the high dose only (Figure 2.6).

We further analyzed the sequence context of induced mutations by considering the flanking base on either side of the mutated base to produce trinucleotide spectra and examine mutational signatures (Alexandrov et al., 2013). This revealed a clear enrichment in T:A>C:T transitions and T:A>A:T transversions, together with a shift from mutations at CpG sites to non CpG sites for C:G>T:A transitions (Supp. Figure 2.6). We compared our trinucleotide frequencies to SBS signatures of the COSMIC Mutational Signatures database (mm10, version 3.3) using cosine similarity. We observed a dose-dependent increase in cosine similarity to several cancer signatures. The signature that displayed the greatest difference between its similarity to the control spectrum and its similarity to the high PRC spectrum was SBS 21, followed by SBS 26, and SBS 12 (Supp. Figure 2.7).

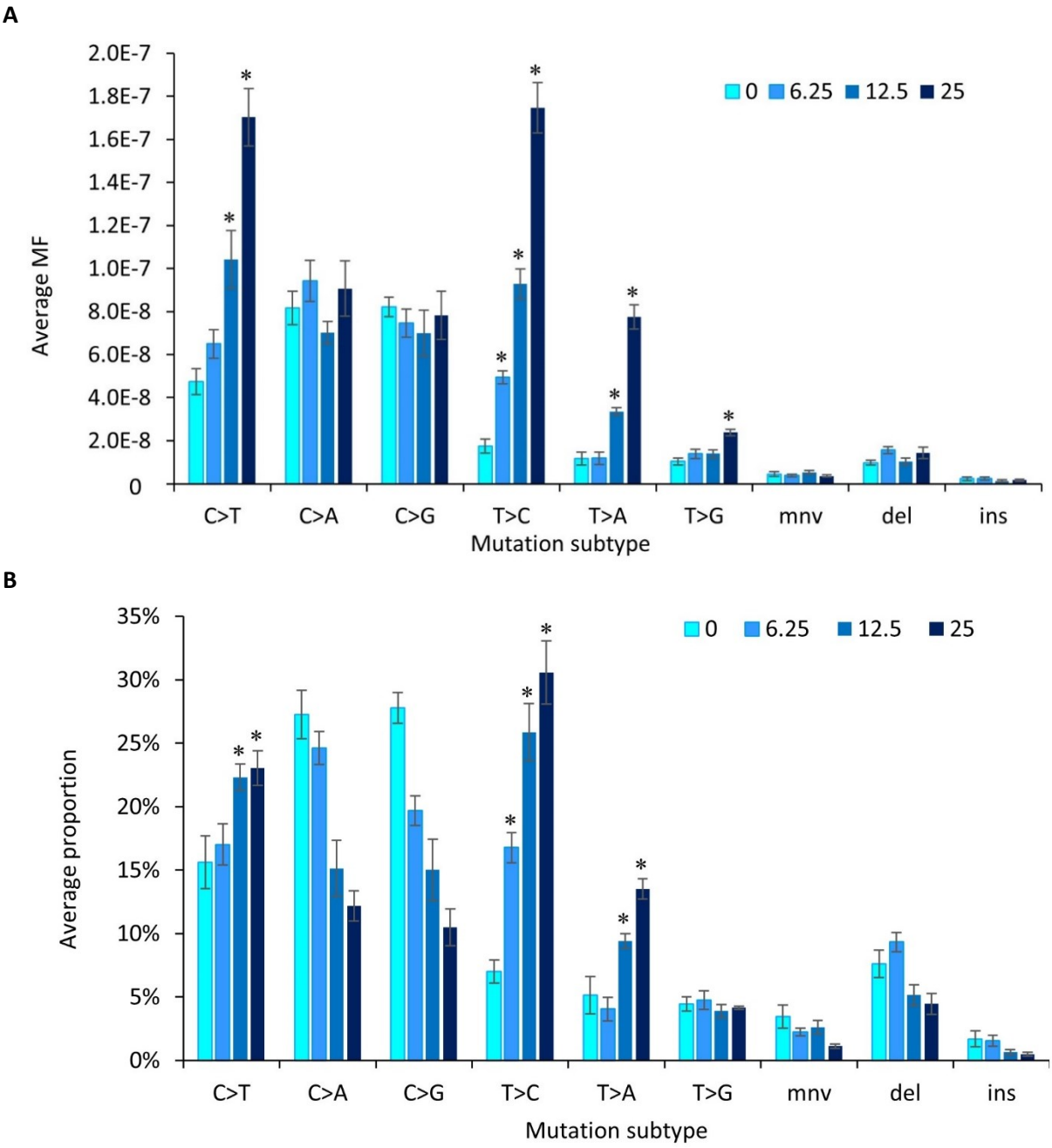

Figure 2.6. **Mutation spectrum of controls and PRC dose groups (mg/kg-bw/d) measured by Duplex Sequencing in the bone marrow of MutaMouse males.** (**A**) Mutation subtypes are presented as the average MF ± SEM. (**B**) Mutation subtypes are represented by the proportion of total mutations. Values are mean ± SEM. Plots represent MF_{Min}. Mutation subtypes include the six single nucleotide variants using a pyrimidine reference, multi-nucleotide variants (mnv), small insertion (ins), and small deletion (del) mutations. Asterisks indicate a significant increase in MF from controls.

2.4.6 Power Analysis for Sample Size and Total Duplex Basepairs

We performed a power analysis on datasets simulated from the observed conditions of our DS experiment. Using our true sample size of six animals per dose, we had >95% power to detect a 1.5-fold increase in MF_{Min} (Table 2.4). Reducing the number to three animals per dose group retained 92% power. The MDES that could be achieved after reducing the sample size to three animals was a 1.4-fold increase in MF from background (Table 2.4). This is higher than the 1.26-fold increase in MF_{Min} that was observed for the lowest PRC dose, but is lower than the 1.55-fold and 2.46-fold increase observed at the middle and high PRC doses. Thus, under the observed conditions of our experiment, a reduction in sample size to three animals per group would result in sufficient power to classify PRC as mutagenic and detect the changes we observed at the middle (95% power) and high (>95% power) PRC dose but would be under-powered to detect the smaller increase observed at the low PRC dose (49% power). The use of MF_{Max} did not alter the results of the power analysis (data not shown). Finally, we assessed whether these results were robust to simulated increases in sample variance. We performed the same analyses as above but with twice the observed sample variance (0.1). We observed an 81% power to detect a 1.5-fold increase in MF_{Min} above background with a sample size of three and the increased sample variance.

Table 2.4. Power analysis for Duplex Sequencing dose-response studies.

	Experimental conditions		**Simulated condition**			
	MF_{Min}		**MF_{Max}**		**Increased Variance**	
Background MF	1.31×10^{-7}		1.41×10^{-7}		1.31×10^{-7}	
Total DS base pairs	7.98×10^{8}		7.98×10^{8}		7.98×10^{8}	
Sample Variance	0.062		0.063		0.10	
Sample Size	**Power (%) 1.5-FC[a]**	**MDES[b]**	**Power (%) 1.5-FC[a]**	**MDES[b]**	**Power (%) 1.5-FC[a]**	**MDES[b]**
6	100	1.23	100	1.22	100	1.27
5	100	1.25	100	1.25	98	1.31
4	100	1.30	99	1.29	95	1.38
3	92	1.40	91	1.38	81	1.51

[a] Power (%) to detect a 1.5-fold-change of MF
[b] MDES: minimum detectable effect size with 80% power

Next, we investigated the number of total duplex bases required for analysis (Figure 2.7). When using a sample size of three animals, and our observed sample variance (0.062), a minimum of 500 million DS bases per animal is required to achieve sufficient power (81%) to detect a 1.5-fold increase in MF_{Min}. However, this reduction in data yield causes analyses to become more susceptible to increases in sample variance. When the sample variance is 0.1, and the sample size is three animals, the power to detect a 1.5-fold increase in MF_{Min} is reduced to 71% and a minimum data yield of ~800 million duplex bases is required to achieve sufficient power. Increasing the number of animals per group to four, with a minimum of 300 million duplex bases, would be sufficient to detect a 50% increase in MF_{Min} for datasets with a sample variance of 0.1 (78.2% power).

A

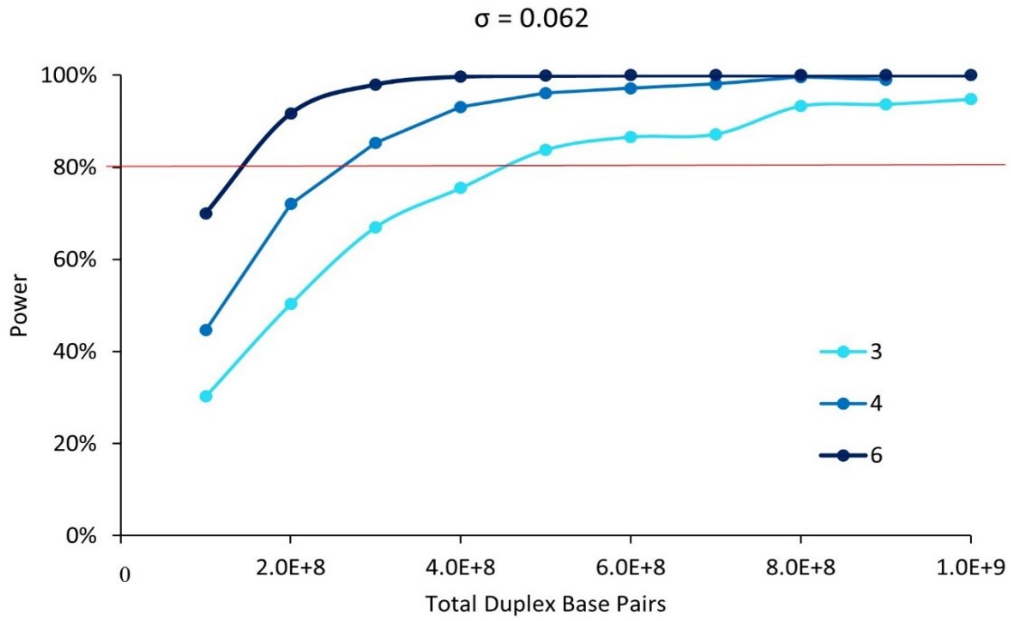

B

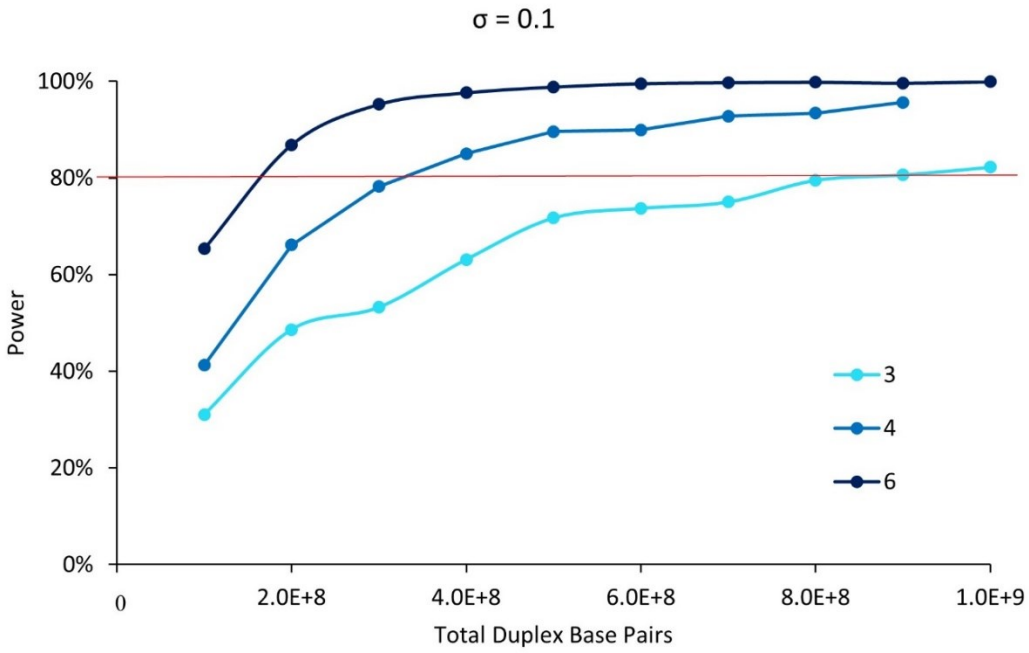

Figure 2.7. The power to detect a 50% increase in MF by Total Duplex Base Pairs. Results are displayed for a sample size of 6 animals per group (dark blue), 4 animals per group (blue) and 3 animals per group (light blue). (**A**) Sample variance of 0.062 (based on current study). (**B**) Sample variance of 0.1. Red line indicates the threshold for > 80% power and $p < 0.05$.

2.5 DISCUSSION

We applied DS to study spontaneous and PRC-induced mutations in the BM of MutaMouse males across a panel of diverse genomic targets and compared the results with those obtained with the OECD TGR assay on the same samples. Low intra-group variability within DS samples resulted in statistically significant increases at all PCR doses, whereas the *lacZ* assay failed to detect a significant increase at the low dose. The *lacZ* assay initially showed a stronger fold-response to PRC than DS based on MF_{Min}; however, when using MF_{Max}, several DS targets had fold-increases consistent with the *lacZ* assay. DS revealed a PRC mutation spectrum that was distinct from the background spectrum, with PRC primarily inducing T:A>C:G transitions, followed by C:G>T:A transitions, and T:A>A:T transversions. Finally, power analyses suggested that reducing the sample size to three animals per dose group and per-sample data yield of 500 million bases retains sufficient power to detect a 1.5-fold increase in MF in our model. Thus, fewer animals per dose-group can be used with respect to the TGR models without losing power to detect an effect. Overall, our study provides strong evidence to support the use of DS in place of the plaque-based TGR assay for qualitative and quantitative chemical mutagenicity assessment with greater sensitivity, richer data and fewer animals.

2.5.1 DS Loci Show Patterns of Mutation Sensitivity Consistent with TCR

There are many genomic and epigenomic features that have been linked to susceptibility to mutation induction including transcription (Monroe et al., 2022; Xia et al., 2020), sequence context (Hodgkinson & Eyre-Walker, 2011), and chromatin state (Hodgkinson et al., 2012; Makova & Hardison, 2015). The use of the Mouse Mutagenesis panel allowed us to observe differences in spontaneous and PRC-induced MF among the 20 targets. Specifically, we found that DS target loci in intergenic regions had a higher response to PRC mutagenesis than loci in genic regions, which is consistent with the protective effect of TCR. Transcribed regions of the genome are subject to increased rates of nucleotide excision repair (Nadkarni et al., 2016) that may contribute to the decreased MF in genic targets. Similar results were observed following BaP exposure in MutaMouse BM (LeBlanc et al., 2022). Remarkably, there was also a consistent pattern of relative sensitivity to mutation induction across targets between the two studies. In fact, the five targets with the highest MF_{Min} at the high PRC dose (chromosome 17, 14, 11, 8, and 16; all intergenic) were the same five targets with the highest MF_{Min} at the high BaP dose. These chemicals have different modes of action, which implies that there is an inherent feature of these loci that

renders them more susceptible to mutagenesis than the others. Our results provide further support for the role of TCR in the variation of mutation among loci.

2.5.2 Clonal Mutations and Target Responsiveness Underlie Discrepancy Between DS and lacZ

One of the main objectives of this study was to assess the concordance of DS with the gold standard TGR assay for *in vivo* mutagenesis testing. Initial analyses comparing the results of the *lacZ* assay with those of DS using MF_{Min} showed a significant positive correlation, but lower fold-increases in MF and a higher BMD for DS compared to *lacZ*. Similarly, an attenuated DS response compared to the Big Blue® plaque-based assay was observed in mouse BM analyzed 3 days following exposure to BaP (Valentine et al., 2020). These authors suggested that the difference might be attributed to unrepaired DNA adducts that were fixed into mutations during the *in vitro* portion of the TGR assay (i.e., *ex vivo* mutations). However, in this study, we had a 42-day waiting period between the last daily exposure and tissue collection. It is highly unlikely that DNA adducts could remain for such an extended period. A similar study using BaP also found the same difference following a 28-day sampling time (LeBlanc et al., 2022). Thus, *ex vivo* mutations are unlikely to contribute to the observed difference between DS and TGR assay. It is possible that applying the MF_{Min} approach to the DS data is too conservative and contributes to the observed difference between the two assay results.

The higher response measured by the *lacZ* assay may be the result of inherent differences between the two assays in how they quantify mutations. The *lacZ* assay scores mutants based on positive selection of plaques carrying mutant *lacZ* genes; thus, it cannot identify synonymous mutations, which do not alter the function of the *lacZ* gene, nor can it discount clonal expansion events unless paired with NGS sequencing. DS, on the other hand, identifies all types of mutations without bias and can easily filter out clonally expanded mutations using the MF_{Min} approach. A single mutation may produce large mutant frequencies following clonal expansion of the mutated cell (Heddle, 1999). Due to the long interval between treatment and sampling time in our experiment, it is possible for the highly proliferative BM to accumulate small clonal populations of mutated cells. Indeed, we found that clonal mutations increased with PRC dose. When we included clonally expanded mutations in our calculations (using the MF_{Max} assumption), we observed that the concordance between DS and the *lacZ* assay improved significantly. DS fold-changes in several endogenous target loci became equivalent to fold changes observed with the *lacZ* gene. Furthermore, BMD confidence intervals generated using MF_{Max} overlapped with those for the *lacZ* BMD. Thus, it is possible that some of the discrepancies between DS

and *lacZ* can be attributed to the exclusion of clonally expanded mutations when analyzing DS data. Whether clonal mutations should be included in the DS mutation counts (MF_{Max}) or corrected for (MF_{Min}) will require consideration of the context with which the assay is performed and should be a subject of further investigation by the expert community.

Differences in the responsiveness of the *lacZ* and DS assays to PRC may also be the result of assessing different genomic loci with differing sensitivities. Several studies have shown that exogeneous bacterial genes, such as the *lacZ* gene, tend to have higher mutant frequencies than endogenous genes. Previous work using Big Blue® mouse splenic tissue demonstrate that the *lacI* transgene exhibits higher spontaneous (Skopek et al., 1995) and BaP-induced (Skopek et al., 1996) mutant frequencies than the endogenous *Hprt* gene. Similarly, Valentine et al. (2020) found that the *cII* transgene has an elevated response to BaP mutagenesis compared to two expressed endogenous genes (*Ctnnb1, Polr1c*) using DS. We posit that the main reason for the seemingly attenuated response of DS compared to the *lacZ* assay is the result of the biologically higher susceptibility of the *lacZ* transgene to mutagenesis relative to many of the endogenous DS loci. The *lacZ* gene may exhibit increased susceptibility to mutation induction because it is a non-transcribed transgene, thus unprotected by TCR. Of the DS loci that had fold-increases in MF_{Max} rivalling that of the *lacZ* transgene, most were in intergenic regions. Future use of DS to directly sequence the *lacZ* gene would aid us in understanding how the differences between the two assays influence MF.

2.5.3 DS Identifies Induction of Mutation Subtypes Not Feasible with TGR

A major benefit of DS is its ability to generate high-quality mutation spectra alongside its measurement of MF. Here, we showed that PRC induces mainly T:A>C:G, C:G>T:A, and T:A>A:T mutations. This is consistent with the known PRC mode of action as a monofunctional SN_1-methylating agent (Fong et al., 1990; Fu et al., 2012; Gerson et al., 2018). The main mutagenic lesions produced by PRC include O_4 and O_2 – methylthymine leading to T:A>C:G and T:A>A:T mutations, respectively (Jenkins et al., 2005), and O_6-methylguanine–a highly mutagenic adduct that results in C:G>T:A transitions (Fu et al., 2012). Previous work on the *lacZ* and *Pig-A* loci did not show significant increases in the proportions of C:G>T:A mutations following PRC exposure (Beal et al., 2020; Pletsa et al., 1997; Revollo et al., 2017). We believe our study is the first to report a significant increase in these mutations. This was likely possible because of the substantially larger amount of spectral data generated by DS than what was produced using laborious manual clone picking and sequencing with the other approaches. Studies

relying on TGR approaches characterized PRC mutation spectrum from only 20-120 mutations. In contrast, our study utilized a total of 3926 mutations, substantially improving the robustness of our analyses. Furthermore, spontaneous C:G>T:A mutations are extremely common at CpG sites as a result of spontaneous deamination of methylated cytosine to form thymine. We observed a dose-dependent proportional reduction in these mutations occurring at CpG sites, alongside an increase in the context of non-CpG cytosine bases, consistent with the formation of O_6-methylguanine adducts by PRC. Previous studies with low mutation counts likely were underpowered to observe a significant increase in C:G>T:A mutations due to their abundance in the VC group. As a mutagenicity test, DS enables the detection of lower frequency changes in specific mutation types to facilitate the discovery of potential secondary mutagenic mechanisms or less prominent DNA lesions induced by the mutagen that would not be observed using traditional assays.

The trinucleotide mutation spectrum generated by DS following PRC exposure was linked to several COSMIC mutational signatures. The PRC mutation spectrum was most similar to SBS 21 and 26, which are both associated with defects in mismatch repair. Interestingly, the mutation spectra of similar acting alkylating agents (N-methyl-N-nitrosourea and N-ethyl-N-nitrosourea) within human pluripotent stem cells (Kucab et al., 2019) also showed high similarity with SBS 26 and SBS 12, suggesting that these SBS may be signatures of alkylation-induced chemicals. Additionally, we observed similarity with SBS 25, a signature observed in several Hodgkin's cell line samples where the patients were treated with chemotherapy (Alexandrov et al., 2020). PRC was historically used to treat Hodgkin's lymphoma; thus, it is possible this cancer signature is related to the exposure of these patients to PRC, or the similar acting methylating agent dacarbazine now used more commonly. These results support the utility of DS mutational signature analyses derived from mutagen-exposed rodents in identifying exposure-associated cancers in humans.

2.5.4 DS Study Design Accommodates Reducing Animal Use and the Cost of Sequencing

The analyses of Piegorsch et al. (1995) revealed that the main source of statistical variability observed in a TGR assay was significant variation between animals within a treatment group. These analyses provided the basis for the number of animals and plaques necessary to define a negative result with acceptable power (80%) for the TGR assay. OECD TG 488 requires a minimum of 5 animals per dose group for *in vivo* mutagenicity testing. In the current study, DS displayed much lower inter-animal variation than is typically observed using the *lacZ* assay. We note that the low sample-to-sample

variability observed with DS is consistent with what other studies have found (LeBlanc et al., 2022). This prompted us to investigate whether the DS study design could be revised to accommodate a reduced number of animals. Our computations suggested that good power (80%) to detect a biologically significant (50%) increase in MF is attainable with as few as three animals and a minimum total depth of 500 million bases per animal. However, to observe more subtle increases in MF, such as that observed in the low PRC dose group, five animals per group is still required. Nevertheless, it appears that DS reduces intragroup variability, thus requiring fewer animals per dose group to detect an effect.

Studies with different variances would require different study designs. To ensure the robustness of our analyses to increased variance, we performed the same analyses with a hypothetical sample variance that was about twice as large as our observed variance (0.1 vs 0.06). We found that a minimum of three animals per group is still sufficient to achieve good power for a 50% increase in MF; however, the minimum number of bases sequenced per sample needs to be increased to 800 million to achieve this power. Overall, our analysis suggests that DS requires fewer animals per group than the TGR assay even when the variance is increased.

In the context of regulatory decision making, there remain many open questions on how to make a hazard call when targets within a panel vary in sensitivity to mutagenesis. For example, should a significant increase in mutations be observed in a single or a small subset of targets, but not with the overall panel, would this be sufficient for a positive result? Further work using DS to test weak and non-mutagenic chemicals across a broad panel of loci is needed to answer this question. Overall, the use of a specific custom panel of targets is an effective methodology to enable an assessment of the various genomic features that influence a chemical's mutagenic effects.

2.6 CONCLUSION

In summary, this study demonstrates the strong potential of DS for assessing *in vivo* mutagenicity and contributes key data towards efforts to understand optimal study design for its application as a regulatory test. With the inclusion of potentially clonally amplified mutations and the use of highly mutable targets, DS displays comparable fold-induction measurements to the gold-standard *lacZ* assay. In addition, DS provides high resolution mutation spectrum data that enable detailed investigations of mutagenic mechanisms and potential contributions to human carcinogenesis. Further advantages of DS with respect to the TGR assay include: (1) the potential to reduce the number of

animals per group necessary to see a significant effect mitigating, in part, the costs associated with DNA sequencing; (2) possible integration with standard toxicity tests, thus negating the need for standalone mutagenicity with TGR animals, and further improving the efficiency and reducing costs and animal use for regulatory testing; and (3) application to any tissue from any species, including humans. Future work to establish DS as a mutagenicity test will require testing DS with different chemicals, including weak mutagenic and non-mutagenic chemicals, and examining response across different loci. Further studies are required to quantify relative mutational sensitivity associated with transcription status, chromatin state, and relationship to 3D genomic architecture across different cell types, tissues, and species to increase our understanding of the underlying biology of mutagenesis. Although there is still much work to be done to standardize DS, it shows great promise for regulatory mutagenicity assessment because it overcomes many of the current limitations faced by traditional assays and provides novel insights into chemical mechanisms that underlie cancer.

Funding

Funding for this research was provided by Health Canada's Genomics Research and Development Initiative to FM. Additional funding support was provided from the Natural Sciences and Engineering Research Council of Canada (NSERC) and the Canada Research Chairs Program to CLY. AED received an NSERC Canada Graduate Scholarship and Ontario Student Assistance Program's Ontario Graduate Scholarship to conduct this work.

Acknowledgments

The authors thank the extended team at TwinStrand Biosciences for their work and continuous bioinformatics and administrative support. Additionally, we thank the two Health Canada internal reviewers for helpful comments on the manuscript.

Conflicts of interest

P.V., F. Y. L., C.C.V., and J.J.S. are employees and equity holders at TwinStrand Biosciences, Inc. and are authors on one or more Duplex Sequencing-related patents.

2.7 REFERENCES

Alexandrov, L. B., Kim, J., Haradhvala, N. J., Huang, M. N., et al. (2020). The repertoire of mutational signatures in human cancer. *Nature 2020 578:7793*, *578*(7793), 94–101. https://doi.org/10.1038/s41586-020-1943-3

Alexandrov, L. B., Nik-Zainal, S., Wedge, D. C., Campbell, P. J., & Stratton, M. R. (2013). Deciphering signatures of mutational processes operative in human cancer. *Cell Reports*, *3*(1), 246–259. https://doi.org/10.1016/J.CELREP.2012.12.008

Beal, M. A., Meier, M. J., LeBlanc, D. P., Maurice, C., O'Brien, J. M., Yauk, C. L., & Marchetti, F. (2020). Chemically induced mutations in a MutaMouse reporter gene inform mechanisms underlying human cancer mutational signatures. *Communications Biology*, *3*(1). https://doi.org/10.1038/S42003-020-01174-Y

Chawanthayatham, S., Valentine, C. C., Fedeles, B. I., Fox, E. J., Loeb, L. A., Levine, S. S., Slocum, S. L., Wogan, G. N., Croy, R. G., & Essigmann, J. M. (2017). Mutational spectra of aflatoxin B1 in vivo establish biomarkers of exposure for human hepatocellular carcinoma. *Proceedings of the National Academy of Sciences of the United States of America*, *114*(15), E3101–E3109. https://doi.org/10.1073/PNAS.1700759114

Fong, L. Y. Y., Jensen, D. E., & Magee, P. N. (1990). DNA methyl-adduct dosimetry and O6-alkylguanine-DNA alkyl transferase activity determinations in rat mammary carcinogenesis by procarbazine and N-methylnitrosourea. *Carcinogenesis*, *11*(3), 411–417. https://doi.org/10.1093/CARCIN/11.3.411

Frankish, A., Diekhans, M., Ferreira, A. M., Johnson, R., et al. (2019). GENCODE reference annotation for the human and mouse genomes. *Nucleic Acids Research*, *47*(D1), D766–D773. https://doi.org/10.1093/NAR/GKY955

Fu, D., Calvo, J. A., & Samson, L. D. (2012). Balancing repair and tolerance of DNA damage caused by alkylating agents. *Nature Reviews Cancer*, *12*(2), 104–121. https://doi.org/10.1038/NRC3185

Gerson, S. L., Caimi, P. F., William, B. M., & Creger, R. J. (2018). Pharmacology and Molecular Mechanisms of Antineoplastic Agents for Hematologic Malignancies. *Hematology: Basic Principles and Practice*, 849–912. https://doi.org/10.1016/B978-0-323-35762-3.00057-3

Gingerich, J. D., Soper, L., Lemieux, C. L., Marchetti, F., & Douglas, G. R. (2014). *Transgenic Rodent Gene Mutation Assay in Somatic Tissues*. 305–321. https://doi.org/10.1007/978-1-4939-1068-7_18

Heddle, J. A. (1999). On clonal expansion and its effects on mutant frequencies, mutation spectra and statistics for somatic mutations in vivo. *Mutagenesis*, *14*(3), 257–260. https://doi.org/10.1093/MUTAGE/14.3.257

Heflich RH, Johnson GE, Zeller A, Marchetti F, Douglas GR, Witt KL, Gollapudi BB, White PA.Environ Mol Mutagen. 2020 Jan;61(1):34-41. doi: 10.1002/em.22338. Epub 2019 Oct 23.PMID: 31600846

Hodgkinson, A., Chen, Y., & Eyre-Walker, A. (2012). The large-scale distribution of somatic mutations in cancer genomes. *Human Mutation*, *33*(1), 136–143. https://doi.org/10.1002/HUMU.21616

Hodgkinson, A., & Eyre-Walker, A. (2011). Variation in the mutation rate across mammalian genomes. *Nature Reviews. Genetics*, *12*(11), 756–766. https://doi.org/10.1038/NRG3098

Højsgaard, S., & Halekoh, U. (2018). *doBy: Groupwise Statistics, LSmeans, Linear Estimates, Utilities* (R package 4.6.10).

IARC Working Group. (1981). Procarbazine Hydrochloride. *IARC Monogr* , *26*, 311–340.

Jackson, M., Marks, L., May, G. H. W., & Wilson, J. B. (2018). The genetic basis of disease. In *Essays in Biochemistry* (Vol. 62, Issue 5, pp. 643–723). Portland Press Ltd. https://doi.org/10.1042/EBC20170053

Jenkins, G. J. S., Doak, S. H., Johnson, G. E., Quick, E., Waters, E. M., & Parry, J. M. (2005). Do dose response thresholds exist for genotoxic alkylating agents? *Mutagenesis*, *20*(6), 389–398. https://doi.org/10.1093/MUTAGE/GEI054

Kennedy, S. R., Schmitt, M. W., Fox, E. J., Kohrn, B. F., Salk, J. J., Ahn, E. H., Prindle, M. J., Kuong, K. J., Shen, J. C., Risques, R. A., & Loeb, L. A. (2014). Detecting ultralow-frequency mutations by Duplex Sequencing. *Nature Protocols*, *9*(11), 2586–2606. https://doi.org/10.1038/NPROT.2014.170

Kucab, J. E., Zou, X., Morganella, S., Joel, M., Nanda, A. S., Nagy, E., Gomez, C., Degasperi, A., Harris, R., Jackson, S. P., Arlt, V. M., Phillips, D. H., & Nik-Zainal, S. (2019). A Compendium of Mutational Signatures of Environmental Agents. *Cell*, *177*(4), 821-836.e16. https://doi.org/10.1016/J.CELL.2019.03.001

Lambert, I. B., Singer, T. M., Boucher, S. E., & Douglas, G. R. (2005). Detailed review of transgenic rodent mutation assays. *Mutation Research*, *590*(1–3), 1–280. https://doi.org/10.1016/J.MRREV.2005.04.002

LeBlanc, D. P. M., Meier, M., Lo, F. Y., Schmidt, E., Valentine, C., Williams, A., Salk, J. J., Yauk, C. L., & Marchetti, F. (2022). Duplex sequencing identifies genomic features that determine susceptibility to benzo(a)pyrene-induced in vivo mutations. *BMC Genomics*, *23*(1). https://doi.org/10.1186/S12864-022-08752-W

Makova, K. D., & Hardison, R. C. (2015). The effects of chromatin organization on variation in mutation rates in the genome. *Nature Reviews. Genetics*, *16*(4), 213. https://doi.org/10.1038/NRG3890

Manders, F., Brandsma, A. M., de Kanter, J., Verheul, M., Oka, R., van Roosmalen, M. J., van der Roest, B., van Hoeck, A., Cuppen, E., & van Boxtel, R. (2022). MutationalPatterns: the one stop shop for the analysis of mutational processes. *BMC Genomics*, *23*(1). https://doi.org/10.1186/S12864-022-08357-3

Marchetti, F., Zhou, G., LeBlanc, D., White, P. A., Williams, A., Yauk, C. L., & Douglas, G. R. (2021). The 28 + 28 day design is an effective sampling time for analyzing mutant frequencies in rapidly proliferating tissues of MutaMouse animals. *Archives of Toxicology*, *95*(3), 1103–1116. https://doi.org/10.1007/S00204-021-02977-6

Maurice, C., Dertinger, S. D., Yauk, C. L., & Marchetti, F. (2019). Integrated In Vivo Genotoxicity Assessment of Procarbazine Hydrochloride Demonstrates Induction of Pig-a and LacZ Mutations, and Micronuclei, in MutaMouse Hematopoietic Cells. *Environmental and Molecular Mutagenesis*, *60*(6), 505–512. https://doi.org/10.1002/EM.22271

Monroe, J. G., Srikant, T., Carbonell-Bejerano, P., Becker, C., Lensink, M., Exposito-Alonso, M., Klein, M., Hildebrandt, J., Neumann, M., Kliebenstein, D., Weng, M. L., Imbert, E., Ågren, J., Rutter, M. T., Fenster, C. B., & Weigel, D. (2022). Mutation bias reflects natural selection in Arabidopsis thaliana. *Nature*, *602*(7895), 101–105. https://doi.org/10.1038/s41586-021-04269-6

Nadkarni, A., Burns, J. A., Gandolfi, A., Chowdhury, M. A., Cartularo, L., Berens, C., Geacintov, N. E., & Scicchitano, D. A. (2016). Nucleotide Excision Repair and Transcription-coupled DNA Repair Abrogate the Impact of DNA Damage on Transcription. *The Journal of Biological Chemistry*, *291*(2), 848–861. https://doi.org/10.1074/JBC.M115.685271

Nik-Zainal, S., Davies, H., Staaf, J. et al. Landscape of somatic mutations in 560 breast cancer whole-genome sequences. Nature 534, 47–54 (2016). https://doi.org/10.1038/nature17676

Piegorsch, W. W., & Bailer, A. J. (1994). Statistical approaches for analyzing mutational spectra: some recommendations for categorical data. *Genetics*, *136*(1), 403–416. https://doi.org/10.1093/GENETICS/136.1.403

Piegorsch, W. W., Margolin, B. H., Shelby, M. D., Johnson, A., French, J. E., Tennant, R. W., & Tindall, K. R. (1995). Study design and sample sizes for a lacI transgenic mouse mutation assay. *Environmental and Molecular Mutagenesis*, *25*(3), 231–245. https://doi.org/10.1002/EM.2850250310

Pletsa, V., Valavanis, C., van Delft, J. H. M., Steenwinkel, M. J. S. T., & Kyrtopoulos, S. A. (1997). DNA damage and mutagenesis induced by procarbazine in lambda lacZ transgenic mice: evidence that

bone marrow mutations do not arise primarily through miscoding by O6-methylguanine. *Carcinogenesis*, *18*(11), 2191–2196. https://doi.org/10.1093/CARCIN/18.11.2191

Revollo, J., Bhalli, J. A., Tebbe, C., Noteboom, J., Thomas, D., McKinzie, P., Felton, N., Pearce, M. G., & Dobrovolsky, V. N. (2017). Spectrum of Pig-a mutations in T lymphocytes of rats treated with procarbazine. *Mutagenesis*, *32*(6), 571–579. https://doi.org/10.1093/MUTAGE/GEX032

Salk, J. J., & Kennedy, S. R. (2020). Next-Generation Genotoxicology: Using Modern Sequencing Technologies to Assess Somatic Mutagenesis and Cancer Risk. *Environmental and Molecular Mutagenesis*, *61*(1), 135–151. https://doi.org/10.1002/EM.22342

Skopek, T. R., Kort, K. L., & Marino, D. R. (1995). Relative sensitivity of the endogenous hprt gene and lacI transgene in ENU-treated big blue™ B6C3F1 mice. *Environmental and Molecular Mutagenesis*, *26*(1), 9–15. https://doi.org/10.1002/EM.2850260103

Skopek, T. R., Kort, K. L., Marino, D. R., Mittal, L. v., Umbenhauer, D. R., Laws, G. M., & Adams, S. P. (1996). Mutagenic Response of the Endogenous hprt Gene and lacI Transgene in Benzo[a]pyrene-Treated Big Blue™ B6C3F1 Mice. *Environmental and Molecular Mutagenesis*, *28*(4), 376–384. https://doi.org/10.1002/(sici)1098-2280(1996)28:4<376::aid-em11>3.0.co;2-c

Souliotis, V. L., Valavanis, C., Boussiotis, V. A., Pangalis, G. A., & Kyrtopoulos, S. A. (1994). Comparative dosimetry of O6-methylguanine in humans and rodents treated with procarbazine. *Carcinogenesis*, *15*(8), 1675–1680. https://doi.org/10.1093/CARCIN/15.8.1675

Suzuki, T., Uno, Y., Idehara, K., Baba, T., Maniwa, J., Ohkouchi, A., Wang, X., Hayashi, M., Sofuni, T., Tsuruoka, M., Miyajima, H., & Kondo, K. (1999). Procarbazine genotoxicity in the MutaMouse; strong clastogenicity and organ-specific induction of lacZ mutations. *Mutation Research*, *444*(2), 269–281. https://doi.org/10.1016/S1383-5718(99)00060-1

Test No. 470: Mammalian Erythrocyte Pig-a Gene Mutation Assay. (2022) OECD Guidelines for the Testing of Chemicals, Section 4, OECD Publishing, Paris, https://doi.org/10.1787/4faea90e-en.

Test No. 471: Bacterial Reverse Mutation Test. (2020) OECD Guidelines for the Testing of Chemicals, Section 4, OECD Publishing, Paris, https://doi.org/10.1787/9789264071247-en.

Test No. 488: Transgenic Rodent Somatic and Germ Cell Gene Mutation Assays. (2022). https://doi.org/10.1787/9789264203907-EN

Valentine, C. C., Young, R. R., Fielden, M. R., Kulkarni, R., Williams, L. N., Li, T., Minocherhomji, S., & Salk, J. J. (2020). Direct quantification of in vivo mutagenesis and carcinogenesis using duplex sequencing. *Proceedings of the National Academy of Sciences of the United States of America*, *117*(52), 33414–33425. https://doi.org/10.1073/PNAS.2013724117/-/DCSUPPLEMENTAL

White, P. A., Long, A. S., & Johnson, G. E. (2020). Quantitative Interpretation of Genetic Toxicity Dose-Response Data for Risk Assessment and Regulatory Decision-Making: Current Status and Emerging Priorities. *Environmental and Molecular Mutagenesis*, *61*(1), 66–83. https://doi.org/10.1002/EM.22351

Xia, B., Yan, Y., Baron, M., Wagner, F., Barkley, D., Chiodin, M., Kim, S. Y., Keefe, D. L., Alukal, J. P.,Boeke, J. D., & Yanai, I. (2020). Widespread Transcriptional Scanning in the Testis Modulates Gene Evolution Rates. *Cell*, *180*(2), 248-262.e21. https://doi.org/10.1016/J.CELL.2019.12.015

CHAPTER THREE

DATA CHAPTER

ANNETTE DODGE

Duplex Sequencing Reveals Dose-Dependent Increases in Mutation Frequency and a Unique Spectrum in Procarbazine-Exposed Male Mouse Germ Cells

Annette E. Dodge[1,2], Danielle P.M. LeBlanc[2], Gu Zhou[2], Andrew Williams[2], Elena Esina[1], Matthew J. Meier[2], Charles C. Valentine[3], Jesse J. Salk[3], Carole L. Yauk[1,4], Francesco Marchetti[2,4]

[1]Department of Biology, University of Ottawa, Ottawa, Ontario, Canada

[2]Environmental Health Science and Research Bureau, Health Canada, Ottawa, Ontario, Canada

[3]TwinStrand Biosciences Inc. Seattle, Washington, USA

[4]Department of Biology, Carleton University, Ottawa, Ontario, Canada

3.1 ABSTRACT

Germ cell mutagenicity testing is essential to protecting population health, though it is often neglected during risk assessment. Duplex Sequencing (DS) is an emerging high-accuracy DNA sequencing technology that provides novel opportunities to deeply characterize germ cell mutagenesis. We used DS to study spontaneous and chemically-induced mutations in the germ cells of MutaMouse males across a panel of 20 diverse genomic targets. Mice were exposed to the antineoplastic agent procarbazine (PRC) at 0, 6.25, 12.5, or 25 mg/kg-bw/day for 28 days by oral gavage. Germ cells of the seminiferous tubules were sampled 28 days post-exposure. The germ cell mutation frequencies and spectra were compared with dose-matched bone marrow samples to contrast mutagenicity profiles. DS detected significant increases in mutation frequencies and changes to mutation spectra at PRC doses comparable to those used during human chemotherapeutic treatment. The genomic features that drove the mutational response of the DS loci differed between germ cells and bone marrow. Furthermore, distinct mutation spectra between tissues suggest that some mutations may arise via different mechanisms in germ cells compared to somatic cells. Our results suggest that male germ cells may have intrinsic mechanisms to reduce mutation burden relative to somatic cells. Ultimately, this work demonstrates clear differences in the mutagenic response of male germ cells compared to the bone marrow using DS. Further characterization of germ cell mutagenicity will enable us to better protect DNA integrity in the germline and thus in the population.

3.2 INTRODUCTION

Germline mutations are the primary force that drive the evolution of species. However, at the individual level, germ cell mutations may have severe negative effects on the health of the offspring. A single mutated germ cell may result in an offspring with the *de novo* mutation in every cell of the body. A broad spectrum of diseases is attributed to *de novo* mutations including rare genetic disorders (Bamshad et al., 2010; Hoischen et al., 2010, 2011), sporadic intellectual disorders (Vissers et al., 2010), autism-spectrum disorders (Alonso-Gonzalez et al., 2018; Iossifov et al., 2012; O'Roak et al., 2011), schizophrenia (Gogos et al., 2011; Rouleau et al., 2011), and cancer (Kuiper et al., 2010). The male germline is the main contributor of inherited *de novo* mutations, and paternal age is directly correlated with mutations inherited by the offspring (Jónsson et al., 2017; Kong et al., 2012; Sasani et al., 2019). However, the contribution of environmental factors to the incidence of *de novo* mutations is almost entirely unknown. Despite decades of research, no human germ cell mutagen has been definitively identified, though over 80 rodent germ cell mutagens are known (Demarini, 2012; Marchetti et al., 2020). Given the consequences of heritable mutations, it is critical that we improve our understanding of germ cell mutagenesis and apply this knowledge to the identification of human germ cell mutagens.

Although a variety of methodologies exist to study germ cell mutations, mutagenicity testing requirements typically focus on somatic cells (OECD, 2017). Indeed, results of comparative studies show that most germ cell mutagens are likely to be detected using somatic cell tests. However, several examples of quantitative and qualitative differences in the mutagenic response of germ cells and somatic cells to chemical toxicants exist. Chemicals that cause mutations in germ cells at doses that do not affect somatic cells include N-hydroxyacrylamide (Witt et al., 2003), side-stream smoke (Marchetti et al., 2011), and various chemotherapy drugs (Cliet et al., 1993; Waters et al., 1994; Yauk et al., 2015). In addition, O'Brien et al. (2016) demonstrated that benzo[a]pyrene (BaP), an established mutagen, induces a distinct mutation spectrum in male mouse germ cells compared to bone marrow. Thus, there appear to be mechanistic and/or chemical-specific effects to germ cells not observed in somatic cells *in vivo*. However, apart from Cliet et al. (1993) and O'Brien et al. (2016), studies comparing germ and somatic cell mutagenesis used different endpoints. Direct comparison of mutation frequency (MF) and spectrum in germ and somatic cells after chemical mutagenesis remains a critical knowledge gap.

There are several notable features that may be contributing to differences between germ cell and somatic cell mutagenesis. Meiosis, for example, may introduce opportunities for mutations to occur (Arbel-Eden & Simchen, 2019) and post-meiotic haploid germ cells cannot rely on sister chromatids for homology-based repair mechanisms (Baarends et al., 2001). The process of spermatogenesis is also characterized by a diminished DNA repair capacity during sperm maturation (Marchetti & Wyrobek, 2008; Olsen et al., 2005). Germ cells are subjected to different epigenetic processes including reprogramming, imprinting, and chromatin remodelling that may modulate the mutational response. The replacement of histones with protamines during spermiogenesis may promote additional opportunities for misrepair of endogenous strand breaks (Rathke et al., 2014). Clearly, these unique germ cell factors may influence their mutagenic responses and would not be effectively captured through the study of somatic cell mutagenesis. Direct analysis of the mechanisms and endogenous factors involved in germ cell mutagenesis will enable better prediction of the hazards posed by mutagenic substances to our germline.

New sequencing-based assays, such as Duplex Sequencing (DS), allow the direct analysis of the mutational response of cells *in vivo* following exposure to mutagenic substances. DS is an error-corrected next-generation sequencing technology that detects ultra-rare mutations using a customizable panel targeting a portion of the endogenous genome (Kennedy et al., 2014). Unlike traditional assays, DS is not restricted to specific test animals and can be widely applied to any species, including humans. Importantly, DS has been used to describe mutational responses of several known mutagens in mouse somatic tissues (Chawanthayatham et al., 2017; Dodge et al., 2023; LeBlanc et al., 2022; Valentine et al., 2020). These studies show that detailed mutation spectra data obtained from sequencing can be used to inform mutagenic mechanisms. Furthermore, DS makes use of genomic targets that encompass a range of chromatin states, transcription statuses, and sequencing contexts; thus, it can inform on the endogenous factors that modulate mutagenesis.

In this study, we used DS to characterize mutation induction in the germ cells of MutaMouse males exposed to procarbazine hydrochloride (PRC). PRC is an anti-neoplastic agent that is classified as a Class 2A probable carcinogen by the International Agency for Research on Cancer (IARC Working Group, 1981). It induces mutations in mouse somatic tissues (Beal et al., 2020; Revollo et al., 2017) and testes (Suzuki et al., 1999) and has tested positive for male germ cell mutagenicity using the specific locus test in mice (Ehling & Neuhäuser, 1977). It is also implicated in impaired male fertility in cancer patients following treatment (Mauz-Körholz et al., 2010; Schellong et al., 1997; Viviani et al., 1985); thus, it

targets male germ cells in both humans and mice. We recently characterized mutations in the bone marrow of MutaMouse males exposed to PRC using DS (Dodge et al., 2023) and found that it induced significant dose-dependent increases in MF and a shift in mutation spectra. Herein, our overall aim is to assess PRC mutagenicity in male germ cells and compare it to bone marrow mutagenicity to explore some of the unique characteristics of germ cell mutagenesis.

The specific objectives of this study are to: 1) use DS to study the dose-response of mutation induction by PRC in germ cells from the seminiferous tubules (hereafter, germ cells) of MutaMouse animals; 2) characterize variability in spontaneous and PRC-induced MF across a panel of 20 DS loci; 3) compare PRC-induced MF and spectrum between germ cells and bone marrow; 4) assess the concordance of DS with the conventional transgenic rodent (TGR) *lacZ* assay; and 5) explore optimal DS study designs for assessing mutagenicity in germ cells by modeling sample size and sequencing data yield.

3.3 METHODS

3.3.1 Animal Exposure and Tissue Collection

All animal handling, exposures and tissue collection were approved by the Health Canada Ottawa Animal Care Committee and followed the Canadian Council on Animal Care guidelines. Adult MutaMouse males, 8-10 weeks of age at the beginning of the experiment were exposed by oral gavage to 6.25, 12.5, or 25 mg/kg-bw/day PRC (CAS 366-70-1; Sigma-Aldrich, Oakville, ON Canada) dissolved in phosphate-buffered saline without calcium and magnesium (PBS; Corning cellgro, Manassas, VA, USA). A sampling time of 28 days post exposure was chosen to ensure that all germ cells were exposed during the proliferative phase of spermatogenesis (Marchetti et al., 2018; OECD 488, 2022). Vehicle control (VC) mice were exposed to PBS for 28 consecutive days and sampled 3 or 28 days post-exposure. There were six mice per treatment group. At euthanasia, germ cells were collected from the seminiferous tubules as previously described (O'Brien et al., 2014), and suspended in Dulbecco's phosphate-buffered saline (D-PBS). The suspension was flash frozen and stored at -80°C (O'Brien et al., 2014). Germ cells from each testis were stored separately and used for the *lacZ* assay and DS, respectively.

3.3.2 DNA Extraction and Library Preparation for Duplex Sequencing

DNA from germ cells was extracted using the Qiagen DNeasy blood and tissue kit, as described in the Qiagen User Manual (Cat. # 69504, Qiagen, Hilden, Germany). DNA quality was assessed using an Agilent Tapestation to ensure a DNA Integrity Number greater than 7.0. DNA was prepared for sequencing using the Duplex Sequencing Kit Mutagenesis Panel (Mouse-50, v1.0) as described in the user manual (Cat. # 06-1006-02, TwinStrand Biosciences, Seattle WA, USA). Briefly, 500 ng of DNA was subjected to enzymatic fragmentation to a mean fragment size of approximately 300 base pairs (bp). The DNA was then end-repaired, A-tailed and ligated to DuplexSeq™ Adapters (TwinStrand Biosciences, Seattle WA, USA). The Mouse Mutagenesis panel was captured using 120mer biotinylated oligo probes (Integrated DNA Technologies, Coalville, IA, USA). This panel was chosen as a balanced representation of the entire genome with respect to location, GC content, trinucleotide abundances and genic status. The DS panel consists of 20 2.4kb targets located on each mouse autosome except for chromosome 1 that has two targets. Nine of the targets are located within genic regions and 11 within intergenic regions (LeBlanc et al., 2022). DS targets were classified as genic or intergenic based on gene intersection information obtained from the gene database GenCode, the Mouse GenCode gene set, version M25 (Frankish et al., 2019).

Prepared libraries were sequenced on a NovaSeq 6000 (Illumina, Sand Diego CA, USA) by Psomagen Inc. (Rockville, MD, USA) to a mean on-target duplex depth of 30,000X. The resulting sequence data were processed through the DS pipeline (TwinStrand Biosciences) as described in Valentine et al. (2020) using the DNANexus platform (v 3.19.3). Bioinformatic processing involved: 1) extraction of Duplex Tags; 2) sequence read alignment; 3) grouping of reads by their unique molecular identifier, quality trimming; 4) error correction of PCR duplicates into a Single-Strand Consensus Sequence (SSCs); 5) error-correction of SSCs by duplex consensus calling; 6) consensus post-processing; 7) re-alignment; and, 8) variant calling. Variants with a variant allele fraction >0.01 were considered germline mutations and were filtered out. Insertions/Deletions larger than 1000bp were called as structural variants. Mutation induction was measured as MF, calculated by dividing mutation counts by total number of duplex bases sequenced (mutations per bp). Mutations that were observed more than once in the same sample were considered under two assumptions as discussed in Dodge et al., (2023): 1) all identical mutations represent the clonal expansion of a single mutational event and are only counted once (MF_{min}); 2) identical mutations represent independent mutational events and are each counted as a unique mutation (MF_{max}). Resulting data from the DS pipeline included a summary of sequencing quality

metrics, MF_{Min} and MF_{Max} (mutations per bp), simple mutation spectra, trinucleotide frequency, and MF per each 2.4 kb target.

3.3.3 Transgenic Rodent Gene Mutation Assay (lacZ assay)

The *lacZ* assay was performed as per the Organisation for Economic Co-operation and Development (OECD) TG 488 (2022). Briefly, genomic DNA was isolated from germ cells using phenol/chloroform extraction (O'Brien et al., 2014). A NanoDrop spectrophotometer (Thermo Scientific Canada, Ottawa, Canada) was used to assess the quantity and purity of DNA. λgt10 phage vectors in genomic DNA were excised using commercial packaging extract kits (Agilent Technology, Santa Clara, CA, USA), according to the manufacturer's instructions. Transgene mutant frequency was determined using the phenyl β-d-galactopyranoside (P-gal)–positive selection assay (Lambert et al., 2005). A minimum number of 300,000 plaque-forming units (pfu) were counted per sample (O'Brien et al., 2014). Mutant frequency (phenotypically selectable mutants per *lacZ* locus) was expressed as the ratio of mutant plaques to total pfu.

3.3.4 Mutation Data Interpretation and Statistical Analysis

Estimated frequencies by dose were obtained for both DS and *lacZ* using generalized linear models (GLM) in the R software with the quasibinomial distribution. Pairwise comparisons were conducted using the doBy R library (Højsgaard & Halekoh, 2018) and these estimates were then back-transformed. The delta method was employed to approximate the back-transformed standard errors (standard error of the mean; SEM) of the estimated MF. A Holm-Sidak correction was applied to adjust p-values for multiple comparisons for both MF_{Min} and MF_{Max}. Next, we estimated MFs for each 2.4 kb target using generalized linear mixed models (GLMM) with a binomial error distribution in the R software. Pairwise comparisons based on dose, location relative to genes, chromatin state, and GC content were conducted using the doBY R library as described above.

The mutation spectra data generated by DS were evaluated by considering first only the mutated base and then by extending the analyses to include the flanking bases. To determine which mutation substitution types differed between control and treated groups, a modified contingency table approach was used as described previously (Piegorsch & Bailer, 1994). Pairwise comparisons as described above were used to determine which mutation types were significantly increased from VC. Subsequently, we generated a 96-trinucleotide mutation spectrum and used cosine similarity to determine the Catalogue

of Somatic Mutations in Cancer (COSMIC) single base substitutions (SBS) signatures (Alexandrov et al., 2020) that most closely resembled the PRC mutation spectra, using the MutationalPatterns package in R (Manders et al., 2022).

3.3.5 Comparison of Germ Cell and Bone Marrow Mutational Responses

DS and *lacZ* data obtained from the germ cells of MutaMouse males were compared to DS and *lacZ* data obtained from the bone marrow of dose-matched MutaMouse males (Dodge et al., 2023). Pairwise comparisons were conducted as described above to determine if MF differed between bone marrow and germ cells for each dose group. A modified contingency table was used to determine if the mutation spectra differed between tissues for each dose group.

3.3.6 Benchmark Dose Comparison

Benchmark dose (BMD) modeling was conducted using the PROAST web application (version 70.1, https://rivm.nl/en/proast) to mathematically model the PRC dose-response curves. The BMD estimated in our study represents a dose that produces a 50% increase (i.e., the benchmark response; BMR) in MF_{Min} or MF_{Max} or *lacZ* mutant frequency. Different mathematical models (Hill, exponential, reverse exponential, and lognormal) were fit to the dose-response data, and the one with the highest Akaike Information Criterion was selected. Statistical evaluation of the differences between BMDs were based on the 95% confidence intervals obtained from model averaging of 200 bootstrap runs. Comparisons were made of BMDs derived from DS versus the *lacZ* assay, and BM data versus germ cell data.

3.3.7 Power Analysis on DS Study Design

A power analysis was used to determine the minimum sample size and total number of duplex base pairs needed to observe a significant increase in MF using DS. Analyses are as described in Dodge et al. (2023). Briefly, simulated "control" and "treated" samples were randomly generated based on the experimental parameters observed in our germ cells and a selected fold-increase of 1.5. Hypothetical mutation counts were generated based on the observed average MF_{Min} from our VC group (2.25×10^{-8} mutations per bp) and the average total number of bases sequenced per animal (depth; 1.45×10^{9} bp). A sample variance of 0.25 was estimated from the standard-deviation obtained from the GLMM used for per target dose-response analysis. The power of the GLM analysis (described above) was then calculated

under the set conditions. The bisection method was used to estimate the minimum detectable effect size (MDES) of the simulated experiment yielding a power of 80% and a $p<0.05$. We varied the sample size and the total sequencing depth and calculated the power and MDES for each condition. Finally, we calculated the minimum total number of duplex bases required to detect a 1.5-fold increase in MF with 80% power under each of the various simulated conditions.

3.4 RESULTS

3.4.1 DS Mutation Frequency

DS reads were distributed evenly across the 24 samples and across the 20 targets (Supp. Figure 3.1). An average of 1.5 billion duplex bases were sequenced per sample for a total of 35 billion across the cohort. All samples met a minimum target of 500 million duplex bases per sample.

DS MF was measured by dividing the number of mutations by the total number of duplex bases sequenced. Mutations included single nucleotide variants (SNVs), small insertions/deletions (indels), multi-nucleotide variants (MNVs), and structural variants (SVs). Under the MF_{Min} assumption, an average of 21, 31, 49, and 79 mutants per mouse were counted for VC, 6.25, 12.5, and 25 mg/kg-bw/day PRC, respectively (Figure 3.1). No statistically significant increase was observed at the low PRC dose. However, PRC induced a significant increase ($P < 0.05$) in MF_{Min} ($\times 10^{-8}$) relative to VC in the middle and high dose groups, from 2.3 ± 0.25 mutations per sample (± SEM) in the VC to 7.7 ± 1.3 at the high PRC dose. A 2.0- and 3.3-fold increase in MF_{Min} was induced relative to VC in the 12.5 and 25 mg/kg-bw/day dose groups, respectively (Table 3.1).

Under the MF_{Max} assumption, an additional 133, 215, 998, and 3486 mutations were identified in total for VC, 6.25, 12.5, and 25 mg/kg-bw/day, respectively (Supp. Figure 3.2a). Large numbers of clonally expanded mutations were identified in several samples that drove MF_{Max} up and caused an increase in inter-individual variability compared to MF_{Min}. Samples were characterized primarily by unique mutations, accounting for roughly 85% of all mutations in each sample (Supp. Figure 3.2b). ~13% of mutations per sample experienced clonal expansion events of 2-50 clones per mutation. Mutations occurring more than 50 times in a single sample accounted for ~1% of total mutations per sample. PRC induced an increase in MF_{Max} ($\times 10^{-8}$ ± SEM), from 4.4 ± 1.6 in the VC to 63 ± 34 in the high dose group. However, MF_{Max} could not be modelled with the GLM approach due to the numerous extreme values. Thus, MF_{Max} was not considered in any further analyses.

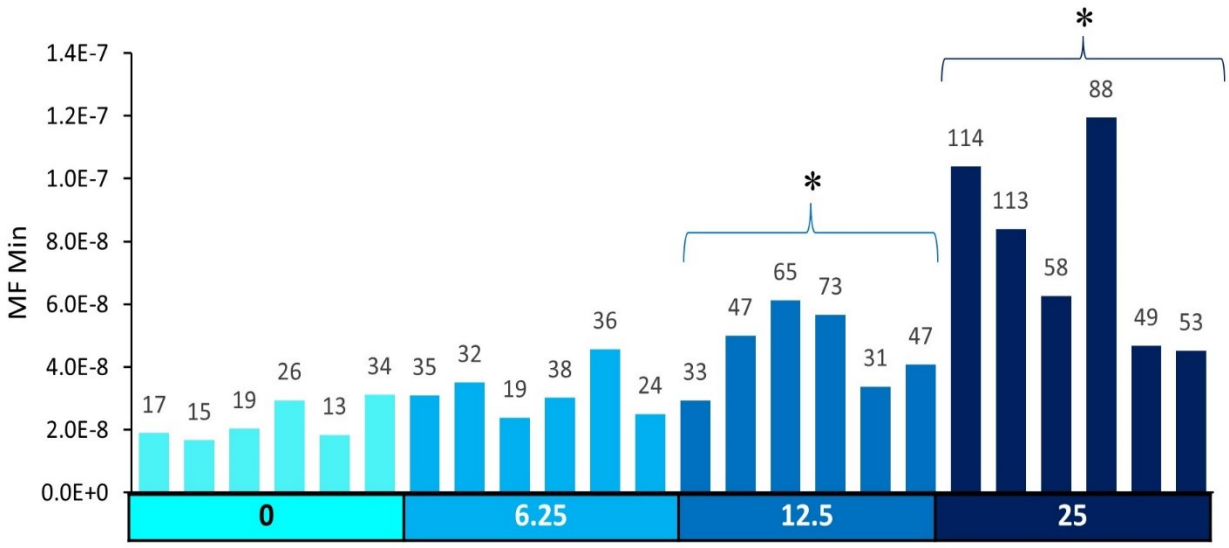

Figure 3.1. Duplex Sequencing mutation frequencies (MF_{Min}) in the germ cells of MutaMouse males at various doses of PRC. Bars represent the MF_{Min} (mutations per bp) for each animal. Data labels indicate the total mutation count per animal. The x-axis indicates the PRC dose group (mg/kg-bw/day). Asterisks indicate a significant difference ($p < 0.05$) relative to VC in the average MF across animals.

Table 3.1. Mean mutation frequency (MF_{Min}) estimates and corresponding pairwise comparisons between dose groups for DS obtained using a GLM.

Dose (mg/kg-bw/day)	Mutant frequency ± SEM (x 10^{-8})	Fold Changes (± SEM)	p-value*
0	2.25 ± 0.25	---	---
6.25	3.19 ± 0.32	1.38 ± 0.35	2.24×10^{-1}
12.5	4.53 ± 0.52	1.99 ± 0.47	**1.57×10^{-2}**
25	7.69 ± 1.3	3.28 ± 0.72	**8.52×10^{-5}**

*bold font indicates p-value < 0.05

3.4.2 DS Mutation Frequency by Target

MF_{Min} was analyzed across the 20 genomic targets (Figure 3.2). Within the VC, a range of 3-13 mutations per locus were identified. PRC induced a significant increase in MF_{Min} relative to VC in 2 of the 20 targets; the target on chromosome 2 (chr2) increased at the middle and high PRC dose and the target on chr13 increased at the high PRC dose. Similar dose-response trends were observed for most of the other targets, though they were not significant.

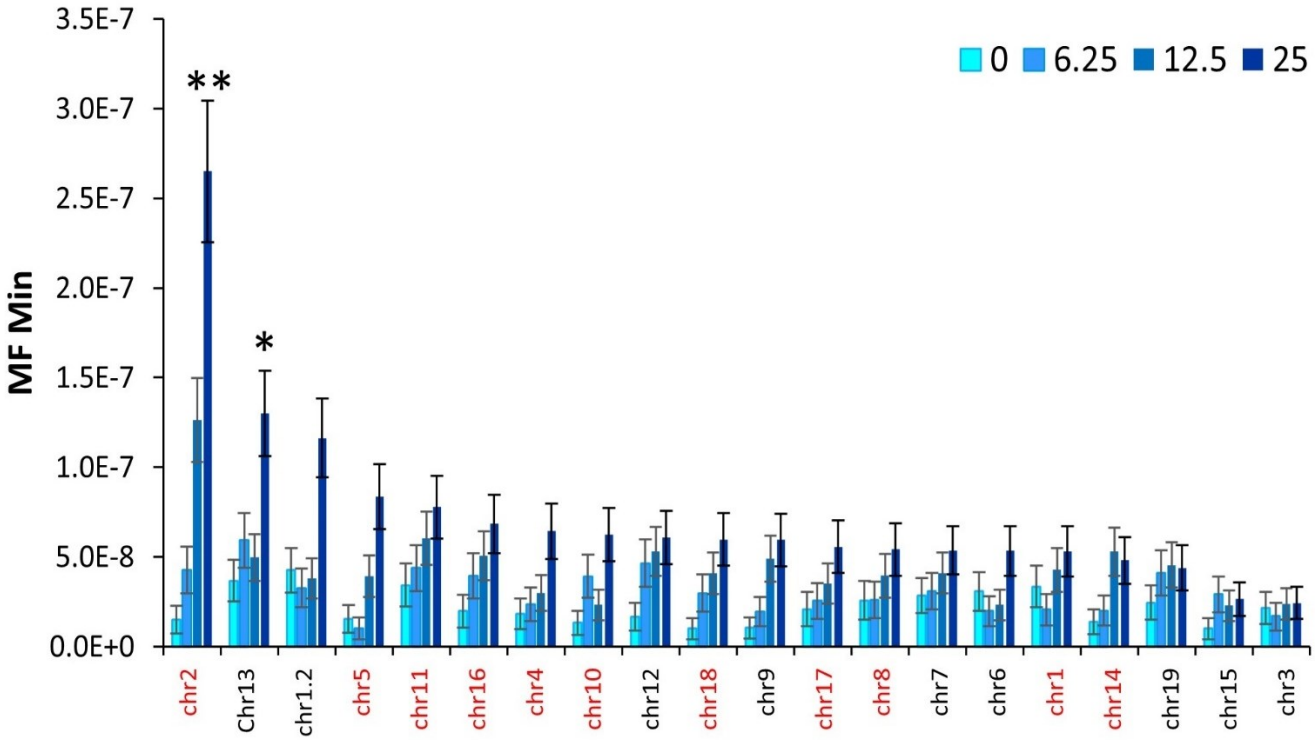

Figure 3.2. Spontaneous and PRC-induced MF by Duplex Sequencing target ordered from highest MF_{Min} in the high PRC dose group to the lowest. Data are mean MF ± SEM mutations per bp, for each target (n = 6), separated by dose (mg/kg-bw/day). Intergenic targets are labelled in red and genic targets are in black along the x-axis. Asterisks indicate a significant increase in the high PRC dose relative to VC. The double asterisk indicates a significant increase in the high and middle PRC doses relative to VC. (Generalized linear mixed model, $p < 0.05$).

Mutation frequencies and response to PRC varied across the 20 DS targets. The background MF_{Min} differed by 4.2-fold across the targets, with the lowest MF_{Min} observed for the target on chr18 (1.00×10^{-8}) and the highest MF_{Min} observed for the second target on chr1 (chr1.2; 4.3×10^{-8}). A larger 11-fold difference was observed for the locus-specific MF_{Min} in the high dose group, from 2.43×10^{-8} on the chr3 target to 26.5×10^{-8} for the target on chr2. We plotted the fold-increase in MF_{Min} for the high dose relative to VC (Figure 3.3) for each locus and noted a high degree of variability in response to PRC across the loci. The chr2 target showed a maximum increase in MF_{Min} relative to VC of 17-fold at the high PRC dose; whereas, the smallest increase in MF_{Min} relative to VC at the high dose was observed for the target on chr3 (1.1-fold). The locus on chr2 showed exceptionally high PRC mutation induction compared to all other targets in the middle and high dose groups, displaying a MF_{Min} that was 2X higher than the targets that achieved the second highest MF_{Min} (chr11; 6.04×10^{-8}, chr13; 13.0×10^{-8}) in their respective dose groups. In contrast, the chr2 locus had the sixth lowest MF_{Min} amongst the targets for the VC (1.51×10^{-8}).

To assess the impact of the extreme mutation induction observed in the chr2 target on the overall dose response, we removed this target's mutation count and sequencing depth from each sample's MFs and reran the GLM analysis (Supp. Figure 3.3). Without chr2, we identified on average, 20, 29, 43, and 65 mutations per sample in the VC, 6.25, 12.5, and 25 mg/kg-bw/d groups, respectively under the MF_{Min} assumption. MF_{Min} remained significantly increased relative to VC at the middle and high dose groups, though their respective fold-increases were reduced to 1.8- and 2.8-fold increase from VC without the chr2 target included.

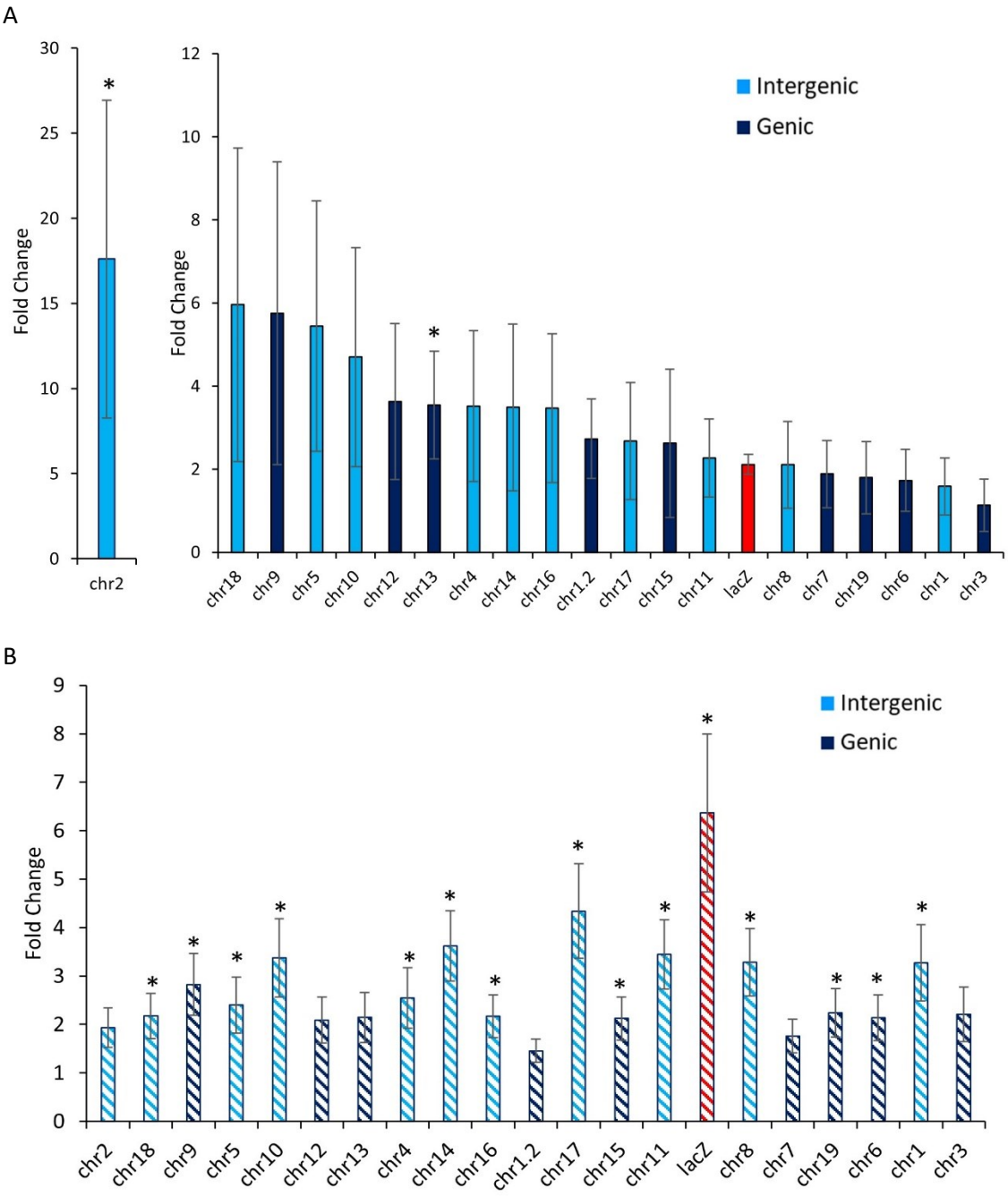

Figure 3.3. Fold change in the MF_{Min} of the high-dose group relative to VC for the 20 DS targets as well as for the *lacZ* gene (red bar). Fold-changes were estimated using a general linear mixed model for (**A**) germ cells and (**B**) bone marrow**.** DS targets are listed along the X-axis. Errors bars are SEM. Asterisks indicate the fold change of MF_{Min} relative to VC was a significantly increased at the high dose,

3.4.3 Comparison of Mutation Frequencies by Genomic Features

To explore the genomic features that may be influencing the responsiveness of the different genomic loci, we compared the MF_{Min} of targets based on their genic status, chromatin state, and GC content. MF_{Min} in targets located within intergenic regions were higher but not significantly different from those located in genic regions for any of the dose groups (Supp. Figure 3.4a). Removal of chr2, an intergenic target, further reduced the difference between intergenic and genic regions (Supp. Figure 3.4b). In contrast, MF_{Min} was significantly increased in targets located within heterochromatin compared to those located within euchromatin in the middle and high PRC dose groups (Supp. Figure 3.5a). However, upon the removal the heterochromatic target on chr2, the difference was no longer significant for any of the dose groups (Supp. Figure 3.5b). Finally, we investigated the correlation between the MF_{Min} of each target and the GC content (%) of that target (Supp. Figure 3.5). There was a moderate but significant positive correlation between the target's GC content and the MF_{Min} at the low dose (Pearson's correlation, $r = 0.59$, $p = 6.5 \times 10^{-3}$). However, no other dose group showed a significant correlation between MF_{Min} and target GC content ($p > 0.3$ for all other doses).

3.4.4 PRC Mutation Spectrum

The mutation spectra for both spontaneous and PRC-induced mutations (MF_{Min}) consisted primarily of SNVs, followed by small deletions, small insertions, MNVs, and lastly, structural variants (Figure 3.4). Pairwise comparison of DS mutation data revealed that the overall mutation spectra were significantly different from VC at the middle and high PRC doses (modified contingency table; $p < 0.05$). PRC primarily induced C:G>T:A transitions, accounting for 40% of total mutations at the high dose, followed by T:A>C:G transitions (23%) and T:A>A:T transversions (10%). This differed from the background mutation spectrum, which consisted primarily of C:G>T:A transitions (26%), C:G>A:T transversions (24%), and small deletions (16%). Removing the mutations observed in chr2 did not significantly change the mutation subtype proportions for any of the dose groups (data not shown; $p > 0.9$). We observed significant dose-dependent increases in T:A>C:G transitions relative to VC; C:G>T:A transitions were significantly increased at the middle and high PRC dose relative to VC; and T:A>A:T transversions were increased at the high dose only. When we expanded our analysis to include the two flanking nucleotides, we observed that C:G>T:A transitions in the VC group primarily occurred at CpG sites (Supp. Figure 3.7). Within the PRC-dose groups, C:G>T:A transitions occurred equally within the context of all nucleotides. Finally, we compared the trinucleotide spectra to the SBS signatures from the

COSMIC database. The cosine similarly between the signatures and our spectra were below 0.5 for all signatures, indicating no strong associations with any of the signatures.

A

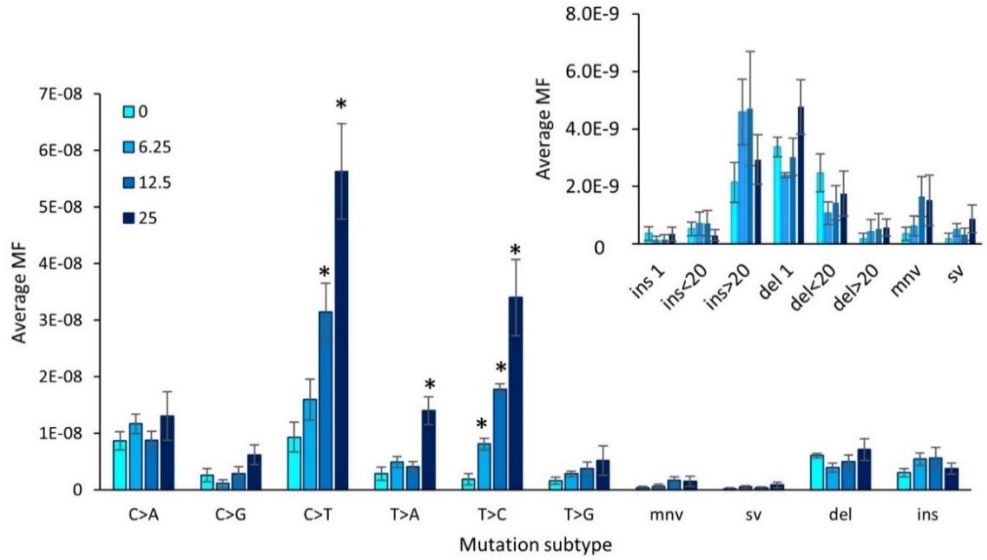

B

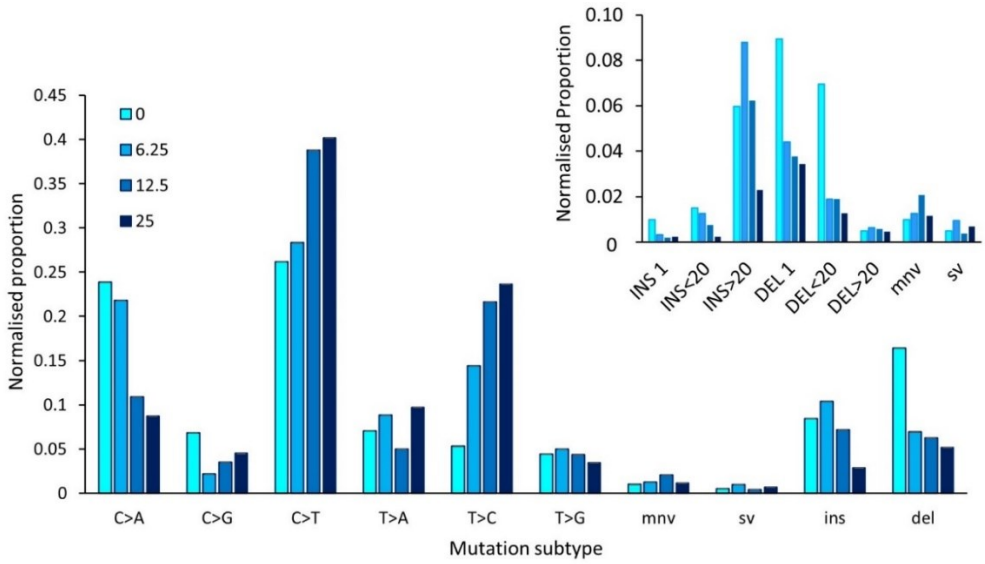

Figure 3.4. Mutation spectrum of controls and PRC dose groups (mg/kg-bw/d)measured by Duplex Sequencing in the germ cells of MutaMouse males. (**A**) Mutation subtypes are presented as the average MF ± SEM. (**B**) Mutation subtypes are represented by the proportion of total mutations normalized to sequencing depth. Plots represent MF_{Min}. Mutation subtypes include the six single nucleotide variants using a pyrimidine reference, multi-nucleotide variants (mnv), structural variants (SV), small insertion (ins), and small deletion (del) mutations. Asterisks indicate a significant increase in MF from controls. Inset figure displays indels categorized by length alongside mnvs and SVs for improved viewing of small MF.

3.4.5 DS Concordance with lacZ Mutant Frequencies

LacZ assay mutant frequency was measured by dividing the number of identified mutant plaques by the total number of plaques counted. Total pfus ranged from 296K – 902K across samples. On average, 8, 10, 15, and 22 mutants were counted for VC, 6.25, 12.5, and 25 mg/kg-bw/day PRC, respectively (Supp. Figure 3.8). PRC induced a significant increase in mutant frequency (x 10^{-5}) relative to VC in the high dose group from 2.25 ± 0.22 mutants per *lacZ* locus (± SEM) in the VC to 4.74 ± 1.94 at the high PRC doses (Table 3.2). No statistically significant increase was observed at the low or middle PRC dose.

Table 3.2. Mean mutant frequency estimates and corresponding pairwise comparisons between dose groups for the *lacZ* assay obtained using a GLM.

Dose (mg/kg-bw/day)	Mutant frequency ± SEM (x 10^{-5})	Fold Changes (± SEM)	p-value*
0	2.25 ± 0.22	---	---
6.25	2.03 ± 0.83	0.91 ± 0.12	0.49
12.5	2.70 ± 1.1	1.15 ± 0.14	0.26
25	4.74 ± 1.9	2.11 ± 0.24	**2.17 x 10^{-6}**

*bold font indicates p-value < 0.05

To assess the concordance between DS and the TGR assay, we compared the DS MF_{Min} to the *lacZ* mutant frequency in the same samples. DS detected a significant increase in MF_{Min} at the middle and high PRC-dose groups, whereas a significant increase in mutant frequency was observed only at the high dose using the TGR assay. Furthermore, a larger fold-increase in MF_{Min} relative to VC at the high dose (3.3-fold) was observed using DS compared to the *lacZ* assay (2.1-fold). DS per-target fold-change in MF_{Min} relative to VC at the high dose exceeded that of the *lacZ* gene for 14 of the 20 DS targets (Figure 3.3). There was a moderate positive correlation between the DS MF_{Min} and *lacZ* mutant frequencies (Supp. Figure 3.9; Pearson's correlation; r=0.62, p = 1.13 x 10^{-3}). Finally, we compared the DS and *lacZ* dose response using BMD modeling to estimate the dose at which a 50% increase in MF occurs above background (Figure 3.5). The BMD (mg/kg-bw/d) for DS MF_{Min} (6.8; 95% CI of 2.9 - 11.3 mg/kg-bw/day) was significantly lower than the BMD for the *lacZ* mutant frequency (17.1; 95% CI 12.4 - 21 mg/kg-bw/day).

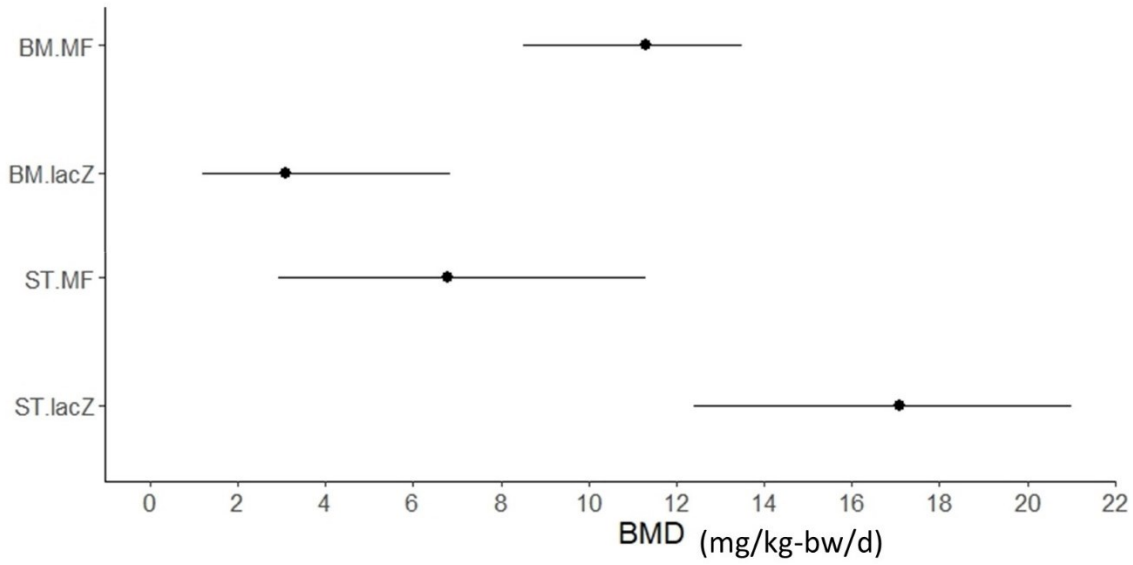

Figure 3.5. 95% confidence intervals (CI) based on BMD model averaging analyses. $\log_{10}$ BMD for a 50% increase of *lacZ* mutant frequency and the Duplex Sequencing MF_{Min} for both germ cells and bone marrow.

3.4.6 Comparison of Mutation Induction Between Male Germ Cells and Bone Marrow

DS data for MutaMouse male germ cells exposed to PRC were compared to DS data described previously from MutaMouse bone marrow for the same dose groups (Dodge et al., 2023). Briefly, PRC induced significant increases in MF_{Min} (x 10^{-8}) relative to VC at all doses in the BM, increasing from 13.1 x 10^{-8} ± 0.75 (± SEM) in the controls to 32.2 ± 1.2 at the high dose. The BM MF_{Min} was significantly higher than in germ cells by a factor of 5.7, 5.2, 4.5, and 4.3 for the VC, 6.25, 12.5 and 25 mg/kg-bw/d dose groups, respectively (Supp. Figure 3.10). However, the germ cells had a larger fold-change in MF_{Min} between controls and the middle (2.0-fold) and high (3.3-fold) dose groups than BM did for the same dose groups (1.6-fold; 2.5-fold respectively) by 1.3X each. The fold-increase relative to VC in germ cells was higher than in BM even upon removal of the chr2 locus mutations.

We next compared the dose response of each tissue using BMD modelling to estimate the dose at which a 50% increase in MF would occur above background (Figure 3.5). For both tissues, we modelled the response of MF_{Min} and the mutant frequency measured by the *lacZ* assay. The BMD (mg/kg-bw/d) for MF_{Min} was 6.8 (95% CI of 2.9 - 11.3 mg/kg-bw/day) for germ cells and 11.29 (95% CI of 8.5 - 13.5 mg/kg-bw/day) for BM; thus, the BMDs for MF_{Min} did not differ significantly between tissues. In contrast to the DS data, the BMD for the *lacZ* mutant frequency was significantly higher for germ cells (17.1; 95% CI 12.4 - 21) than it was for BM (3.1; 95% CI 1.2 - 6.9).

Within the BM, we have observed consistent patterns of relative target susceptibility to mutation induction following exposures to different chemicals (LeBlanc et al., 2022; Dodge et al., 2023). In contrast, our results show very different patterns of target responsiveness in germ cells relative to BM (Figure 3.3). Only one (chr1.2) of the top five targets with the highest background MF_{Min} was consistent between germ cells and BM. Similarly, only chr10 was within the top five targets with the lowest background MF_{Min} for both germ cells and BM. The other four targets are different between tissues. The fold-change (FC) in MF_{Min} between the high dose and VC for each target also differed between tissues. Within germ cells, the top five most responsive targets were on chr2 (FC 17.6), chr18, (FC 5.96), chr9 (FC 5.75), chr5 (FC 5.44) and chr10 (FC 4.70). In contrast, the most responsive targets in the BM were, the *lacZ* gene as measured by the *lacZ* assay (FC 6.37), chr17 (FC 4.34), chr14 (FC 3.62), chr11 (FC 3.46), and chr10 (FC 3.38).

A modified contingency table was used to compare the overall mutation spectra between germ cells and BM. The proportion of mutation subtypes differed significantly between the two tissues for each dose group (Figure 3.6). First, germ cells had significantly higher proportions of indels than BM. Second, there was a shift from C:G>G:C transversions to C:G>T:A transitions in germ cells that was not observed in BM.

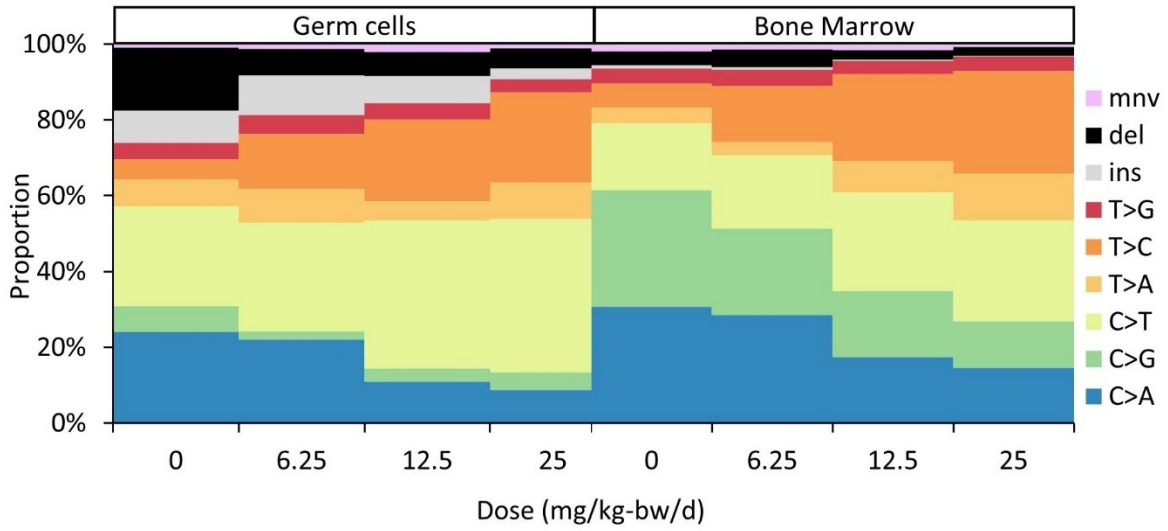

Figure 3.6. Normalized proportion of mutation subtypes at various doses of PRC (mg/kw-bw/d) within MutaMouse germ cells and bone marrow.

3.4.7 Power Analysis to Explore DS Study Designs.

We conducted a power analysis to explore the study design of DS as a mutagenicity test for male mouse germ cells. Data sets were simulated from the observed conditions of our DS experiment including background MF_{Min} of 2.25×10^{-8} and sample variance of 0.25. Within our experiment, we used six animals per group, and sequenced an average of 1.5×10^{9} duplex bases per animal. Under these conditions, we had 58% power and 95% power to detect a 1.5-fold and a 2-fold increase in MF_{Min}, respectively. The MDES that could be achieved under the conditions of our experiment was 1.7-fold. PRC induced a non-significant 1.4-fold increase in MF_{Min} in the low dose group; thus, we were underpowered to detect this effect.

We investigated the power to detect a 1.5-fold increase in MF_{Min} for a range of sample sizes and duplex depths (Figure 3.7). We determined that a minimum of eight animals per group, each sequenced to 3 billion duplex bases, would achieve sufficient power (80%) to detect a 1.5-fold increase. Thus, even upon increasing the sample size, we would also need to sequence twice as deeply to observe this effect with DS in male mouse germ cells. A sample size of six will not yield sufficient power to detect a 1.5-fold increase even upon sequencing 10 billion duplex bases per animal. Our power analyses indicates that 5 animals per group and 600 million duplex bases per animal would achieve sufficient power to detect a 2-fold increase.

A

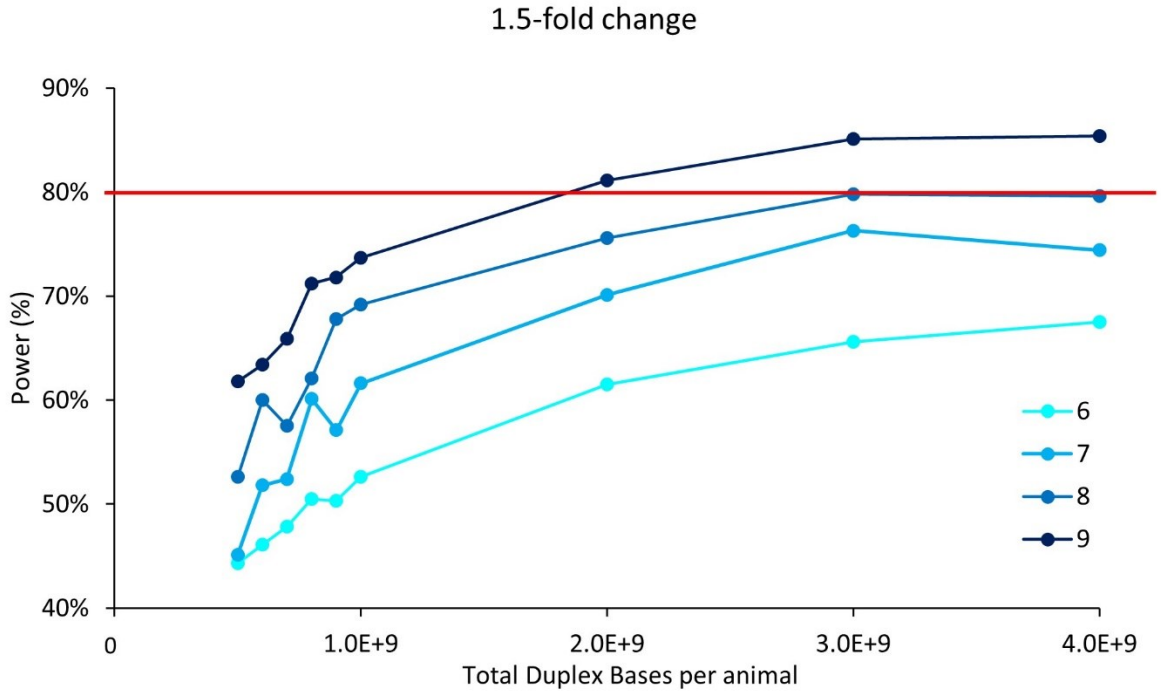

B

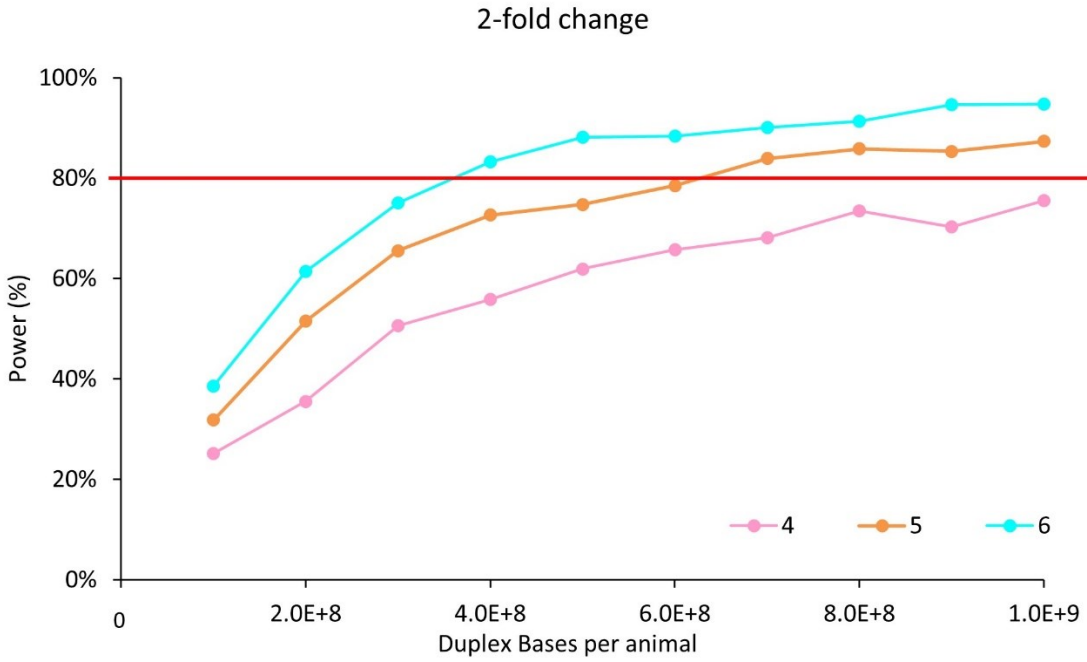

Figure 3.7. The power to detect an increase in MF in MutaMouse germ cells by Total Duplex Base Pairs. Results are displayed for a sample size of 4, 5, and 6 animals per group. (**A**) a 50% increase in MF. (**B**) A 100% increase in MF. The red line indicates the threshold for > 80% power and $p < 0.05$.

3.5 DISCUSSION

We applied DS to study mutations in the germ cells of MutaMouse males following exposure to the chemotherapy agent PRC. Our results clearly demonstrate that PRC is a mouse germ cell mutagen, causing dose-dependent increases in MF by DS and a robust shift in the mutation spectrum. We observed dose-dependent increases in T:A>C:G, T:A>A:T, and C:G>T:A mutations. These results are consistent with the methylation of thymine and guanine residues by PRC. There was a high degree of variability across the target loci both at baseline and following PRC exposures. The *lacZ* locus, measured using the TGR assay, was among the bottom third of responsive loci examined. All these findings differed from results obtained applying DS and the TGR assay to the bone marrow of dose-matched animals, suggesting the contribution of unique mutational mechanisms operating in male germ cells. As discussed below, our findings on the mutagenic susceptibility of mice to PRC are highly relevant to humans receiving chemotherapy, as the doses used in the study are within the same range as those used in the clinic. Overall, deep characterization of MF using DS identified distinct features of germ cell spontaneous and PRC-induced mutagenicity.

3.5.1 Germs Cells Display Reduced Mutagenesis Compared to Somatic Tissues

We compared mutation induction in germ cells to bone marrow in the MutaMouse males. The male germline is the main contributor of inherited *de novo* mutations (Conrad et al., 2011; Crow, 2000; Kong et al., 2012), making it an important target tissue for mutagenicity assessment. We observed that both spontaneous and PRC-induced mutations were nearly ten-fold more frequent in the BM than in germ cells. Our results suggest that there may be intrinsic mechanisms unique to germ cells that protect the germline from mutations so that genetic information may be passed down unaltered.

Proliferation rates may partially explain the difference between tissues. DNA replication is the main mechanism for DNA lesions to be fixed into mutations; thus, MF is correlated with cellular proliferation (Busuttil et al., 2006). BM proliferates very quickly compared to spermatogonial stem cells, providing more opportunities for mutations to occur during DNA replication. However, many studies have reported that mouse and human somatic cells display a higher mutation rate than germ cells even after correcting for proliferation rates (Lynch, 2010; Milholland et al., 2017; Werner & Sottoriva, 2018). The rates of DNA repair may also differ by tissue and would heavily influence the MF. There is evidence that germ cells of the seminiferous tubules maintain their telomere length throughout the ageing process while somatic

cells do not (Moore et al., 2021), suggesting that repair mechanisms differ between tissues. Finally, the distribution of PRC may differ between tissues, with lower levels reaching the testes than the BM. However, we do not know of any study that has characterised the tissue distribution of this chemical.

It should be noted that technical differences between the DNA fragmentation methods may contribute to the differences observed between the germ cells and BM. BM samples were ultrasonically sheared while germ cell samples were subjected to enzymatic fragmentation. Both methods produced high quality reads; however, there is evidence that sonication can induce oxidative nucleotide modifications (Ma et al., 2019). As such, additional errors induced by sonication may partially contribute to the elevated MF observed in BM samples compared to germ cells. Additional work ongoing in the lab have reported that MF in germ cells is reduced by 5-fold when enzymatic fragmentation is used rather than sonication. More thorough comparisons of DNA fragmentation methods should be performed within the same tissue to evaluate its impact on variant calling to clarify our findings.

3.5.2 Germ Cell Mutagenicity is Influenced by Different Genomic Features than Bone Marrow

We next investigated the relative susceptibility of the 20 DS targets to spontaneous and PRC-induced mutagenesis. As it has been reported previously for other chemical exposures (Dodge et al., 2023; LeBlanc et al., 2022; Valentine et al., 2020), the DS targets displayed differential susceptibility to mutagenesis in both VC and PRC dose groups. The pattern of relative susceptibility observed across targets was highly consistent with that observed for other DS studies in MutaMouse male germ cells exposed to BaP, ENU, and coal tar (unpublished data). Most prominently, in all these studies, the target on chr2 has consistently displayed exceptionally high MF following exposure to different mutagens. Similarly, alongside the target on chr2, the target on chr11 and the second target on chr1 (chr1.2) were within the five targets with the highest MF at the high dose group for all studies. This suggests that there is an intrinsic property of these targets that renders them more susceptible to chemical mutagenesis than the other targets. Interestingly, we observed that the pattern of relative susceptibility to mutagenesis of the DS targets differed by tissue. For instance, chr2 displayed the highest fold-change relative to control at the high dose for germ cells. However, it had the third smallest fold-change relative to control in the BM. This suggests that the mechanisms influencing the susceptibility of the DS targets to PRC-mutagenesis are tissue-specific.

We performed comparative analyses between targets to investigate the features that may influence mutagenicity in germ cells and BM. *De novo* mutations and somatic mutations in cancer have been reported to occur at higher rates in closed chromatin states compared to open states (Habig et al., 2021; Michaelson et al., 2012; Schuster-Böckler & Lehner, 2012). Open chromatin states may allow for greater recognition and damage-correction by DNA-repair enzymes leading to reduced mutation rates within euchromatin compared to heterochromatin (Makova & Hardison, 2015). In germ cells, we observed that MF was significantly higher in targets located in heterochromatic regions than those in euchromatic regions, though this effect was largely driven by the target on chr2. No significant effect of chromatin state was observed in the BM following PRC exposure (data not shown) or BaP exposure (LeBlanc et al., 2022). It is unclear why we are observing this effect in germ cells and not somatic cells. More work in characterizing the epigenetic features that modulate chromatin accessibility within the male germline may better enable us to further investigate this phenomenon.

Previous studies using DS to quantify mutations in mouse BM reported that spontaneous, BaP-induced (LeBlanc et al., 2022), and PRC-induced (Dodge et al., 2023) mutations occurred more frequently in intergenic targets than in genic targets. This is consistent with transcription-coupled repair (TCR) in which transcribed regions of the genome are subjected to higher rates of DNA repair. We observed no difference in MF between intergenic and genic targets within germ cells. Importantly, without expression levels for our genic targets it is impossible to draw a firm conclusion on the effects of transcription within germ cells. However, the testis expresses the largest number of genes of any mammalian organ, including over 80% of all protein-coding genes in mice, humans, and other mammals (Melé et al., 2015; Schmidt & Schibler, 1995; Soumillon et al., 2013). Transcription is most prevalent in meiotic spermatocytes and postmeiotic spermatids, however expression levels are also elevated in spermatogonial stem cells and differentiating spermatogonia (Soumillon et al., 2013). As such, we do expect our genic targets to be transcribed.

There are several contradicting views concerning the influence of transcription on germ cell mutagenesis. The widespread transcriptional scanning hypothesis suggests that developing male germ cells use widespread transcription to facilitate germline DNA repair through TCR (Xia et al., 2020). Our results do not support this hypothesis and similar research in humans has reported that elevated transcription levels are associated with decreased mutations within somatic cells, but not within the germ cells of the seminiferous tubules (Moore et al., 2021). Another study reported that with increasing levels of gene expression, somatic mutation rates decreased but mutation rates in the testes actually

increased, suggesting that transcription may be mutagenic within the germline (Chen et al., 2017). The temporary single-stranded state of DNA during transcription may render it more susceptible to damage resulting in elevated mutation rates in highly expressed genes (Jinks-Robertson & Bhagwat, 2014; Xia et al., 2020). It is possible that the balance between TCR and damage differs between tissues, with transcription-coupled damage potentially occurring in germ cells, and TCR dominating in the soma.

3.5.3 Mutation Spectra Suggest Mutagenic Mechanisms Differ Between Tissues

The mutation spectrum provides insights into the mechanisms involved in mutagenesis. DS provides high-quality mutation spectra data that enable a thorough analysis of mutation induction within the tissues. Within the germ cell samples, we observed dose-dependent increases in C:G>T:A transitions, T:A>C:G transitions, and T:A>A:T transversions. This mutation spectrum is consistent with the creation of the mutagenic lesions O_6-methylguanine and O_4- and O_2 – methylthymine by PRC (Fong et al., 1990; Fu et al., 2012; Gerson et al., 2018). Similar dose-dependent increases in these mutation subtypes were observed within the BM by DS.

Despite similarities in response to PRC, there were several notable differences in the mutation spectra of germ cells and BM. We observed a shift in the prevailing spontaneous mutations from C:G>G:C transversions in the BM to C:G>T:A transitions in germ cells. Enrichment of C:G>T:A mutations in the germline compared to the soma has been observed previously (Milholland et al., 2017). It is possible that C:G>T:A transitions are abundant in the germline as a result of increased spontaneous deamination of methylated cytosine. Male germ cells are one of the most methylated cell types, with over 80% of the CpG sites methylated (Popp et al., 2010), providing more opportunities for C:G>T:A mutations to occur. Alternatively, differences in oxidative stress levels between the two tissues may contribute to higher levels of C:G>G:C transversions within the BM. Spermatogonia and spermatogonial stem cells are highly tolerant to reactive oxygen species thanks to elevated levels of base-excision repair and antioxidants (Celino et al., 2011; Chuma et al., 2021; Mori et al., 2021). C:G>G:C transitions are mainly caused by oxidative damage to cells (Kino & Sugiyama, 2001); therefore, it is possible that germ cells reduce these mutations through alternate repair pathways that help prevent oxidative damage.

Germ cells also displayed a higher proportion of spontaneous deletion mutations than the BM. As mentioned, male germ cells are subjected to high rates of transcription, which has been suggested to cause small deletions (Jinks-Robertson & Bhagwat, 2014). Alternatively, technical differences due to DNA

fragmentation methods may induce differences in the mutation spectrum. There is some evidence that enzymatic fragmentation, such as was used on the germ cell libraries, can increase the frequency of insertions and deletions (Knierim et al., 2011). Further analysis comparing DNA fragmentation methods for DS must be done before we can draw a firm conclusion.

3.5.4. DS is More Sensitive to Detecting PRC Mutagenesis in Male Germ Cells Than the TGR Assay

Before DS can be accepted as a regulatory test, its performance should be compared to current, approved assays. We observed a significant positive correlation between DS MF_{Min} and the *lacZ* mutant frequency, but with higher fold-increases in MF_{Min} and a lower BMD for DS compared to *lacZ.* Significant increases in MF_{Min} were observed at lower doses by DS than with the *lacZ* assay. This is the first study to report an elevated response in MF_{Min} by DS compared to the *lacZ* assay. Previously, DS targets showed lower fold-increases and higher BMDs than the *lacZ* assay within the BM following exposure to both PRC (Dodge et al., 2023) and BaP (LeBlanc et al., 2022). As noted above, we observed differences in the susceptibility of genomic loci between tissues; herein, the *lacZ* gene is less susceptible to PRC-induced mutagenesis in the germ cells than in the BM. Interestingly, following exposure to BaP in MutaMouse germ cells, *lacZ* showed an elevated response compared to DS targets, suggesting that there may be a chemical-locus interaction that is influencing the susceptibility to mutagenesis. Future work to test DS with different chemicals will enable us to explore how different mutagenic mechanisms affect the differential susceptibility of genomic loci to mutagenicity in different tissues.

Previous studies in BM that assessed concordance of DS and *lacZ* observed that the correlation between the two assays improved when using MF_{Max} over MF_{Min} (Dodge et al, 2023). The *lacZ* assay is unable to differentiate between mutations that arise independently from those that arise via clonal expansion. As such, the *lacZ* assay is always reporting "MF_{Max}". However, comparison with MF_{Max} was not valid herein given the major clonal expansion events that occurred in the germ cells at the DS targets. In this study, we observed that MF_{Max} was highly variable due to several extreme instances of clonal mutations. The germ cells of the seminiferous tubules arise from a relatively small population of spermatogonial stem cells. Mutations that occur in the stem cells are propagated to all descendants; thus, large instances of clonal mutations are likely a result of a mutation occurring in a stem cell. Our results suggest that using MF_{Max} for mutagenicity testing in germ cells would hinder the assessment of the chemical.

3.5.5 DS Study Designs in Male Germ Cells Require Elevated Sample Sizes and Deeper Sequencing Compared to Bone Marrow

DS shows great promise to revolutionize mutagenicity testing; however, a limitation of DS is the high cost of library preparation and sequencing. We explored the DS study design to determine ways in which we could minimize the sample size or sequencing data yield to reduce expenses. Previous work in MutaMouse BM revealed remarkably low sample variance within DS data (0.062), enabling sample size to be reduced to three animals per group and still retain sufficient power to detect a 50% increase in MF (Dodge et al 2023). Upon performing the same analysis for our germ cell data, we found that our study was underpowered to detect a 1.5-fold increase in MF even with six animals per group. Our study had enough power to detect at minimum a 70% increase in MF. This is in accordance with our statistical analysis; the 1.4-fold change at the low PRC dose was not significant.

The low power in our experiment stems from the relatively high sample variance (0.25) in germ cells compared to BM. This sample variance is consistent with other germ cell studies on MutaMouse males exposed to BaP, ENU, and coal-tar alongside vehicle controls (data not published). Furthermore, the lower MF in germ cells compared to the BM also decreases the power to detect an effect. As such, moving forward, a larger sample size and/or deeper sequencing should be used when assessing chemical mutagenicity in germ cells. Our analysis suggests that a minimum of eight animals per group are necessary to detect a 50% increase in MF. However, germ cell risk assessment may warrant an even lower response threshold. A 50% increase was chosen to compare our results with those obtained in the BM and to reflect current recommendations for BMD analysis by White et al. (2020). Recent studies have suggested that even a modest 25% increase in male germ cell mutations could significantly increase the incidence of detrimental diseases within the population (Beal et al., 2017). Therefore, it may be prudent when performing risk assessment for male germ cells to aim for enough power to detect smaller increases in MF.

3.5.6 Relevance to Humans

During chemotherapy, patients are generally administered 60-100 mg/m^2 PRC daily for 14 days (Diehl & Fuchs, 2007; Solimando & Waddell, 2017). Assuming a mouse body weight/surface area ratio of 3.2 kg/m^2 (Cheung et al., 2009), our mouse exposures correspond roughly to 20 mg/m^2, 40 mg/m^2, and 79 mg/m^2 per day. Our estimated BMD at which a 50% increase in MF occurs was 6.8 mg/kg-bw/d which

is roughly equivalent to 21.8 mg/m^2. Thus, mutagenic effects are observed in mice at doses lower than those used to treat patients. PRC is typically used in combination with other chemotherapy drugs, making it difficult to assess its impact on human health. However, several combination therapies that include PRC are suspected of inducing secondary leukemias (Brusamolino et al., 1998; IARC, 1987; Schellong et al., 1997) and male infertility (Mauz-Körholz et al., 2010; Schellong et al., 1992; Viviani et al., 1985) in patients following treatment. Our results support these effects and suggest that we would expect to see an increased MF and a similar mutation spectrum in PRC-treated patients.

3.6 CONCLUSION

We make use of the many advantages of DS to investigate germ cell mutagenesis in MutaMouse males compared to BM. Our data support that male germ cells have intrinsic mechanisms to protect DNA integrity and reduce mutation burden relative to somatic cells. We observe that both the mutagenic mechanisms and the genomic features influencing mutagenesis differ between tissues. The susceptibility of genomic loci to mutagenesis is further influenced by chemical. This study ultimately supports the assessment of germ cell mutagenicity independently from somatic cells, though we note that a larger sample size is required to measure smaller effects that are more relevant to population health. Furthermore, study of germ cell mutagenesis would benefit from a more thorough understanding of germ cell genetic processes that may modulate mutagenesis including transcription, chromatin state, and other epigenetic features. Additionally, more work testing germ cells with different chemicals will enable us to assess how different mutagenic mechanisms respond within the germline. Finally, we observed an extreme example of differential susceptibility to mutagenesis within the DS panel in this study. The target on chr 2 showed a uniquely high response to chemical mutagenesis within the germline, which raises both biological and technical questions. Characterizing the factors that are responsible for such an extreme mutagenic response may illuminate some of the unique mutagenic mechanisms at play within the germline. In addition, more thought must be given to how outlying loci such as chr2 should be handled during application of DS in a regulatory testing context. Overall, we demonstrate clear differences in the mutagenic response of male germ cells compared to the BM using DS. PRC has effectively been used to treat Hodgkin' lymphoma and other cancers for the past 70 years. In this study we show that PRC induces mutagenic effects in the germ cells of MutaMouse males at doses lower than those used during chemotherapy, suggesting that similar effects may arise in treated patients. The work provides insight into how the germ cells respond to mutagens that will enable us to develop methodologies to better protect the population from genetic disease.

3.7 REFERENCES

Alexandrov, L. B., Kim, J., Haradhvala, N. J., Huang, M. N., Tian Ng, A. W., Wu, Y., Boot, A., Covington, K. R., Gordenin, D. A., Bergstrom, E. N., Islam, S. M. A., Lopez-Bigas, N., Klimczak, L. J., McPherson, J. R., Morganella, S., Sabarinathan, R., Wheeler, D. A., Mustonen, V., Boutros, P., … Yu, W. (2020). The repertoire of mutational signatures in human cancer. *Nature 2020 578:7793*, *578*(7793), 94–101. https://doi.org/10.1038/s41586-020-1943-3

Alonso-Gonzalez, A., Rodriguez-Fontenla, C., & Carracedo, A. (2018). De novo mutations (DNMs) in autism spectrum disorder (ASD): Pathway and network analysis. *Frontiers in Genetics*, *9*(SEP), 406. https://doi.org/10.3389/FGENE.2018.00406/BIBTEX

Arbel-Eden, A., & Simchen, G. (2019). Elevated Mutagenicity in Meiosis and Its Mechanism [Article]. *BioEssays*, *41*(4), e1800235-n/a. https://doi.org/10.1002/bies.201800235

Baarends, W., van der Laan, R., & Grootegoed, J. (2001). DNA repair mechanisms and gametogenesis [Article]. *Reproduction (Cambridge, England)*, *121*(1), 31–39. https://doi.org/10.1530/rep.0.1210031

Bamshad, M. J., Shendure, J., Ng, S. B., Bigham, A. W., Buckingham, K. J., Hannibal, M. C., McMillin, M. J., Gildersleeve, H. I., Beck, A. E., Tabor, H. K., Cooper, G. M., Mefford, H. C., Lee, C., Turner, E. H., Smith, J. D., Rieder, M. J., Yoshiura, K., Matsumoto, N., Ohta, T., … Nickerson, D. A. (2010). Exome sequencing identifies MLL2 mutations as a cause of Kabuki syndrome [Article]. *Nature Genetics*, *42*(9), 790–793. https://doi.org/10.1038/ng.646

Beal, M. A., Meier, M. J., LeBlanc, D. P., Maurice, C., O'Brien, J. M., Yauk, C. L., & Marchetti, F. (2020). Chemically induced mutations in a MutaMouse reporter gene inform mechanisms underlying human cancer mutational signatures. *Communications Biology*, *3*(1). https://doi.org/10.1038/S42003-020-01174-Y

Beal, M. A., Yauk, C. L., & Marchetti, F. (2017). From sperm to offspring: Assessing the heritable genetic consequences of paternal smoking and potential public health impacts. *Mutation Research/Reviews in Mutation Research*, *773*, 26–50. https://doi.org/10.1016/J.MRREV.2017.04.001

Brusamolino, E., Anselmo, A. P., Klersy, C., Santoro, M., Orlandi, E., Pagnucco, G., Lunghi, F., Maurizi-Enrici, R., Baroni, C. D., Lazzarino, M., Mandelli, F., & Bernasconi, C. (1998). The risk of acute leukemia in patients treated for Hodgkin's disease is significantly higher aft [see bined modality programs than after chemotherapy alone and is correlated with the extent of radiotherapy and type and duration of chemotherapy: a case-control study. *Haematologica*, *83*(9), 812–823.

Busuttil, R. A., Rubio, M., Dollé, M. E. T., Campisi, J., & Vijg, J. (2006). Mutant frequencies and spectra depend on growth state and passage number in cells cultured from transgenic lacZ-plasmid reporter mice [Article]. *DNA Repair*, *5*(1), 52–60. https://doi.org/10.1016/j.dnarep.2005.07.006

Celino, F. T., Yamaguchi, S., Miura, C., Ohta, T., Tozawa, Y., Iwai, T., & Miura, T. (2011). Tolerance of Spermatogonia to Oxidative Stress Is Due to High Levels of Zn and Cu/Zn Superoxide Dismutase. *PLoS ONE*, *6*(2), e16938. https://doi.org/10.1371/journal.pone.0016938

Chawanthayatham, S., Valentine, C. C., Fedeles, B. I., Fox, E. J., Loeb, L. A., Levine, S. S., Slocum, S. L., Wogan, G. N., Croy, R. G., & Essigmann, J. M. (2017). Mutational spectra of aflatoxin B_1 in vivo establish biomarkers of exposure for human hepatocellular carcinoma [Article]. *Proceedings of the National Academy of Sciences - PNAS*, *114*(15), E3101–E3109. https://doi.org/10.1073/pnas.1700759114

Chen, C., Qi, H., Shen, Y., Pickrell, J., & Przeworski, M. (2017). Contrasting Determinants of Mutation Rates in Germline and Soma. *Genetics*, *207*(1), 255–267. https://doi.org/10.1534/genetics.117.1114

Cheung, M. C., Spalding, P. B., Gutierrez, J. C., Balkan, W., Namias, N., Koniaris, L. G., & Zimmers, T. A. (2009). Body Surface Area Prediction in Normal, Hypermuscular, and Obese Mice [Article]. *The Journal of Surgical Research*, *153*(2), 326–331. https://doi.org/10.1016/j.jss.2008.05.002

Chuma, S., Kanatsu-Shinohara, M., Katanaya, A., Hosokawa, M., & Shinohara, T. (2021). Genomic stability of mouse spermatogonial stem cells in vitro. *Scientific Reports*, *11*(1), 24199. https://doi.org/10.1038/s41598-021-03658-1

Cliet, I., Melcion, C., & Cordier, A. (1993). Lack of predictivity of bone marrow micronucleus test versus testis micronucleus test: comparison with four carcinogens [Article]. *Mutation Research*, *292*(2), 105–111. https://doi.org/10.1016/0165-1161(93)90137-O

CONRAD, D. F., KEEBLER, J. E. M., ZILVERSMIT, M., CARTWRIGHT, R., ROULEAU, G. A., DALY, M., STONE, E. A., HURLES, M. E., AWADALLA, P., DEPRISTO, M. A., LINDSAY, S. J., YUJUN ZHANG, CASALS, F., IDAGHDOUR, Y., HARTL, C. L., TORROJA, C., & GARIMELLA, K. V. (2011). Variation in genome-wide mutation rates within and between human families [Article]. *Nature Genetics*, *43*(7), 712–714. https://doi.org/10.1038/ng.862

Crow, J. F. (2000). The origins, patterns and implications of human spontaneous mutation [Article]. *Nature Reviews. Genetics*, *1*(1), 40–47. https://doi.org/10.1038/35049558

Demarini, D. M. (2012). Declaring the existence of human germ-cell mutagens. *Environmental and Molecular Mutagenesis*, *53*(3), 166–172. https://doi.org/10.1002/EM.21685

Diehl, V., & Fuchs, M. (2007). Will BEACOPP be the standard for high risk Hodgkin lymphoma patients in advanced stages? *Transfusion and Apheresis Science*, *37*(1), 37–41. https://doi.org/10.1016/j.transci.2007.04.004

Dodge, A.E., LeBlanc, P.M., Zhou, G., Williams, A., Meier, M.J., Van, P., Lo, F.Y., Valentine, C.C., Salk, J.J., Yauk, C.L., Marchetti, F. (2023) Duplex Sequencing Provides Detailed Characterization of Mutation Frequencies and Spectra in the Bone Marrow of MutaMouse Males Exposed to Procarbazine Hydrochloride. *Archives of Toxicology.* Post-print.

Ehling, U. H., & Neuhäuser, A. (1977). Procarbazine-induced specific locus mutations in male mice [Article]. *Mutation Research/Environmental Mutagenesis and Related Subjects*, *46*(3), 218–218. https://doi.org/10.1016/0165-1161(77)90065-6

Fong, L. Y. Y., Jensen, D. E., & Magee, P. N. (1990). DNA methyl-adduct dosimetry and O6-alkylguanine-DNA alkyl transferase activity determinations in rat mammary carcinogenesis by procarbazine and N-methylnitrosourea. *Carcinogenesis*, *11*(3), 411–417. https://doi.org/10.1093/CARCIN/11.3.411

Frankish, A., Diekhans, M., Ferreira, A. M., Johnson, R., Jungreis, I., Loveland, J., Mudge, J. M., Sisu, C., Wright, J., Armstrong, J., Barnes, I., Berry, A., Bignell, A., Carbonell Sala, S., Chrast, J., Cunningham, F., di Domenico, T., Donaldson, S., Fiddes, I. T., … Flicek, P. (2019). GENCODE reference annotation for the human and mouse genomes. *Nucleic Acids Research*, *47*(D1), D766–D773. https://doi.org/10.1093/NAR/GKY955

Fu, D., Calvo, J. A., & Samson, L. D. (2012). Balancing repair and tolerance of DNA damage caused by alkylating agents. *Nature Reviews. Cancer*, *12*(2), 104–120. https://doi.org/10.1038/NRC3185

Gerson, S. L., Caimi, P. F., William, B. M., & Creger, R. J. (2018). Pharmacology and Molecular Mechanisms of Antineoplastic Agents for Hematologic Malignancies. *Hematology: Basic Principles and Practice*, 849–912. https://doi.org/10.1016/B978-0-323-35762-3.00057-3

Gogos, J. A., Karayiorgou, M., Xu, B., Roos, J. L., Dexheimer, P., Boone, B., Plummer, B., & Levy, S. (2011). Exome sequencing supports a de novo mutational paradigm for schizophrenia [Article]. *Nature Genetics*, *43*(9), 864–868. https://doi.org/10.1038/ng.902

Habig, M., Lorrain, C., Feurtey, A., Komluski, J., & Stukenbrock, E. H. (2021). Epigenetic modifications affect the rate of spontaneous mutations in a pathogenic fungus. *Nature Communications*, *12*(1), 5869. https://doi.org/10.1038/s41467-021-26108-y

Hoischen, A., Bon, B. W. M. van, Gilissen, C. F. H. A., Arts, P. J. W., Lier, B. van, Steehouwer, M., Vries, P. F. de, Reuver, R. de, Wieskamp, N. A. W., Mortier, G., Devriendt, K., Amorim, M. Z., Revencu, N., Kidd, A., Barbosa, M., Turner, A., Smith, J., Oley, C., Henderson, A., … Veltman, J. A. (2010). De novo mutations of SETBP1 cause Schinzel-Giedion syndrome [Article]. *Nature Genetics*, *42*(6), 483–485. https://doi.org/10.1038/ng.581

Hoischen, A., van Bon, B. W. M., Roíguez-Santiago, B., Gilissen, C., Vissers, L. E. L. M., de Vries, P., Janssen, I., van Lier, B., Hastings, R., Smithson, S. F., Newbury-Ecob, R., Kjaergaard, S., Goodship, J., McGowan, R., Bartholdi, D., Rauch, A., Peippo, M., Cobben, J. M., Wieczorek, D., … de Vries, B. B. B. A. (2011). De novo nonsense mutations in ASXL1 cause Bohring-Opitz syndrome [Article]. *Nature Genetics*, *43*(8), 729–731. https://doi.org/10.1038/ng.868

Højsgaard, S., & Halekoh, U. (2018). *doBy: Groupwise Statistics, LSmeans, Linear Estimates, Utilities* (R package 4.6.10).

IARC. (1987). MOPP AND OTHER COMBINED CHEMOTHERAPY INCLUDING ALKYLATING AGENTS (Group 1). In *Overall Evaluations of Carcinogenicity: An Updating of IARC Monographs* (7th ed., Vols. 1–42).

IARC Working Group. (1981). Procarbazine Hydrochloride. *IARC Monogr* , *26*, 311–340.

Iossifov, I., Ronemus, M., Levy, D., Wang, Z., Hakker, I., Rosenbaum, J., Yamrom, B., Lee, Y., Narzisi, G., Leotta, A., Kendall, J., Grabowska, E., Ma, B., Marks, S., Rodgers, L., Stepansky, A., Troge, J., Andrews, P., Bekritsky, M., … Wigler, M. (2012). De Novo Gene Disruptions in Children on the Autistic Spectrum [Article]. *Neuron (Cambridge, Mass.)*, *74*(2), 285–299. https://doi.org/10.1016/j.neuron.2012.04.009

Jinks-Robertson, S., & Bhagwat, A. S. (2014). Transcription-associated mutagenesis. *Annual Review of Genetics*, *48*, 341–359. https://doi.org/10.1146/ANNUREV-GENET-120213-092015

Jónsson, H., Sulem, P., Kehr, B., Kristmundsdottir, S., Zink, F., Hjartarson, E., Hardarson, M. T., Hjorleifsson, K. E., Eggertsson, H. P., Gudjonsson, S. A., Ward, L. D., Arnadottir, G. A., Helgason, E. A., Helgason, H., Gylfason, A., Jonasdottir, A., Jonasdottir, A., Rafnar, T., Frigge, M., … Stefansson, K. (2017). Parental influence on human germline de novo mutations in 1,548 trios from Iceland [Article]. *Nature (London)*, *549*(7673), 519–522. https://doi.org/10.1038/nature24018

Kennedy, S. R., Schmitt, M. W., Fox, E. J., Kohrn, B. F., Salk, J. J., Ahn, E. H., Prindle, M. J., Kuong, K. J., Shen, J. C., Risques, R. A., & Loeb, L. A. (2014). Detecting ultralow-frequency mutations by Duplex Sequencing. *Nature Protocols*, *9*(11), 2586–2606. https://doi.org/10.1038/NPROT.2014.170

Kino, K., & Sugiyama, H. (2001). Possible cause of G·C→C·G transversion mutation by guanine oxidation product, imidazolone. *Chemistry & Biology*, *8*(4), 369–378. https://doi.org/10.1016/S1074-5521(01)00019-9

Knierim, E., Lucke, B., Schwarz, J. M., Schuelke, M., & Seelow, D. (2011). Systematic Comparison of Three Methods for Fragmentation of Long-Range PCR Products for Next Generation Sequencing. *PLoS ONE*, *6*(11), e28240. https://doi.org/10.1371/journal.pone.0028240

KONG, A., FRIGGE, M. L., WONG, W. S. W., SIGURDSSON, G., BRAGI WALTERS, G., STEINBERG, S., HELGASON, H., THORLEIFSSON, G., GUDBJARTSSON, D. F., HELGASON, A., MAGNUSSON, O. T., THORSTEINSDOTTIR, U., MASSON, G., STEFANSSON, K., BESENBACHER, S., SULEM, P., MAGNUSSON, G., GUDJONSSON, S. A., SIGURDSSON, A., … JONASDOTTIR, A. (2012). Rate of de novo mutations and the importance of father's age to disease risk [Article]. *Nature (London)*, *488*(7412), 471–475. https://doi.org/10.1038/nature11396

Kuiper, R. P., Ligtenberg, M. J., Hoogerbrugge, N., & Geurts van Kessel, A. (2010). Germline copy number variation and cancer risk [Article]. *Current Opinion in Genetics & Development*, *20*(3), 282–289. https://doi.org/10.1016/j.gde.2010.03.005

Lambert, I. B., Singer, T. M., Boucher, S. E., & Douglas, G. R. (2005). Detailed review of transgenic rodent mutation assays. *Mutation Research*, *590*(1–3), 1–280. https://doi.org/10.1016/J.MRREV.2005.04.002

LeBlanc, D. P. M., Meier, M., Lo, F. Y., Schmidt, E., Valentine, C., Williams, A., Salk, J. J., Yauk, C. L., & Marchetti, F. (2022). Duplex sequencing identifies genomic features that determine susceptibility to benzo(a)pyrene-induced in vivo mutations. *BMC Genomics*, *23*(1). https://doi.org/10.1186/S12864-022-08752-W

Lynch, M. (2010). Evolution of the mutation rate. *Trends in Genetics*, *26*(8), 345–352. https://doi.org/10.1016/j.tig.2010.05.003

Ma, X., Shao, Y., Tian, L., Flasch, D. A., Mulder, H. L., Edmonson, M. N., Liu, Y., Chen, X., Newman, S., Nakitandwe, J., Li, Y., Li, B., Shen, S., Wang, Z., Shurtleff, S., Robison, L. L., Levy, S., Easton, J., & Zhang, J. (2019). Analysis of error profiles in deep next-generation sequencing data. *Genome Biology*, *20*(1), 50. https://doi.org/10.1186/s13059-019-1659-6

Makova, K. D., & Hardison, R. C. (2015). The effects of chromatin organization on variation in mutation rates in the genome. *Nature Reviews. Genetics*, *16*(4), 213. https://doi.org/10.1038/NRG3890

Manders, F., Brandsma, A. M., de Kanter, J., Verheul, M., Oka, R., van Roosmalen, M. J., van der Roest, B., van Hoeck, A., Cuppen, E., & van Boxtel, R. (2022). MutationalPatterns: the one stop shop for the analysis of mutational processes. *BMC Genomics*, *23*(1). https://doi.org/10.1186/S12864-022-08357-3

Marchetti, F., Aardema, M., Beevers, C., van Benthem, J., Douglas, G. R., Godschalk, R., Yauk, C. L., Young, R., & Williams, A. (2018). Simulation of mouse and rat spermatogenesis to inform genotoxicity testing using OECD test guideline 488. *Mutation Research/Genetic Toxicology and Environmental Mutagenesis*, *832–833*, 19–28. https://doi.org/10.1016/J.MRGENTOX.2018.05.020

Marchetti, F., Douglas, G. R., & Yauk, C. L. (2020). A Return to the Origin of the EMGS: Rejuvenating the Quest for Human Germ Cell Mutagens and Determining the Risk to Future Generations. *Environmental and Molecular Mutagenesis*, *61*(1), 42–54. https://doi.org/10.1002/EM.22327

Marchetti, F., Rowan-Carroll, A., Williams, A., Polyzos, A., Berndt-Weis, M. L., & Yauk, C. L. (2011). Sidestream tobacco smoke is a male germ cell mutagen. *Proceedings of the National Academy of Sciences of the United States of America*, *108*(31), 12811–12814. https://doi.org/10.1073/PNAS.1106896108/ASSET/44FF636A-C271-4F00-937E-3534B52DD8C4/ASSETS/GRAPHIC/PNAS.1106896108FIG01.JPEG

Marchetti, F., & Wyrobek, A. J. (2008). DNA repair decline during mouse spermiogenesis results in the accumulation of heritable DNA damage [Article]. *DNA Repair*, *7*(4), 572–581. https://doi.org/10.1016/j.dnarep.2007.12.011

Mauz-Körholz, C., Hasenclever, D., Dörffel, W., Ruschke, K., Pelz, T., Voigt, A., Stiefel, M., Winkler, M., Vilser, C., Dieckmann, K., Karlén, J., Bergsträsser, E., Fosså, A., Mann, G., Hummel, M., Klapper, W., Stein, H., Vordermark, D., Kluge, R., & Körholz, D. (2010). Procarbazine-Free OEPA-COPDAC Chemotherapy in Boys and Standard OPPA-COPP in Girls Have Comparable Effectiveness in Pediatric Hodgkin's Lymphoma: The GPOH-HD-2002 Study. *Journal of Clinical Oncology*, *28*(23), 3680–3686. https://doi.org/10.1200/JCO.2009.26.9381

Melé, M., Ferreira, P. G., Reverter, F., DeLuca, D. S., Monlong, J., Sammeth, M., Young, T. R., Goldmann, J. M., Pervouchine, D. D., Sullivan, T. J., Johnson, R., Segrè, A. V., Djebali, S., Niarchou, A., Wright, F. A., Lappalainen, T., Calvo, M., Getz, G., Dermitzakis, E. T., … Guigó, R. (2015). The human transcriptome across tissues and individuals. *Science (New York, N.Y.)*, *348*(6235), 660. https://doi.org/10.1126/SCIENCE.AAA0355

Michaelson, J. J., Shi, Y., Gujral, M., Zheng, H., Malhotra, D., Jin, X., Jian, M., Liu, G., Greer, D., Bhandari, A., Wu, W., Corominas, R., Peoples, Á., Koren, A., Gore, A., Kang, S., Lin, G. N., Estabillo, J.,

Gadomski, T., … Sebat, J. (2012). Whole-genome sequencing in autism identifies hot spots for de novo germline mutation. *Cell*, *151*(7), 1431–1442. https://doi.org/10.1016/J.CELL.2012.11.019

Milholland, B., Dong, X., Zhang, L., Hao, X., Suh, Y., & Vijg, J. (2017). ARTICLE Differences between germline and somatic mutation rates in humans and mice. *Nature Communications*, *8*. https://doi.org/10.1038/ncomms15183

Moore, L., Cagan, A., Coorens, T. H. H., Neville, M. D. C., Sanghvi, R., Sanders, M. A., Oliver, T. R. W., Leongamornlert, D., Ellis, P., Noorani, A., Mitchell, T. J., Butler, T. M., Hooks, Y., Warren, A. Y., Jorgensen, M., Dawson, K. J., Menzies, A., O'Neill, L., Latimer, C., … Rahbari, R. (2021). The mutational landscape of human somatic and germline cells [Article]. *Nature (London)*, *597*(7876), 381–386. https://doi.org/10.1038/s41586-021-03822-7

Mori, Y., Ogonuki, N., Hasegawa, A., Kanatsu-Shinohara, M., Ogura, A., Wang, Y., McCarrey, J. R., & Shinohara, T. (2021). OGG1 protects mouse spermatogonial stem cells from reactive oxygen species in culture†. *Biology of Reproduction*, *104*(3), 706–716. https://doi.org/10.1093/biolre/ioaa216

O'Brien, J. M., Beal, M. A., Gingerich, J. D., Soper, L., Douglas, G. R., Yauk, C. L., & Marchetti, F. (2014). Transgenic Rodent Assay for Quantifying Male Germ Cell Mutant Frequency [Article]. *Journal of Visualized Experiments*, *90*, e51576. https://doi.org/10.3791/51576

O'Brien, J. M., Beal, M. A., Yauk, C. L., & Marchetti, F. (2016). Next generation sequencing of benzo(a)pyrene-induced lacZ mutants identifies a germ cell-specific mutation spectrum [Article]. *Scientific Reports*, *6*(1), 36743–36743. https://doi.org/10.1038/srep36743

OECD. (2017). *Test No. 238 Overview on genetic toxicology TGs*. OECD. https://doi.org/10.1787/9789264274761-en

OECD 488. (2022). *Test No. 488: Transgenic Rodent Somatic and Germ Cell Gene Mutation Assays*. OECD. https://doi.org/10.1787/9789264203907-en

Olsen, A.-K., Lindeman, B., Wiger, R., Duale, N., & Brunborg, G. (2005). How do male germ cells handle DNA damage? [Article]. *Toxicology and Applied Pharmacology*, *207*(2), 521–531. https://doi.org/10.1016/j.taap.2005.01.060

O'ROAK, B. J., DERIZIOTIS, P., RIEDER, M. J., NICKERSON, D. A., BERNIER, R., FISHER, S. E., SHENDURE, J., EICHLER, E. E., LEE, C., VIVES, L., SCHWARTZ, J. J., GIRIRAJAN, S., KARAKOC, E., MACKENZIE, A. P., NG, S. B., & BAKER, C. (2011). Exome sequencing in sporadic autism spectrum disorders identifies severe de novo mutations [Article]. *Nature Genetics*, *43*(6), 585–589. https://doi.org/10.1038/ng.835

Piegorsch, W. W., & Bailer, A. J. (1994). Statistical approaches for analyzing mutational spectra: some recommendations for categorical data. *Genetics*, *136*(1), 403–416. https://doi.org/10.1093/GENETICS/136.1.403

Popp, C., Dean, W., Feng, S., Cokus, S. J., Andrews, S., Pellegrini, M., Jacobsen, S. E., & Reik, W. (2010). Genome-wide erasure of DNA methylation in mouse primordial germ cells is affected by AID deficiency. *Nature*, *463*(7284), 1101–1105. https://doi.org/10.1038/nature08829

Rathke, C., Baarends, W. M., Awe, S., & Renkawitz-Pohl, R. (2014). Chromatin dynamics during spermiogenesis [Article]. *Biochimica et Biophysica Acta. Gene Regulatory Mechanisms*, *1839*(3), 155–168. https://doi.org/10.1016/j.bbagrm.2013.08.004

Revollo, J., Bhalli, J. A., Tebbe, C., Noteboom, J., Thomas, D., McKinzie, P., Felton, N., Pearce, M. G., & Dobrovolsky, V. N. (2017). Spectrum of Pig-a mutations in T lymphocytes of rats treated with procarbazine. *Mutagenesis*, *32*(6), 571–579. https://doi.org/10.1093/MUTAGE/GEX032

Rouleau, G. A., Girard, S. L., Gauthier, J., Noreau, A., Xiong, L., Zhou, S., Jouan, L., Dionne-Laporte, A., Spiegelman, D., Henrion, E., Diallo, O., Thibodeau, P., Bachand, I., Bao, J. Y. J., Tong, A. H. Y., Lin, C.-H., Millet, B., Jaafari, N., Joober, R., … Krebs, M.-O. (2011). Increased exonic de novo mutation rate

in individuals with schizophrenia [Article]. *Nature Genetics*, *43*(9), 860–863. https://doi.org/10.1038/ng.886

Sasani, T. A., Pedersen, B. S., Gao, Z., Baird, L., Przeworski, M., Jorde, L. B., & Quinlan, A. R. (2019). Large, three-generation human families reveal post-zygotic mosaicism and variability in germline mutation accumulation [Article]. *ELife*, *8*. https://doi.org/10.7554/eLife.46922

Schellong, G., Brämswig, J. H., & Hörnig-Franz, I. (1992). Treatment of children with Hodgkin's disease – Results of the German Pediatric Oncology Group. *Annals of Oncology*, *3*, S73–S76. https://doi.org/10.1093/annonc/3.suppl_4.S73

Schellong, G., Riepenhausen, M., Creutzig, U., Ritter, J., Harbott, J., Mann, G., & Gadner, H. (1997). Low risk of secondary leukemias after chemotherapy without mechlorethamine in childhood Hodgkin's disease. German-Austrian Pediatric Hodgkin's Disease Group. *Journal of Clinical Oncology*, *15*(6), 2247–2253. https://doi.org/10.1200/JCO.1997.15.6.2247

Schmidt, E. E., & Schibler, U. (1995). High accumulation of components of the RNA polymerase II transcription machinery in rodent spermatids. *Development (Cambridge, England)*, *121*(8), 2373–2383. https://doi.org/10.1242/DEV.121.8.2373

Schuster-Böckler, B., & Lehner, B. (2012). Chromatin organization is a major influence on regional mutation rates in human cancer cells. *Nature*, *488*(7412), 504–507. https://doi.org/10.1038/NATURE11273

Solimando, D. A., & Waddell, J. A. (2017). Procarbazine, Lomustine, and Vincristine (PCV) Regimen for Central Nervous System Tumors. *Hospital Pharmacy*, *52*(2), 98–104. https://doi.org/10.1310/hpj5202-98

Soumillon, M., Necsulea, A., Weier, M., Brawand, D., Zhang, X., Gu, H., Barthès, P., Kokkinaki, M., Nef, S., Gnirke, A., Dym, M., deMassy, B., Mikkelsen, T. S., & Kaessmann, H. (2013). Cellular source and mechanisms of high transcriptome complexity in the mammalian testis. *Cell Reports*, *3*(6), 2179–2190. https://doi.org/10.1016/J.CELREP.2013.05.031

Suzuki, T., Uno, Y., Idehara, K., Baba, T., Maniwa, J., Ohkouchi, A., Wang, X., Hayashi, M., Sofuni, T., Tsuruoka, M., Miyajima, H., & Kondo, K. (1999). Procarbazine genotoxicity in the MutaMouse; strong clastogenicity and organ-specific induction of lacZ mutations. *Mutation Research*, *444*(2), 269–281. https://doi.org/10.1016/S1383-5718(99)00060-1

Test No. 488: Transgenic Rodent Somatic and Germ Cell Gene Mutation Assays. (2022). https://doi.org/10.1787/9789264203907-EN

Valentine, C. C., Young, R. R., Fielden, M. R., Kulkarni, R., Williams, L. N., Li, T., Minocherhomji, S., & Salk, J. J. (2020). Direct quantification of in vivo mutagenesis and carcinogenesis using duplex sequencing. *Proceedings of the National Academy of Sciences of the United States of America*, *117*(52), 33414–33425. https://doi.org/10.1073/PNAS.2013724117/-/DCSUPPLEMENTAL

Vissers, L. E. L. M., Ligt, J. de, Gilissen, C. F. H. A., Janssen, I. M., Steehouwer, M., Vries, P. F. de, Lier, B. van, Arts, P. J. W., Wieskamp, N. A. W., Rosario, M. del, Bon, B. W. M. van, Hoischen, A., Vries, L. B. A. de, Brunner, H. G., & Veltman, J. A. (2010). A de novo paradigm for mental retardation [Article]. *Nature Genetics*, *42*(12), 1109–1112. https://doi.org/10.1038/ng.712

Viviani, S., Santoro, A., Ragni, G., Bonfante, V., Bestetti, O., & Bonadonna, G. (1985). Gonadal toxicity after combination chemotherapy for Hodgkin's disease. Comparative results of MOPP vs ABVD [Article]. *European Journal of Cancer & Clinical Oncology*, *21*(5), 601–605. https://doi.org/10.1016/0277-5379(85)90088-4

Waters, M. D., Stack, H. F., Jackson, M. A., Bridges, B. A., & Adler, I.-D. (1994). The performance of short-term tests in identifying potential germ cell mutagens: a qualitative and quantitative analysis [Article]. *Mutation Research*, *341*(2), 109–131. https://doi.org/10.1016/0165-1218(94)90093-0

Werner, B., & Sottoriva, A. (2018). *Variation of mutational burden in healthy human tissues suggests non-random strand segregation and allows measuring somatic mutation rates*. https://doi.org/10.1371/journal.pcbi.1006233

White, P. A., Long, A. S., & Johnson, G. E. (2020). Quantitative Interpretation of Genetic Toxicity Dose-Response Data for Risk Assessment and Regulatory Decision-Making: Current Status and Emerging Priorities. *Environmental and Molecular Mutagenesis*, *61*(1), 66–83. https://doi.org/10.1002/EM.22351

Witt, K. L., Hughes, L. A., Burka, L. T., McFee, A. F., Mathews, J. M., Black, S. L., & Bishop, J. B. (2003). Mouse bone marrow micronucleus test results do not predict the germ cell mutagenicity of N-hydroxymethylacrylamide in the mouse dominant lethal assay. *Environmental and Molecular Mutagenesis*, *41*(2), 111–120. https://doi.org/10.1002/EM.10139

Xia, B., Yan, Y., Baron, M., Wagner, F., Barkley, D., Chiodin, M., Kim, S. Y., Keefe, D. L., Alukal, J. P., Boeke, J. D., & Yanai, I. (2020). Widespread Transcriptional Scanning in the Testis Modulates Gene Evolution Rates. *Cell*, *180*(2), 248-262.e21. https://doi.org/10.1016/J.CELL.2019.12.015

Yauk, C. L., Aardema, M. J., Benthem, J. van, Bishop, J. B., Dearfield, K. L., DeMarini, D. M., Dubrova, Y. E., Honma, M., Lupski, J. R., Marchetti, F., Meistrich, M. L., Pacchierotti, F., Stewart, J., Waters, M. D., & Douglas, G. R. (2015). Approaches for identifying germ cell mutagens: Report of the 2013 IWGT workshop on germ cell assays [Article]. *Mutation Research. Genetic Toxicology and Environmental Mutagenesis*, *783*, 36–54. https://doi.org/10.1016/j.mrgentox.2015.01.008

CHAPTER FOUR

DISCUSSION

ANNETTE DODGE

4.1 SUMMARY OF STUDY OUTCOMES

Assessment of the mutagenic potential of environmental exposures is essential to evaluate the risks posed to human health. *In vivo* mutagenicity assays are used to screen chemicals for potential oncogenic hazard and negative germline effects (Erickson, 2003; Godschalk et al., 2020; Jackson et al., 2018; Marchetti et al., 2020; OECD, 2017). Current practices focus largely on hazard identification (Salk & Kennedy, 2020). However, recently there has been a shift towards understanding the endogenous and exogenous mechanisms that lead to mutagenic outcomes and quantitatively characterizing effects to determine potential human health risks. Advances in this area are providing an empirical link between chemical exposures and incidences of human disease (Alexandrov et al., 2013; Salk & Kennedy, 2020). Unfortunately, the limitations of current mutagenicity assays render them impractical to study mutagenic mechanisms effectively (Salk & Kennedy, 2020; Valentine et al., 2020); thus, there has been a call to improve current testing practices to better reflect 21st century technologies. DS presents a potential alternative to traditional assays that would overcome many of the current challenges involved in characterising mutagenic responses *in vivo* (LeBlanc et al., 2022; Schmitt et al., 2012; Valentine et al., 2020). As such, developing DS for effective mutagenicity testing is essential for modernising mutagenicity testing.

The overarching objectives of this study were to: 1) demonstrate the potential of DS as a robust *in vivo* mutagenicity test that could replace the TGR assay as the next gold-standard in research and regulatory applications; and 2) explore the rich data provided by DS to gain a better understanding of spontaneous and PRC-induced mutagenicity in somatic and germ cells. MutaMouse bone marrow and germ cells were exposed to three doses of PRC alongside controls and then DNA was sequenced using DS to quantify mutation induction. Results were compared to those obtained using the *lacZ* TGR assay on the same samples to assess concordance with OECD-approved methods. As described herein, DS analyses revealed significant increases in mutation frequencies and shifts in the mutation spectra, thus demonstrating its utility in identifying mutagenic hazards in parallel with providing mechanistic insights. Analysis of the DS genomic loci revealed intrinsic differences in the mutagenic response between the two tissues. Overall, this work supports the integration of DS into standard testing strategies and provides recommendations for future work towards this goal.

4.2 FULFILLMENT OF THESIS OBJECTIVES

Objective 1. Evaluate the performance of DS for effective assessment of in vivo spontaneous and induced mutations in bone marrow and germ cells following exposure to PRC.

DS was used to analyse MF in the bone marrow and germ cells of MutaMouse males exposed to PRC alongside vehicle controls. We report a significant dose-response of MF in both tissues, that builds on the work done in previous studies to characterise PRC mutagenicity with the TGR (Beal et al., 2020; Suzuki et al., 1999) and Pig-a assay (Revollo et al., 2017). We assessed the performance of DS by comparing the MF by DS to the mutant frequency obtained by using the OECD-approved *lacZ* TGR assay on the same samples. Significant positive correlations between the two assays were found for both tissues. DS detected significant increases in MF at lower doses than the *lacZ* assay in both tissues. In the bone marrow, DS fold-changes were lower, and BMDs were higher than the *lacZ* assay; however, concordance improved upon the inclusion of potentially clonally expanded mutations in DS frequencies. Mutation spectra in the bone marrow was concordant with what has previously been characterised using the TGR assay, though DS provided higher-resolution data that enabled the detection of secondary mutation subtypes. In the germ cells, DS detected higher fold-changes and a lower BMD than the *lacZ* assay. Overall, DS performs comparably with the gold-standard *lacZ* TGR assay, with improved sensitivity to detect small changes in mutations.

Objective 2. Assess genomic features that drive mutational response and whether they differ between bone marrow and germ cells.

We compared the MF of the twenty 2.4kb genomic targets of the DS mutagenesis panel to investigate which genomic factors might influence the mutation response to genotoxic agents in bone marrow and germ cells. We observed that for both tissues, the relative susceptibility of the targets to both spontaneous and PRC-induced mutations varied. The relative pattern of mutagenic susceptibility of the 20 DS targets and the *lacZ* gene were tissue-specific and influenced by chemical. Within the bone marrow, PRC-induced MF was potentially influenced by transcription status, in which intergenic targets demonstrated higher MF than genic targets. This is consistent with TCR. In contrast, germ cells showed no effect of transcription status, but PRC-induced MF was influenced by chromatin state. Heterochromatic targets had higher MF than euchromatic targets consistent with inefficient DNA repair

in closed chromatin states. Our results suggest that the genomic features that drive the mutational response of genomic loci potentially differ between somatic and germ cells.

Objective 3. Use bioinformatic approaches to characterize mutagenic mechanisms and determine the mutational signature of PRC in bone marrow and germ cells of MutaMouse males.

We characterized a robust shift in the mutation spectra following exposure to PRC in bone marrow and germ cells. In both tissues, dose-dependent increases in C:G>T:A, T:A>C:G, and T:A>A:T mutations were observed, consistent with the methylation of thymine and guanine residues by PRC. In bone marrow, the PRC mutation spectra could be linked to mechanism-associated mutation signatures observed in human cancers. In particular, our spectra were associated with a mutational signature derived from Hodgkin's cell line samples of patients treated with chemotherapy. No mutation signature was associated with the PRC spectra in germ cells. We observed distinct mutation spectra for our two tissues that further supports that there are differences in the mutagenic mechanisms involved in somatic versus germ cell mutagenesis.

Objective 4. Explore optimal DS study designs for assessing mutagenicity by modeling sample size and sequencing data yield within mouse bone marrow and germ cells.

A power analysis was used to determine if sample size and total bases sequenced per animal could be reduced without compromising the quality of the data obtained. Low sample variance within mouse bone marrow allows for the reduction of sample size to three animals per dose group while maintaining power to detect a 50% increase in MF. This is an improvement over the TGR assay, which typically requires five animals per group. In contrast, in the germ cells a lower background MF and a higher sample variance require studies to have at least eight animals per group to detect a 50% increase in MF. As such, moving forward, studies in germ cells should consider larger sample sizes and a higher depth of sequencing tailored to the relevant effect sizes they are striving to detect.

4.3 CONTRIBUTION TO SCIENTIFIC KNOWLEDGE

This thesis contributes to scientific knowledge in three important areas: 1) demonstrating the potential of DS to revolutionize mutagenicity assessment for regulatory toxicology and contributing to efforts to establish it as a mutagenicity test; 2) providing evidence for distinct mutational responses in

germ cells compared to somatic cells that supports the need for independent assessment of germ cell mutagenesis during regulatory testing; 3) characterisation of PRC mutagenicity in mouse tissues.

4.3.1 DS Shows Strong Potential for Mutagenicity Assessment

This work demonstrates the strong potential of DS for assessing *in vivo* mutagenicity within both somatic and germ cells. We provide a thorough evaluation of the performance of DS compared to the OECD-approved *lacZ* assay and highlight many of the advantages that DS has over traditional testing methods. DS overcomes many of the limitations faced by current assays (Kennedy et al., 2014). We clearly demonstrate using the DS panel that the *lacZ* reporter gene for mutagenicity testing has a higher degree of variability in the mutagenic response compared to analysis of MF_{min} of different endogenous genomic loci. In our second study, we further demonstrate that the relative susceptibility of genomic loci varies between tissues and by chemical. As such, quantification of mutations from a single reporter gene, such as the *lacZ* gene, cannot inform on the many endogenous factors that influence mutagenesis. DS offers a better representation of the whole genome by quantifying mutations in a panel of loci that encapsulates a broad spectrum of genomic features. Further advantages of DS over traditional assays include improved ability to measure mutation spectra, possible integration with other toxicity tests, and the application to any tissue or model organism, including humans.

This work also contributes to the effort aimed at establishing DS as a mutagenicity test by broadening the range of chemicals and tissues that have been tested. Before an assay can be accepted for regulatory testing, thorough evaluation of its performance across a range of chemicals and tissues is required to assess its precision. Previously DS had only been tested using established mutagens such as BaP (LeBlanc et al., 2022) and ENU (Valentine et al., 2020), which are known to have potent mutagenic effects. Herein we demonstrate that DS shows excellent sensitivity to detect smaller changes in mutations by a less potent mutagen. Furthermore, we characterize the variable mutagenic responses of the DS loci between tissues and chemicals. Finally, we inform on DS study design in both the bone marrow and male germ cells using power analyses to determine minimum sample sizes and sequencing depths needed to detect biologically relevant effects. This work will help guide future DS studies.

Lastly, we demonstrate the utility of DS for analysis of mutagenic mechanisms. High-resolution mutation spectra identified increases in mutation subtypes not detectable by the TGR assay, likely resulting from an improved ability to detect secondary mutagenic lesions. Furthermore, we demonstrate

how DS mutation spectra can be used to empirically link chemical exposures to mechanisms relevant to human cancers through mutational signature analyses. PRC is an antineoplastic agent used to treat Hodgkin's lymphoma (Andrieu et al., 2016). Herein we show that PRC-mutation spectra are associated with the mutational signature observed in Hodgkin's cell line samples of people treated with chemotherapy and errors in mismatch repair. Providing empirical evidence towards the contribution of a chemical towards the mutational signature of human cancers will improve both chemical mutagenicity assessment and aid in finding potential aetiologies for incidences of human cancers. Overall, our work strongly supports the use of DS in mutagenicity testing and provides useful information on study design that will provide a framework for future studies.

4.3.2 Germ Cells Demonstrate Distinct Mutational Responses Compared to Somatic Cells

Historically, regulatory authorities assumed that decisions based on evidence of chemical mutagenicity in somatic cells, such as the bone marrow, will by default protect the germline. However, there are several examples of mutagens inducing changes in germ cells at doses that do not elicit a response in somatic cells (Marchetti et al., 2011; Witt et al., 2003). In this work we provide evidence of distinct mutagenic mechanisms operating within male germ cells compared to somatic cells. Differences in background mutation spectra may underlie differences in intrinsic mutagenic mechanisms or DNA repair pathways. Furthermore, differences in the genetic factors that drive mutagenesis result in differential sensitivity of genomic loci to mutagenesis between tissues. As such, genomic loci that may be negative in the bone marrow, may be positive in the germline. Our work supports the independent assessment of germ cell mutagenesis from somatic cells and provides insight into some of the unique features of germ cell mutagenicity.

4.3.3 PRC Mutagenic Effects are Observed in MutaMouse tissues at Human-Relevant Doses

We provide a thorough characterization of PRC mutagenicity within the bone marrow and germ cells of MutaMouse males. We observe significant increases in mutation frequencies and robust shift in the mutation spectra in both tissues. Mice were exposed to 0, 6.25, 12.5, and 25 mg/kg-bw/d PRC orally for 28 days. This is roughly equivalent to 20 mg/m^2, 40 mg/m^2, and 79 mg/m^2 per day (Cheung et al., 2009). During chemotherapy, patients typically receive 60-100mg/m^2 PRC orally for 14 days in a cycle, and typically undergo 4-8 cycles of treatment (Diehl & Fuchs, 2007; Solimando & Waddell, 2017). Though

our exposure period is longer, we observe significant effects in mice at doses much lower than those used to treat patients; 20mg/m^2 in the bone marrow and 40 mg/m^2 in germ cells. This is an incredibly important finding concerning the risks of developing secondary malignancies because of PRC treatment.

4.4 FUTURE DIRECTIONS

There are three main areas for future work following this study: 1) DS optimization and performance evaluation; 2) use of DS in regulatory decision-making; and 3) advancing biological understanding.

4.4.1 DS Optimization and Performance Evaluation

This thesis contributes towards implementing DS as a mutagenicity test; however, there remains much work to be done to establish DS as an approved method for regulatory testing. First, standard DS protocols must be established for optimal testing strategies. We took steps towards this by characterizing optimal DS study designs based on the parameters of our experiments. Work should continue to confirm the reproducibility of DS; this involves testing a variety of chemicals with different mutagenic potencies across different tissues, model organisms, and across testing facilities. Another priority is to establish a historical control for DS data amongst our tissues of interest. This will involve quantifying the mutation frequency from many control animals across several different tissues to confirm that results are precise and establish inter-study variance. Furthermore, a well-established control mutation spectrum will enable the isolation of true differences from confounding factors during analysis of mutagenic mechanisms. This work and previous studies have so far assessed DS in bone marrow (LeBlanc et al., 2022) and male germ cells. There are many more tissues that are target tissues for cancer and other genetic diseases. Further testing is required to establish study design parameters for these tissues.

Another important parameter to consider is sample variance. As we observed in our power analyses, this plays a large role in determining the minimum detectable effect size of the study. Exposure studies in our lab within bone marrow (LeBlanc et al., 2022) and germ cells (data not published) have so far shown consistent sample variances for each tissue; however, more work should be done in different laboratories to confirm these observations. Establishing the main sources of variation within a DS study will be a great asset when designing future studies (Piegorsch et al., 1995). Once reproducible

background mutation frequencies and sample variance have been established, the optimal number of animals and depth of sequencing can be calculated for a DS mutagenicity assay.

It is essential that DS is tested with a broad range of chemicals before it is accepted as a mutagenicity test. First, DS should be tested with mutagens of different modes of action. So far, DS has been tested on a relatively small range of mutagenic mechanisms (LeBlanc et al., 2022; Valentine et al., 2020). BaP induces bulky adducts whilst ENU and PRC both act as alkylating agents. Other mechanisms should be evaluated to ensure that analysis of the mutagenic mechanism by DS can be applied more widely. Furthermore, as noted in our second data chapter, the susceptibility of genomic loci to mutagenesis may vary based on the chemical. As such, work to characterise the susceptibility of the DS loci to different chemicals should be done. Second, DS must be tested with low doses of mutagens and non-mutagenic compounds. While it is important to determine that DS can detect a positive mutagenic effect, it is equally important to assess its performance with negative compounds. This work has demonstrated DS to be highly sensitive, therefore it is important to determine its specificity (i.e., its ability to correctly identify non-mutagenic chemicals).

DS is a novel technology and is still being improved; however, a standard protocol must be in place before it can be used for mutagenicity testing. In this work, our comparison between bone marrow and germ cells was potentially confounded by differences in DNA fragmentation methods. Although there has been some evidence in our lab to suggest that enzymatic fragmentation might result in lower mutation frequencies than ultrasonication, no direct comparison has yet been made. It will be important in the future to thoroughly compare how changes to the DS protocol might affect results. Future work should directly compare mutation frequencies and spectra between protocols within the same tissue as the technology evolves. Additionally, previous work *in vitro* has shown strong inter-lab reproducibility in DS results, however, reproducibility of *in vivo* studies has yet to be tested in depth. Therefore, inter-lab comparisons of *in vivo* DS studies are recommended.

Finally, it should be noted that DS is not the only error-corrected technology available. Other studies have made use of similar technologies to great success (Bae et al., 2023). While this work focuses on the performance of DS in a mutagenicity test setting, work should also expand to show the benefits of sequencing technologies as a whole for mutagenicity testing.

4.4.2. DS in Regulatory Decision-Making

Further consideration must be given to how a regulatory call should be made based on a panel of targets. Previous mutagenicity assays have relied on the use of a single reporter gene to quantify mutagenesis. DS moves away from that approach and quantifies mutations within 20 genomic loci. However, as discussed throughout this thesis, the genomic loci show variable susceptibility to mutagenesis. As such, questions remain on how to approach a regulatory assessment should only a few loci demonstrate a positive response. A conservative approach would be to base the call on loci with a higher susceptibility to mutagenesis. This will ensure the genome is well protected but could also lead to false positives. It is possible that a similar approach has been unintentionally used with the *lacZ* assay, which has proven to be relatively more susceptible to mutations compared to the DS loci in some tissues. Additional consideration should be given to the response of the DS loci in different tissues. As we observed in the second data chapter, target susceptibility to mutagenesis depends on the tissue of interest. This gives more weight to the use of a panel of targets for mutagenicity testing, as mutational responses in specific tissues are less likely to be missed in a panel rather than a single target.

Next, it will also be important to establish a threshold for relevant mutation induction by DS. During hazard characterisation in risk assessment, the nature of the dose-response relationship is explored in detail. Regulatory authorities identify from toxicity studies a dose that will be deemed acceptable for human intake i.e., a dose under which it is confidently expected that there would be no appreciable adverse health effects (More et al., 2022). Previous work based on the TGR assays recommend a 50% increase in mutant frequency as a point of departure (White et al., 2020). However, as previously described, it is expected that even a 25% increase in mutation frequency of the male germline could detrimentally affect human populations (Beal et al., 2017). As such, a lower threshold may be prudent to allow for a more conservative approach to risk assessment. Furthermore, the threshold must be re-established based on DS data. As noted throughout this thesis, DS and the TGR assay report different response levels to chemical-induced mutagenesis stemming from the use of a panel versus a single reporter gene. Therefore, we must conduct a series of DS exposure studies to re-establish a threshold that will reflect DS sensitivity. However, it should be noted that 50% my still be a useful threshold that can continue to be used for potency comparisons. In this thesis, we made use of the 50% threshold to compare the performance of different assays and the mutagenic response of different tissues to the same doses.

4.4.3. Advancing Biological Understanding

Throughout the course of this study several interesting areas of research were identified that require further investigation. First, more work is required to characterise the factors driving the susceptibility of different loci to mutagenesis. In this study we identified some genomic features that are likely influencing the mutagenic response of the DS loci. However, a more thorough analysis of these features would be helpful. Most importantly, steps should be taken to measure the expression levels of the genic loci within the DS panel for each tissue of interest. This will allow a more relevant analysis of the effects transcription has on mutagenesis. Next, one large gap remains the influence of epigenetic factors on mutagenicity. In this study, we observed differences due to chromatin state within germ cells but not bone marrow. It is uncertain whether chromatin state differs between germ cells and bone marrow, or if the mechanisms involved differ between tissues. A more detailed map of the epigenetic markers within the tissues of interest would allow for a more comprehensive analysis of different epigenetic processes on mutagenesis. Finally, a more powerful analysis would sequence an entire genome with DS to conduct an analysis of the factors that are influencing the mutagenic response. While DS remains very costly, it may be worth investing in a study of the whole genome and look beyond the relatively small DS panel. Not only would this provide an opportunity to study many genomic factors involved in mutagenesis, but it will also enable us to compare the performance of the DS panel in reflecting whole genome mutagenicity.

The target on chromosome 2 was particularly interesting as it displayed a uniquely high mutagenic response in the germ cells of MutaMouse males but not the bone marrow. Future work should aim to study this locus specifically to understand the factors driving its extreme response. Work should detail the mutation frequency and spectra of this target across several studies and tissues to identify any locations that may be mutation hotspots. Furthermore, it would be helpful to study the epigenetic factors at this locus in germ cells to see if there are any unique factors that may be influencing the response. It will be important to understand the biological reasons behind the extreme response of this target in order to make an informed decision on how to handle it during regulatory testing. It may be prudent to remove this target from the panel.

The results of this thesis suggest that there are unique mutagenic mechanisms in male MutaMouse germ cells compared to bone marrow. Investigation of these germ cell-specific mechanisms would greatly enhance our understanding of germline mutagenesis. Work should continue to

characterise the DNA repair mechanisms within male germ cells, especially during the mitotic phases of spermatogenesis when the majority of mutations are occurring. It would also be beneficial to investigate mutations that may be specific to meiosis. To this end, research comparing the mutation spectra at different phases of spermatogenesis (i.e., mitotic phase, meiotic phase, etc.) would help us elucidate if there are any meiotic-specific mutations occurring. Further work with mechanism-associated mutational signatures may also help elucidate differences between somatic and germ cells. We did not find any strong associations between our germ cell spectra and the SBS signatures of the COSMIC database. However, recent work has extracted germline-specific mutational signatures (Seplyarskiy et al., 2021) that may better reflect the mechanisms at work within the male germline compared to signatures extracted from human cancers.

Lastly, this study detailed the mutagenic effects of PRC within MutaMouse tissues at doses that were comparable to those used during chemotherapy. It would be prudent to continue the assessment of PRC mutagenic risk within human samples. Effects in both bone marrow and male germ cells are of concern. Patients who underwent combination treatments that included PRC have been known to develop secondary leukemias (Henry-Amar, 1992; IARC, 1981; Kaldor et al., 1988), suggesting that mutagenic effects in the bone marrow may lead to secondary cancer. Historically, it has been difficult to distinguish the effects of PRC from the effects of other compounds as it is almost always used in combination with other chemotherapy agents. Comparing the mutational signatures of these secondary leukemias to PRC mutation spectra may allow us to find evidence of PRC's contribution to the disease even amongst confounding effects of other compounds. Human effects in male germ cells often lead to life-long infertility, though some men do regain fertility several years after treatment (Viviani et al., 1985; Schellong et al., 1992; Mauz-Körholz et al., 2010). In this case, mutagenic effects in male germ cells would be of concern to the health of potential offspring that may be fathered following treatment. Previous work has reported several cases of high levels of de novo mutations in children of men who underwent chemotherapy (Kaplanis et al., 2022). As such, further investigation into the mutagenic effects of PRC in humans is recommended.

4.5 CONCLUDING REMARKS

This study demonstrated the strong potential of DS as an *in vivo* mutagenicity test that could ultimately replace the TGR assay as the next gold-standard. DS successfully identified mutagenic hazard of a known mutagen, PRC, in both somatic and germ cells. Although the results were highly comparable

to those obtained using the *lacZ* assay, key added advantages include increased sensitivity, multi-locus responses that increases the human-relevance and weight of evidence for decision-making, and the availability of high-resolution mutation spectra that provided mechanistic insight into the mutagenic response. Analysis of the relative susceptibility of the DS loci revealed intrinsic differences between bone marrow and germ cells that may underlie differences in mutagenic mechanisms or DNA repair. Importantly, this is the first germ cell study applying DS and one of only a handful of other studies exploring its use in chemical mutagenicity assessment. Thus, the work provides essential data to inform DS study design that will facilitate future research. Overall, our findings strongly support the very high value of DS as a mutagenicity test to revolutionize regulatory testing.

4.6 REFERENCES

Alexandrov, L. B., Nik-Zainal, S., Wedge, D. C., Campbell, P. J., & Stratton, M. R. (2013). Deciphering signatures of mutational processes operative in human cancer. *Cell Reports*, *3*(1), 246–259. https://doi.org/10.1016/J.CELREP.2012.12.008

Andrieu, J. M., Ifrah, N., Payen, C., Fermanian, J., Coscas, Y., & Flandrin, G. (2016). Increased risk of secondary acute nonlymphocytic leukemia after extended-field radiation therapy combined with MOPP chemotherapy for Hodgkin's disease. *Https://Doi.Org/10.1200/JCO.1990.8.7.1148*, *8*(7), 1148–1154. https://doi.org/10.1200/JCO.1990.8.7.1148

Bae, J. H., Liu, R., Roberts, E., Nguyen, E., Tabrizi, S., Rhoades, J., Blewett, T., Xiong, K., Gydush, G., Shea, D., An, Z., Patel, S., Cheng, J., Sridhar, S., Liu, M. H., Lassen, E., Skytte, A.-B., Grońska-Pęski, M., Shoag, J. E., … Adalsteinsson, V. A. (2023). Single duplex DNA sequencing with CODEC detects mutations with high sensitivity [Article]. *Nature Genetics*, *55*(5), 871. https://doi.org/10.1038/s41588-023-01376-0

Beal, M. A., Meier, M. J., LeBlanc, D. P., Maurice, C., O'Brien, J. M., Yauk, C. L., & Marchetti, F. (2020). Chemically induced mutations in a MutaMouse reporter gene inform mechanisms underlying human cancer mutational signatures. *Communications Biology*, *3*(1). https://doi.org/10.1038/S42003-020-01174-Y

Beal, M. A., Yauk, C. L., & Marchetti, F. (2017). From sperm to offspring: Assessing the heritable genetic consequences of paternal smoking and potential public health impacts. *Mutation Research/Reviews in Mutation Research*, *773*, 26–50.

Cheung, M. C., Spalding, P. B., Gutierrez, J. C., Balkan, W., Namias, N., Koniaris, L. G., & Zimmers, T. A. (2009). Body Surface Area Prediction in Normal, Hypermuscular, and Obese Mice [Article]. *The Journal of Surgical Research*, *153*(2), 326–331. https://doi.org/10.1016/j.jss.2008.05.002

Diehl, V., & Fuchs, M. (2007). Will BEACOPP be the standard for high risk Hodgkin lymphoma patients in advanced stages? *Transfusion and Apheresis Science*, *37*(1), 37–41. https://doi.org/10.1016/j.transci.2007.04.004

Erickson, R. P. (2003). Somatic gene mutation and human disease other than cancer. *Mutation Research/Reviews in Mutation Research*, *543*(2), 125–136. https://doi.org/10.1016/S1383-5742(03)00010-3

Godschalk, R. W. L., Yauk, C. L., van Benthem, J., Douglas, G. R., & Marchetti, F. (2020). In utero Exposure to Genotoxicants Leading to Genetic Mosaicism: An Overlooked Window of Susceptibility in Genetic Toxicology Testing? *Environmental and Molecular Mutagenesis*, *61*(1), 55–65. https://doi.org/10.1002/EM.22347

Henry-Amar, M. (1992). Second cancer after the treatment for Hodgkin's disease: a report from the International Database on Hodgkin's Disease [Article]. *Annals of Oncology*, *3*(suppl-4), S117–S128. https://doi.org/10.1093/annonc/3.suppl_4.S117

IARC. (1981). Evaluations of the Carcinogenic Risk of Chemicals o Humans; Some Antineoplastic and Immunosuppressive Agents. *International Agency for Research on Cancer. WHO*, *26*, 311–340.

Jackson, M., Marks, L., May, G. H. W., & Wilson, J. B. (2018). The genetic basis of disease. In *Essays in Biochemistry* (Vol. 62, Issue 5, pp. 643–723). Portland Press Ltd. https://doi.org/10.1042/EBC20170053

Kaldor, J. M., Day, N. E., & Hemminki, K. (1988). Quantifying the carcinogenicity of antineoplastic drugs [Article]. *European Journal of Cancer & Clinical Oncology*, *24*(4), 703–711. https://doi.org/10.1016/0277-5379(88)90302-1

Kaplanis, J., Ide, B., Sanghvi, R., Neville, M., Danecek, P., Coorens, T., Prigmore, E., Short, P., Gallone, G., McRae, J., Genomics England Research Consortium, Carmichael, J., Barnicoat, A., Firth, H., O'Brien,

P., Rahbari, R., & Hurles, M. (2022). Genetic and chemotherapeutic influences on germline hypermutation. Nature, 605(7910), 503–508. https://doi.org/10.1038/s41586-022-04712-2

Kennedy, S. R., Schmitt, M. W., Fox, E. J., Kohrn, B. F., Salk, J. J., Ahn, E. H., Prindle, M. J., Kuong, K. J., Shen, J. C., Risques, R. A., & Loeb, L. A. (2014). Detecting ultralow-frequency mutations by Duplex Sequencing. *Nature Protocols*, *9*(11), 2586–2606. https://doi.org/10.1038/NPROT.2014.170

LeBlanc, D. P. M., Meier, M., Lo, F. Y., Schmidt, E., Valentine, C., Williams, A., Salk, J. J., Yauk, C. L., & Marchetti, F. (2022). Duplex sequencing identifies genomic features that determine susceptibility to benzo(a)pyrene-induced in vivo mutations. *BMC Genomics*, *23*(1). https://doi.org/10.1186/S12864-022-08752-W

Marchetti, F., Douglas, G. R., & Yauk, C. L. (2020). A Return to the Origin of the EMGS: Rejuvenating the Quest for Human Germ Cell Mutagens and Determining the Risk to Future Generations. *Environmental and Molecular Mutagenesis*, *61*(1), 42–54. https://doi.org/10.1002/EM.22327

Marchetti, F., Rowan-Carroll, A., Williams, A., Polyzos, A., Berndt-Weis, M. L., & Yauk, C. L. (2011). Sidestream tobacco smoke is a male germ cell mutagen. *Proceedings of the National Academy of Sciences of the United States of America*, *108*(31), 12811–12814. https://doi.org/10.1073/PNAS.1106896108/ASSET/44FF636A-C271-4F00-937E-3534B52DD8C4/ASSETS/GRAPHIC/PNAS.1106896108FIG01.JPEG

Mauz-Körholz, C., Hasenclever, D., Dörffel, W., Ruschke, K., Pelz, T., Voigt, A., Stiefel, M., Winkler, M., Vilser, C., Dieckmann, K., Karlén, J., Bergsträsser, E., Fosså, A., Mann, G., Hummel, M., Klapper, W., Stein, H., Vordermark, D., Kluge, R., & Körholz, D. (2010). Procarbazine-free OEPA-COPDAC chemotherapy in boys and standard OPPA-COPP in girls have comparable effectiveness in pediatric Hodgkin's lymphoma: the GPOH-HD-2002 study. Journal of clinical oncology : official journal of the American Society of Clinical Oncology, 28(23), 3680–3686. https://doi.org/10.1200/JCO.2009.26.9381

More, S. J., Bampidis, V., Benford, D., Bragard, C., Halldorsson, T. I., Hernández-Jerez, A. F., Bennekou, S. H., Koutsoumanis, K., Lambré, C., Machera, K., Mennes, W., Mullins, E., Nielsen, S. S., Schrenk, D., Turck, D., Younes, M., Aerts, M., Edler, L., Sand, S., . . . Schlatter, J. (2022). Guidance on the use of the benchmark dose approach in risk assessment. *EFSA Journal*, *20*(10), e07584. https://doi.org/10.2903/j.efsa.2022.7584

OECD. (2017). *Test No. 238 Overview on genetic toxicology TGs*. OECD. https://doi.org/10.1787/9789264274761-en

Piegorsch, W. W., Margolin, B. H., Shelby, M. D., Johnson, A., French, J. E., Tennant, R. W., & Tindall, K. R. (1995). Study design and sample sizes for a lacI transgenic mouse mutation assay. *Environmental and Molecular Mutagenesis*, *25*(3), 231–245. https://doi.org/10.1002/EM.2850250310

Revollo, J., Bhalli, J. A., Tebbe, C., Noteboom, J., Thomas, D., McKinzie, P., Felton, N., Pearce, M. G., & Dobrovolsky, V. N. (2017). Spectrum of Pig-a mutations in T lymphocytes of rats treated with procarbazine. *Mutagenesis*, *32*(6), 571–579. https://doi.org/10.1093/MUTAGE/GEX032

Salk, J. J., & Kennedy, S. R. (2020). Next-Generation Genotoxicology: Using Modern Sequencing Technologies to Assess Somatic Mutagenesis and Cancer Risk. *Environmental and Molecular Mutagenesis*, *61*(1), 135–151. https://doi.org/10.1002/EM.22342

Schellong, G., Brämswig, J. H., & Hörnig-Franz, I. (1992). Treatment of children with Hodgkin's disease--results of the German Pediatric Oncology Group. Annals of oncology : official journal of the European Society for Medical Oncology, 3 Suppl 4, 73–76. https://doi.org/10.1093/annonc/3.suppl_4.s73

Schmitt, M. W., Kennedy, S. R., Salk, J. J., Fox, E. J., Hiatt, J. B., & Loeb, L. A. (2012). Detection of ultra-rare mutations by next-generation sequencing. *Proceedings of the National Academy of Sciences of the*

United States of America, *109*(36), 14508–14513. https://doi.org/10.1073/PNAS.1208715109/-/DCSUPPLEMENTAL/PNAS.201208715SI.PDF

Seplyarskiy, V. B., Soldatov, R. A., Koch, E., McGinty, R. J., Goldmann, J. M., Hernandez, R. D., Barnes, K., Correa, A., Burchard, E. G., Ellinor, P. T., McGarvey, S. T., Mitchell, B. D., Vasan, R. S., Redline, S., Silverman, E., Weiss, S. T., Arnett, D. K., Blangero, J., Boerwinkle, E., He, J., … Sunyaev, S. (2021). Population sequencing data reveal a compendium of mutational processes in the human germ line. Science (New York, N.Y.), 373(6558), 1030–1035.

Solimando, D. A., & Waddell, J. A. (2017). Procarbazine, Lomustine, and Vincristine (PCV) Regimen for Central Nervous System Tumors. *Hospital Pharmacy*, *52*(2), 98–104. https://doi.org/10.1310/hpj5202-98

Suzuki, T., Uno, Y., Idehara, K., Baba, T., Maniwa, J., Ohkouchi, A., Wang, X., Hayashi, M., Sofuni, T., Tsuruoka, M., Miyajima, H., & Kondo, K. (1999). Procarbazine genotoxicity in the MutaMouse; strong clastogenicity and organ-specific induction of lacZ mutations. *Mutation Research*, *444*(2), 269–281. https://doi.org/10.1016/S1383-5718(99)00060-1

Valentine, C. C., Young, R. R., Fielden, M. R., Kulkarni, R., Williams, L. N., Li, T., Minocherhomji, S., & Salk, J. J. (2020). Direct quantification of in vivo mutagenesis and carcinogenesis using duplex sequencing. *Proceedings of the National Academy of Sciences of the United States of America*, *117*(52), 33414–33425. https://doi.org/10.1073/PNAS.2013724117/-/DCSUPPLEMENTAL

Viviani, S., Santoro, A., Ragni, G., Bonfante, V., Bestetti, O., & Bonadonna, G. (1985). Gonadal toxicity after combination chemotherapy for Hodgkin's disease. Comparative results of MOPP vs ABVD. European journal of cancer & clinical oncology, 21(5), 601–605. https://doi.org/10.1016/0277-5379(85)90088-4

White, P. A., Long, A. S., & Johnson, G. E. (2020). Quantitative Interpretation of Genetic Toxicity Dose-Response Data for Risk Assessment and Regulatory Decision-Making: Current Status and Emerging Priorities. *Environmental and Molecular Mutagenesis*, *61*(1), 66–83. https://doi.org/10.1002/EM.22351

Witt, K. L., Hughes, L. A., Burka, L. T., McFee, A. F., Mathews, J. M., Black, S. L., & Bishop, J. B. (2003). Mouse bone marrow micronucleus test results do not predict the germ cell mutagenicity of N-hydroxymethylacrylamide in the mouse dominant lethal assay. *Environmental and Molecular Mutagenesis*, *41*(2), 111–120. https://doi.org/10.1002/EM.10139

SUPPLEMENTARY MATERIALS

CHAPTER TWO

Supplementary Table 2.1. Mutagenesis panel targets and their chromosomal locations*

Target	Start Location	End Location	Genic Context	Chromatin State	%GC
chr1	69304217	69306617	Intergenic	Euchromatin	37.3
chr1.2	155235938	155238338	Genic	Heterochromatin	54
chr2	50833175	50835575	Intergenic	Heterochromatin	45.3
chr3	109633160	109635560	Genic	Euchromatin	39.2
chr4	96825280	96827680	Intergenic	Euchromatin	39.4
chr5	18210612	18213012	Intergenic	Euchromatin	35.6
chr6	119170706	119173106	Genic	Euchromatin	40.5
chr7	142683053	142685453	Genic	Euchromatin	45.9
chr8	43954521	43956921	Intergenic	Euchromatin	35.6
chr9	28648072	28650472	Genic	Euchromatin	37.3
chr10	21442014	21444414	Intergenic	Euchromatin	46.3
chr11	37934364	37936764	Intergenic	Heterochromatin	35.8
chr12	80601542	80603942	Genic	Heterochromatin	52
chr13	74030071	74032471	Genic	Euchromatin	50.4
chr14	13076171	13078571	Intergenic	Heterochromatin	42.2
chr15	66779762	66782162	Genic	Euchromatin	44
chr16	72381580	72383980	Intergenic	Heterochromatin	38.3
chr17	94009028	94011428	Intergenic	Euchromatin	35.2
chr18	81262078	81264478	Intergenic	Euchromatin	47.3
chr19	4618813	4621213	Genic	Heterochromatin	56.1

* mm10 coordinates; from LeBlanc et al., 2022.

Supplementary Table 2.2. Summary of DS mutation induction within the 24 MutaMouse bone marrow samples.

Sample	Dose	Mut Depth Min	Mut Depth Max	Total Depth	MF_{Min}	MF_{Max}
DNA02444	0	114	129	728699669	1.56443E-07	1.77028E-07
DNA02445	0	122	135	817107673	1.50531E-07	1.65217E-07
DNA02447	0	110	113	846953699	1.31058E-07	1.59395E-07
DNA02448	0	87	96	780873955	1.11414E-07	1.4471E-07
DNA02449	0	96	101	770727712	1.24558E-07	1.24558E-07
DNA02450	0	94	99	826612593	1.13717E-07	1.22185E-07
DNA02446	6.25	113	135	657402286	1.71889E-07	1.50593E-07
DNA02451	6.25	138	189	820030039	1.68287E-07	2.30479E-07
DNA02452	6.25	155	188	782634215	1.99327E-07	2.40214E-07
DNA02453	6.25	108	141	853755000	1.265E-07	1.65153E-07
DNA02454	6.25	146	181	855903938	1.71748E-07	2.11472E-07
DNA02455	6.25	155	179	978513059	1.59426E-07	1.82931E-07
DNA02456	12.5	169	213	763679775	2.22606E-07	2.78913E-07
DNA02457	12.5	164	216	809078854	2.027E-07	2.6697E-07
DNA02458	12.5	142	195	706111588	2.01101E-07	2.7616E-07
DNA02459	12.5	177	238	891637902	1.98511E-07	2.66924E-07
DNA02460	12.5	137	197	729478918	1.87805E-07	2.70056E-07
DNA02461	12.5	152	233	750681115	2.03815E-07	3.10385E-07
DNA02462	25	295	419	793981642	3.71545E-07	5.2772E-07
DNA02463	25	275	431	841255951	3.26892E-07	5.12329E-07
DNA02464	25	221	346	791686322	2.80414E-07	4.37042E-07
DNA02465	25	243	374	756161273	3.22682E-07	4.94603E-07
DNA02466	25	274	448	936111894	2.927E-07	4.78575E-07
DNA02467	25	229	289	666280326	3.452E-07	4.33751E-07

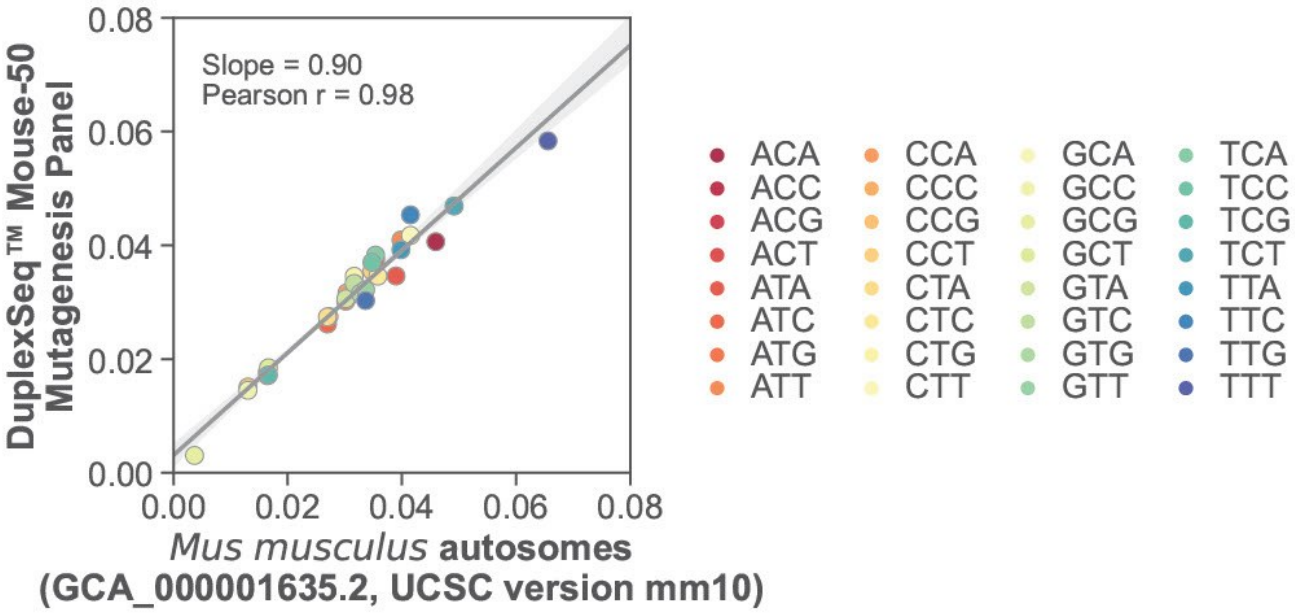

Supplementary Figure 2.1. Correlation of the trinucleotide composition between the DS Mouse-50 Mutagenesis Panel and the mm10 Mus musculus autosomes. Data represents the proportion of trinucleotides.

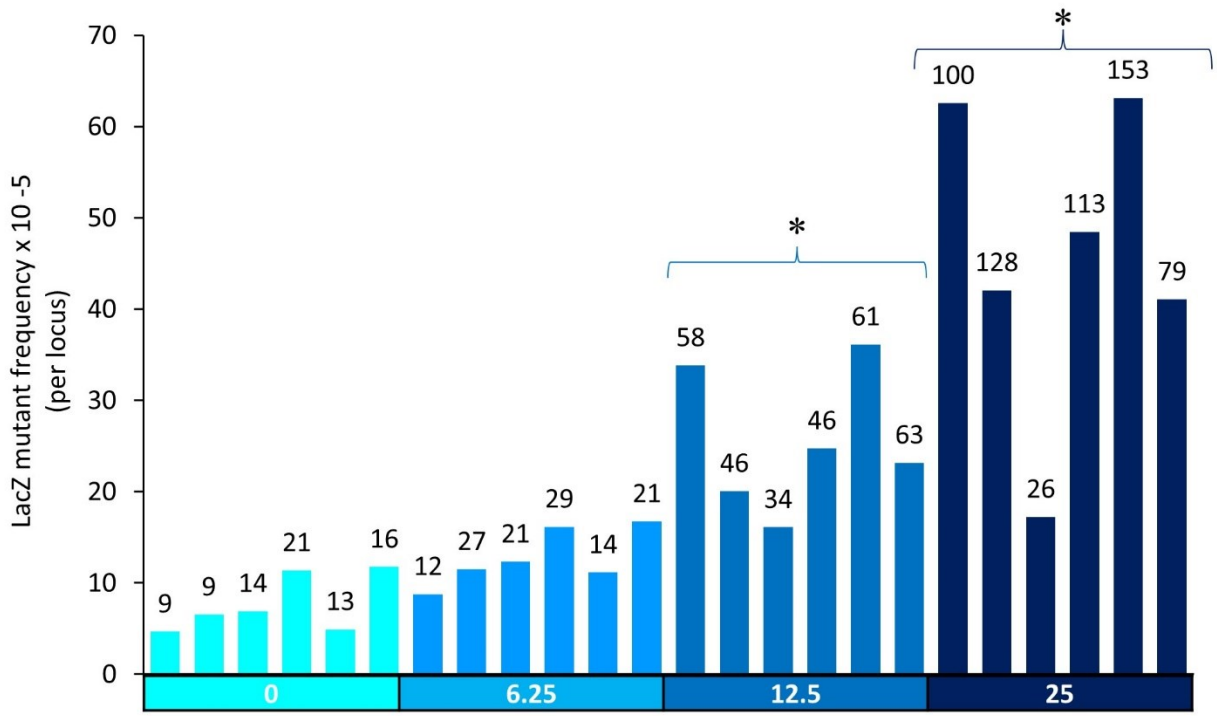

Supplementary Figure 2.2. *LacZ* mutant frequencies in the bone marrow of MutaMouse males at various doses of PRC. Bars represent mutant frequency (mutations per locus) for each animal. Data labels indicate total number of mutant plaques counted for each animal. The X-axis indicates PRC dose group (mg/kg-bw/day). Asterisks indicate a significant difference relative to the controls in the average mutant frequency across animals.

A

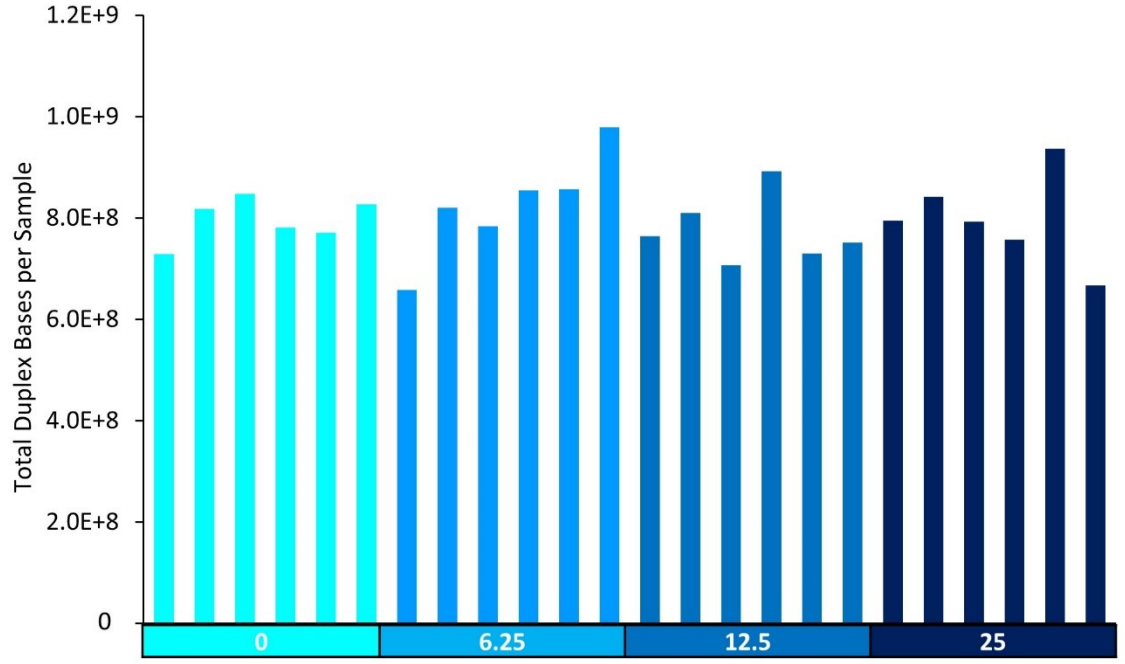

B

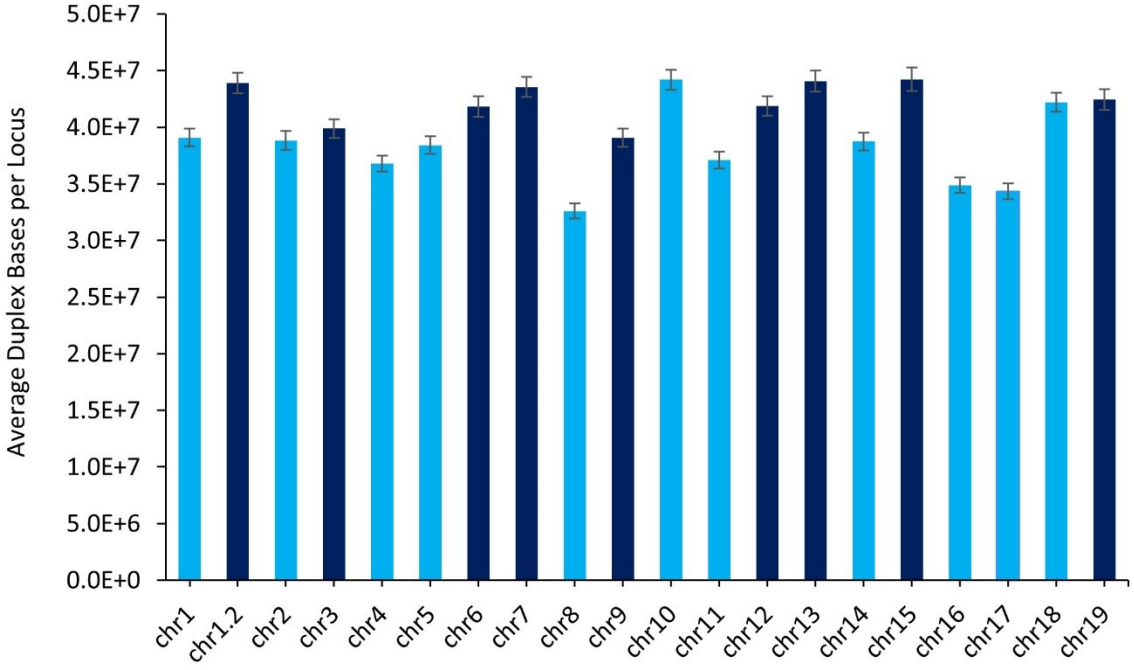

Supplementary Figure 2.3. Duplex data yields. (A) Total duplex bases per individual animal. X-axis indicates dose group (mg/kg-bw/day PRC). (B) Average duplex bases per chromosome location per animal. Error bars represent standard error of the mean (SEM).

A

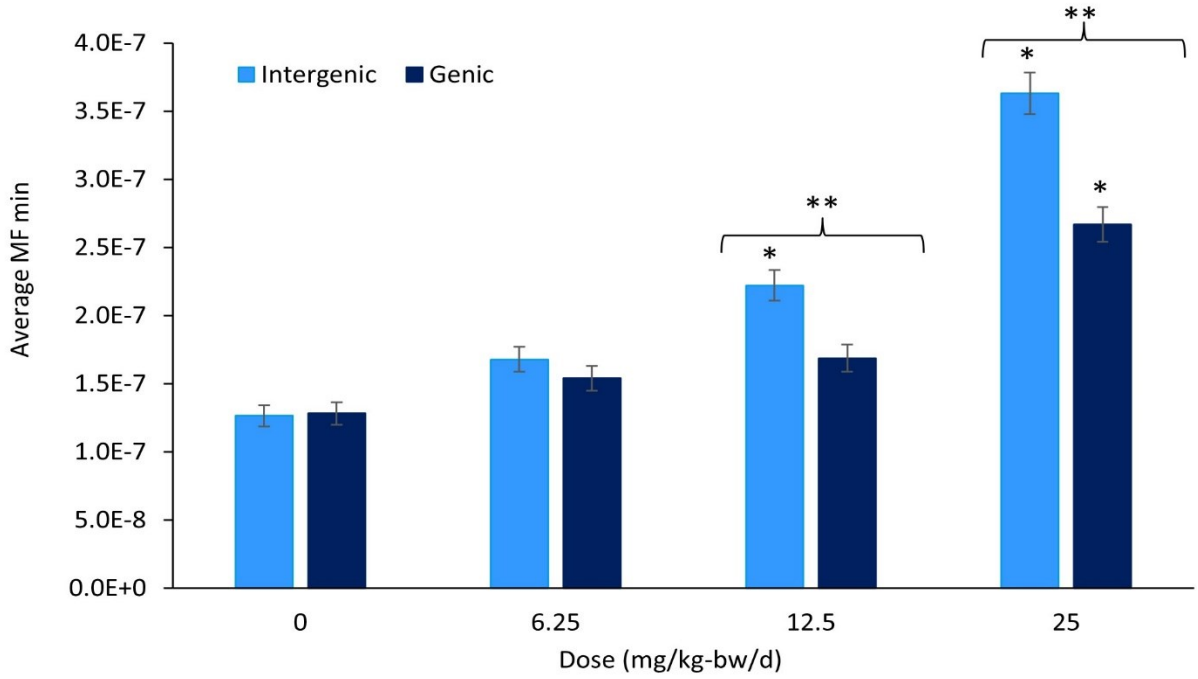

B

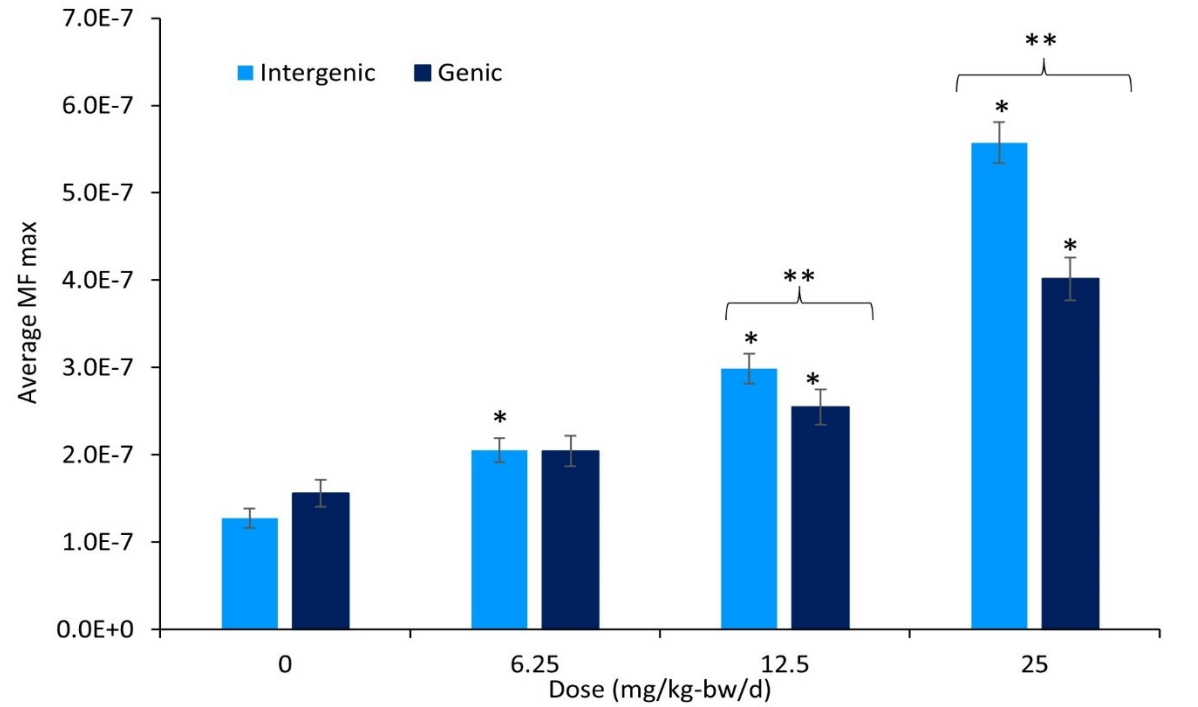

Supplementary Figure 2.4. MF of intergenic targets compared to genic targets for various doses of PRC using A) MF_{Min} and B) MF_{Max}. Data are represented as the mean ± SEM (mutations per bp). Asterisks indicate a significant difference in MF of dose groups relative to controls (GLM, $p < 0.05$). Double asterisks indicate a significant difference in MF between intergenic and genic targets within a dose group (GLMM, $p < 0.05$).

A

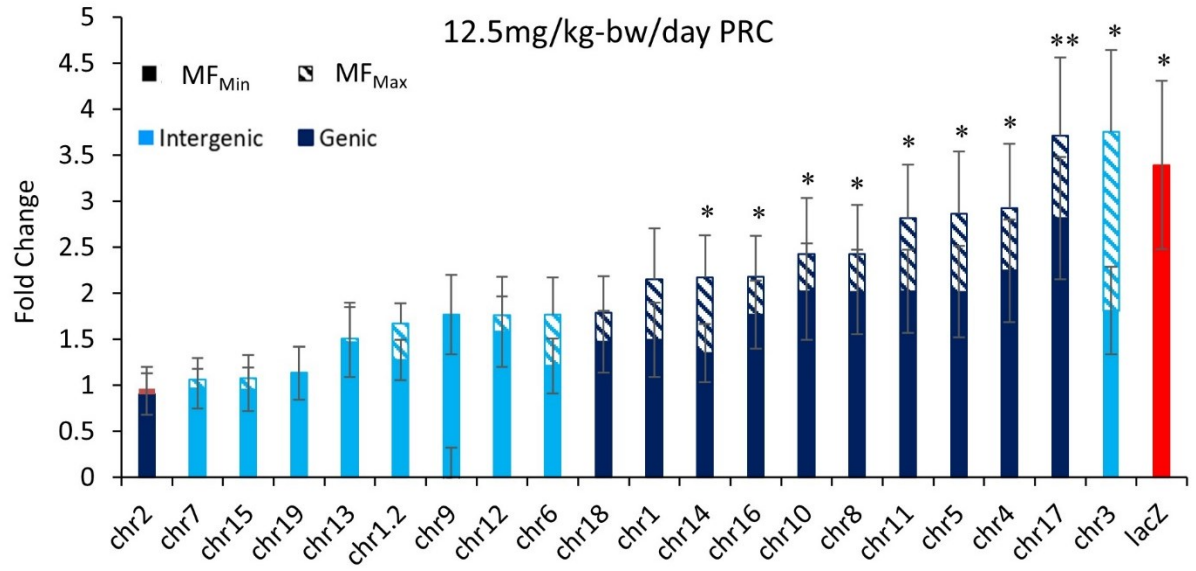

B

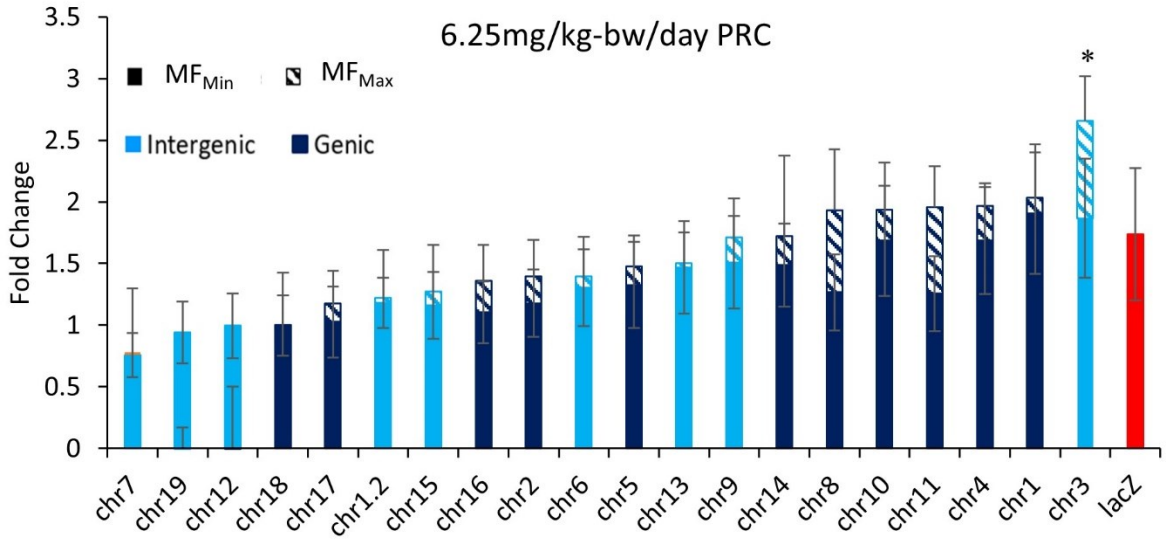

Supplementary Figure 2.5. Fold change in MF between PRC VC (**A**) and middle-dose group (**B**) and low-dose group for the 20 DS targets as well as for the *lacZ* gene (red bar), estimated using a general linear mixed model. DS targets are listed along the X-axis. Errors bars are SEM. Asterisks indicate the fold change was a significant increase in MF_{Max} from VC. Double asterisks indicate a significant increase for both MF_{Max} and MF_{Min}.

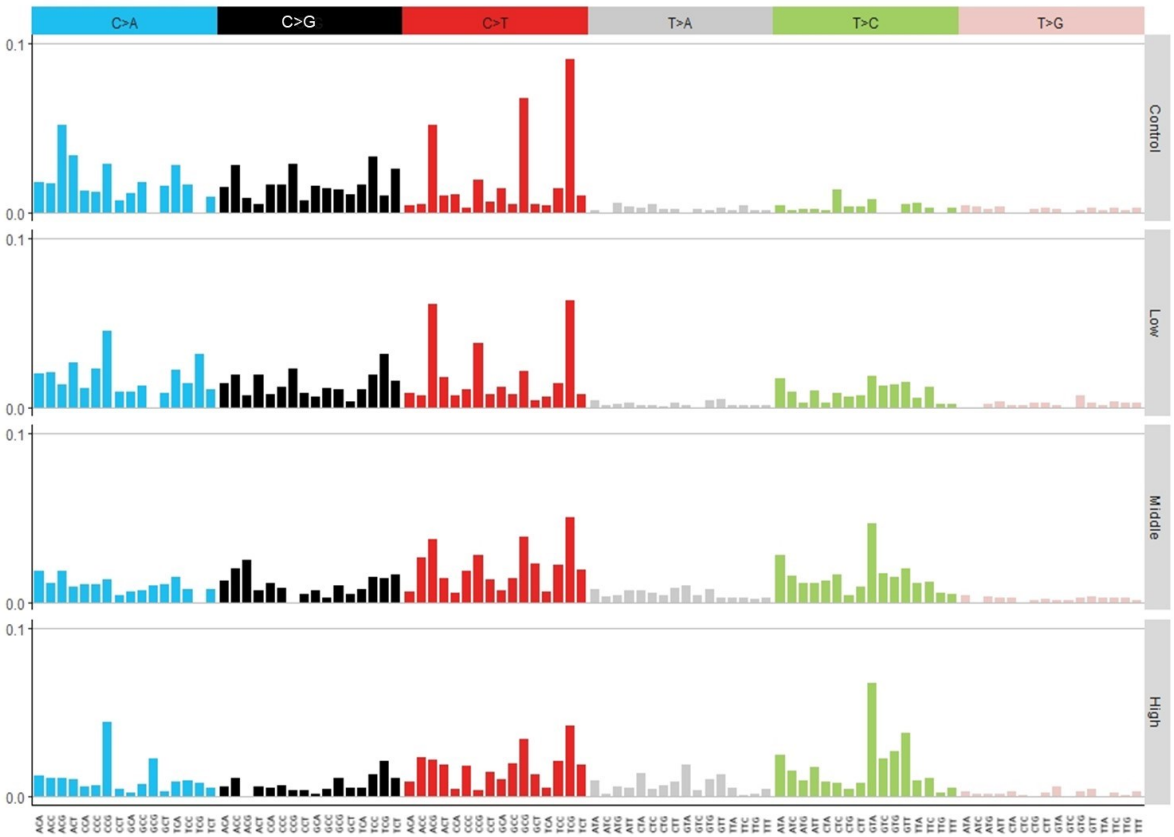

Supplementary Figure 2.6. Mutation spectra with trinucleotide context of controls and PRC dose groups measured by Duplex Sequencing in the bone marrow of MutaMouse males. Dose groups are listed along the right: 6.25 mg/kg-bw/d (Low), 12.5 mg/kg-bw/d (Middle), 25 mg/kg-bw/d (High). The substitution subtype is listed along the top, the mutation including the two flanking nucleotides are listed along the bottom. Mutation subtypes are represented by the proportion of total mutations.

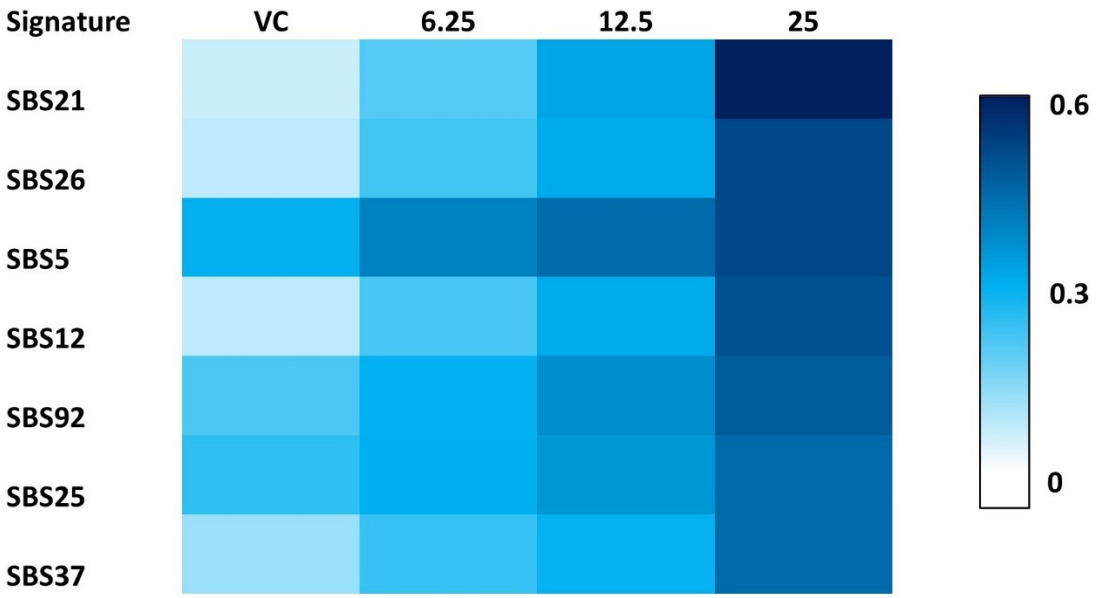

Supplementary Figure 2.7. Cosine similarity of COSMIC SBS signatures to the trinucleotide mutation spectrum of each dose group. Data represents mean cosine value for the dose group.

Supplementary Table 3.1. Summary of DS mutation induction within the 24 MutaMouse germ cell samples.

Sample	Dose (mg/kw-bw/d)	Depth (bp)	Mut Count Min	Mut Count Max	Mfmin	Mfmax
PRC_ST_113.1	0	8.99E+08	17	18	1.89E-08	2.00E-08
PRC_ST_114.1	0	9.03E+08	15	16	1.66E-08	1.77E-08
PRC_ST_115.1	0	9.35E+08	19	21	2.03E-08	2.25E-08
PRC_ST_116.1	0	8.84E+08	26	67	2.94E-08	7.58E-08
PRC_ST_119.1	0	7.07E+08	13	13	1.84E-08	1.84E-08
PRC_ST_120.1	0	1.09E+09	34	122	3.11E-08	1.12E-07
PRC_ST_137.1	6.25	1.13E+09	35	74	3.09E-08	6.54E-08
PRC_ST_138.1	6.25	9.13E+08	32	115	3.51E-08	1.26E-07
PRC_ST_139.1	6.25	7.96E+08	19	20	2.39E-08	2.51E-08
PRC_ST_140.1	6.25	1.26E+09	38	86	3.02E-08	6.83E-08
PRC_ST_143.1	6.25	7.88E+08	36	52	4.57E-08	6.60E-08
PRC_ST_144.1	6.25	9.58E+08	24	52	2.50E-08	5.43E-08
PRC_ST_169.1	12.5	1.13E+09	33	37	2.93E-08	3.29E-08
PRC_ST_173.1	12.5	9.41E+08	47	171	5.00E-08	1.82E-07
PRC_ST_174.1	12.5	1.06E+09	65	865	6.12E-08	8.14E-07
PRC_ST_175.1	12.5	1.29E+09	73	83	5.66E-08	6.43E-08
PRC_ST_185.1	12.5	9.18E+08	31	88	3.38E-08	9.59E-08
PRC_ST_186.1	12.5	1.15E+09	47	50	4.08E-08	4.34E-08
PRC_ST_201.1	25	1.10E+09	114	164	1.04E-07	1.49E-07
PRC_ST_202.1	25	1.35E+09	113	2363	8.39E-08	1.75E-06
PRC_ST_203.1	25	9.26E+08	58	74	6.26E-08	7.99E-08
PRC_ST_206.1	25	7.37E+08	88	1221	1.19E-07	1.66E-06
PRC_ST_207.1	25	1.05E+09	49	54	4.67E-08	5.15E-08
PRC_ST_208.1	25	1.17E+09	53	85	4.52E-08	7.24E-08

A

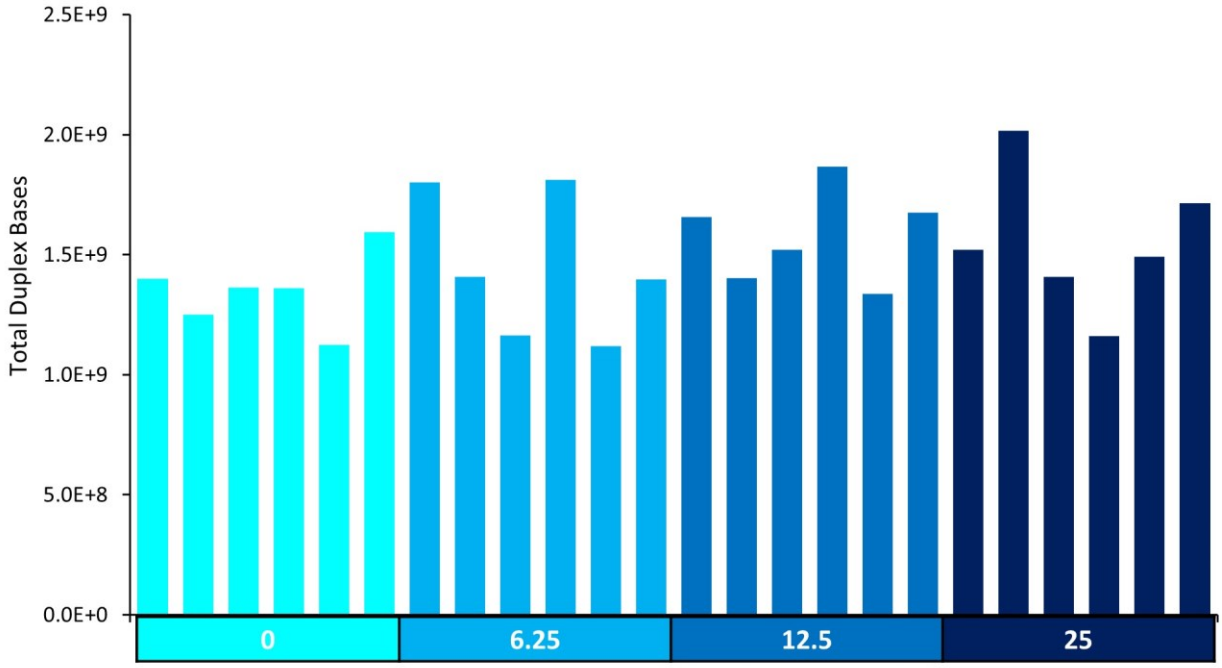

B

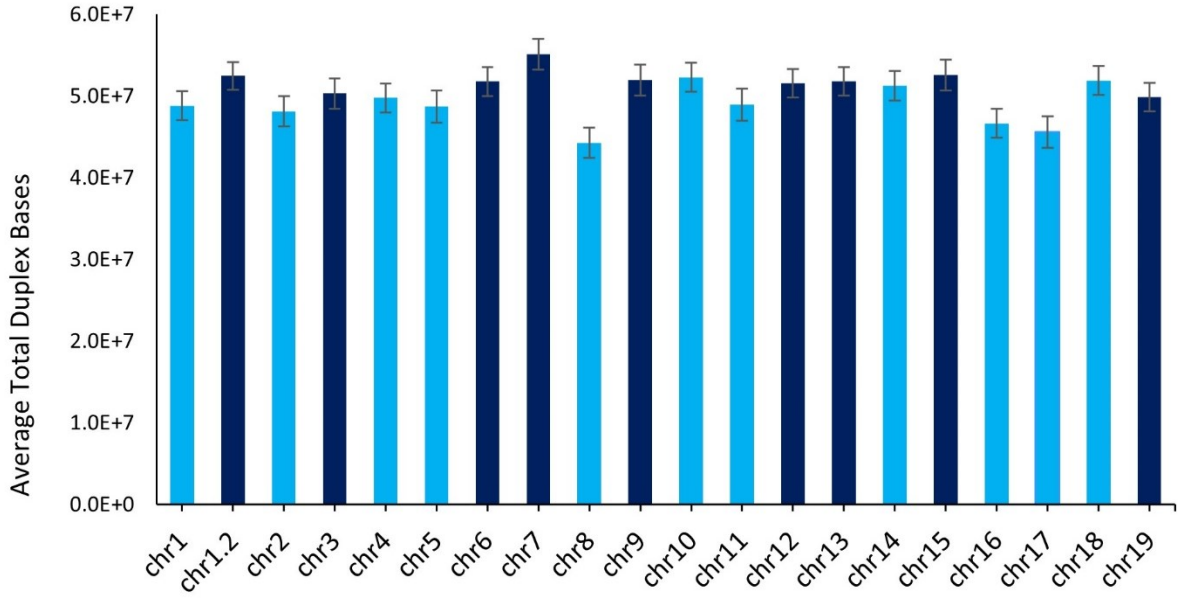

Supplementary Figure 3.1. Duplex data yields. (A) Total duplex bases per individual animal. X-axis indicates dose group (mg/kg-bw/day PRC). (B) Average duplex bases per target per animal. Error bars represent the standard error of the mean (SEM). Light blue bars represent intergenic targets. Dark blue bars represent genic targets.

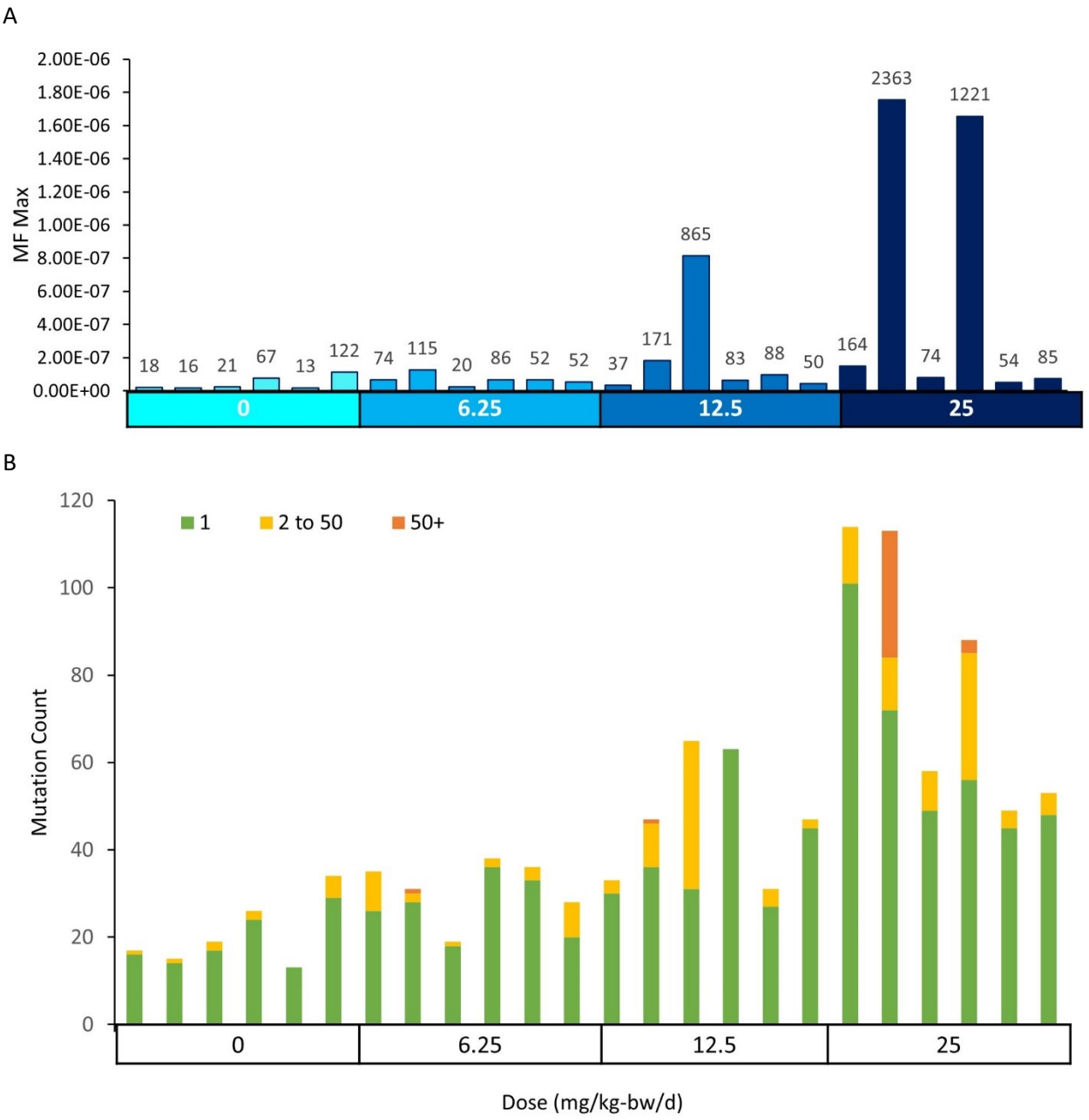

Supplementary Figure 3.2. Duplex Sequencing mutation frequencies (MF_{Max}) in the germ cells of MutaMouse males at various doses of PRC. **(A)** MF_{Max} (mutations per bp) for each animal. Data labels indicate the total mutation count per animal. X-axis indicates the PRC dose group (mg/kg-bw/day). **(B)** Distribution of clonal expansion events. Bars represent the unique mutation count for each animal. Green bars represent the number of mutations that appeared only once in the sample. Yellow bars represent the number of mutations that appeared 20-50 times in a single sample. Orange bars represent the number of mutations that appeared more than 50 times in a single sample. X-axis indicates the PRC dose group (mg/kg-bw/day).

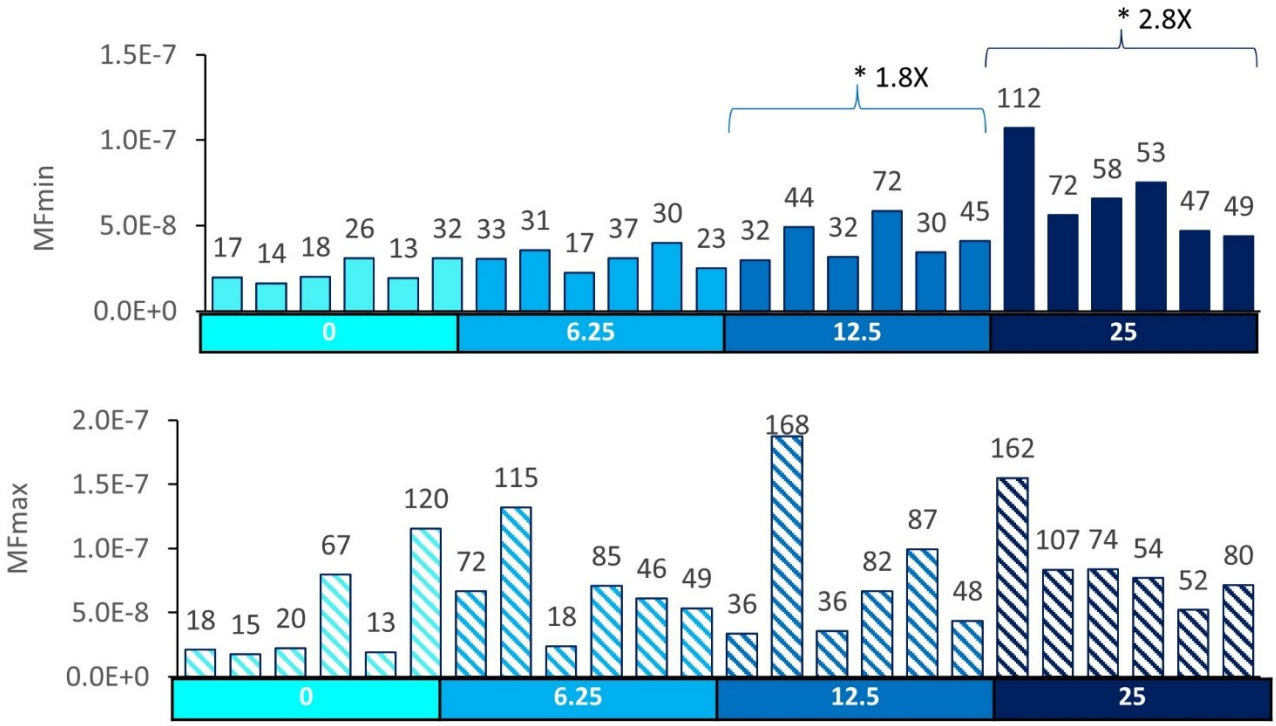

Supplementary Figure 3.3. Duplex Sequencing mutation frequencies (MF) without chr2 mutations for MutaMouse germ cells at various doses of PRC. Bars represent (A) the MF_{Min} (mutations per bp) and (B) MF_{Max} for each animal. Data labels indicate the total mutation count per animal. X-axis indicates the PRC dose group (mg/kg-bw/day). Asterisks indicate a significant difference ($p < 0.05$ relative to the control in the average MF across animals).

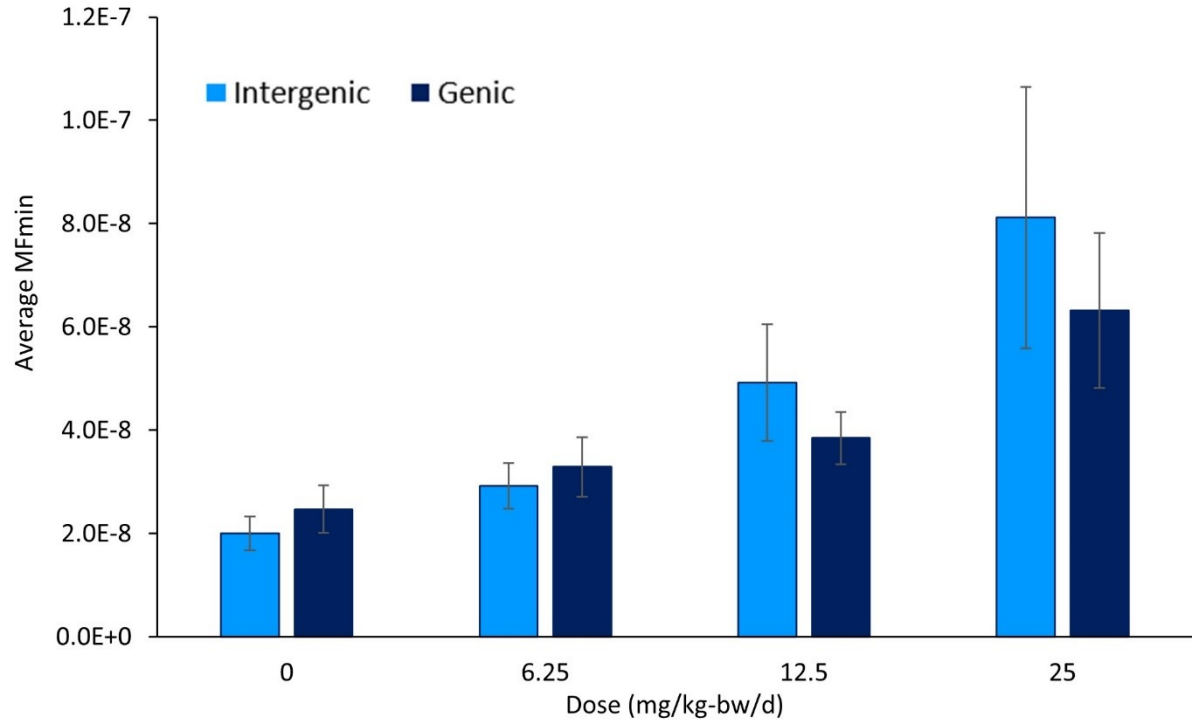

A

B

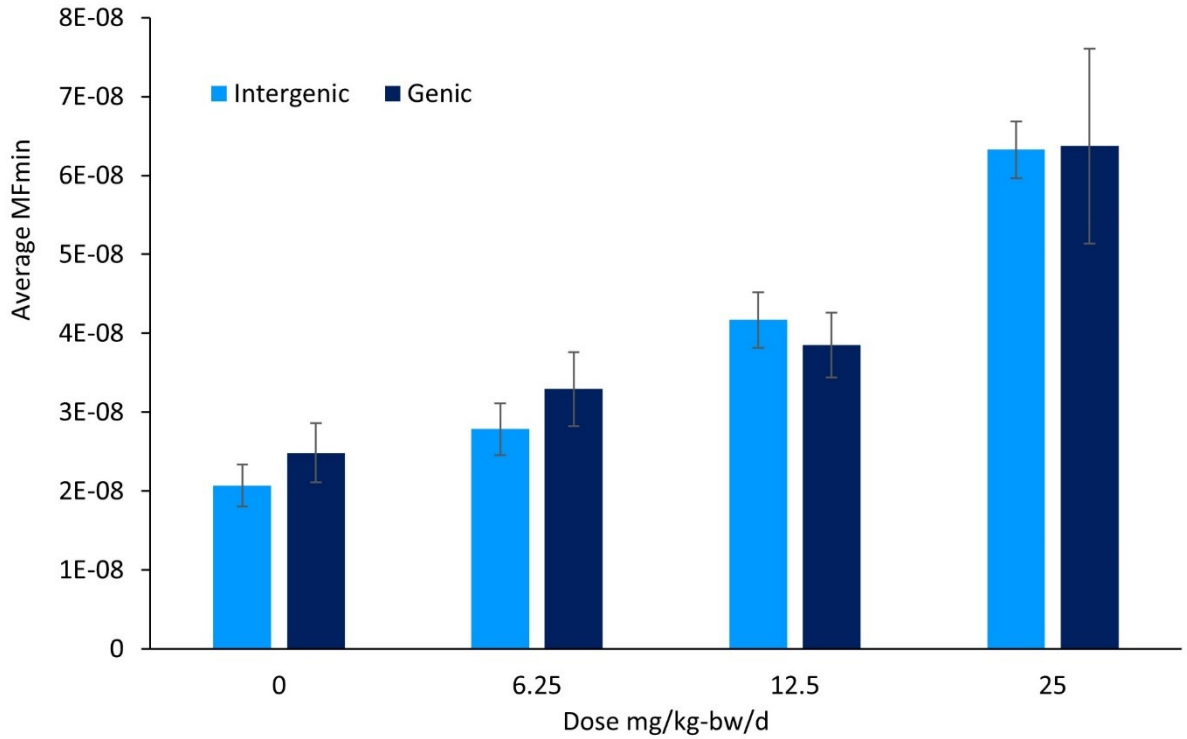

Supplementary Figure 3.4. MF_{Min} of intergenic targets compared to genic targets for various doses of PRC using (**A**) all data and (**B**) data without chr2**.** Data are represented as the mean ± SEM (mutations per bp).

A

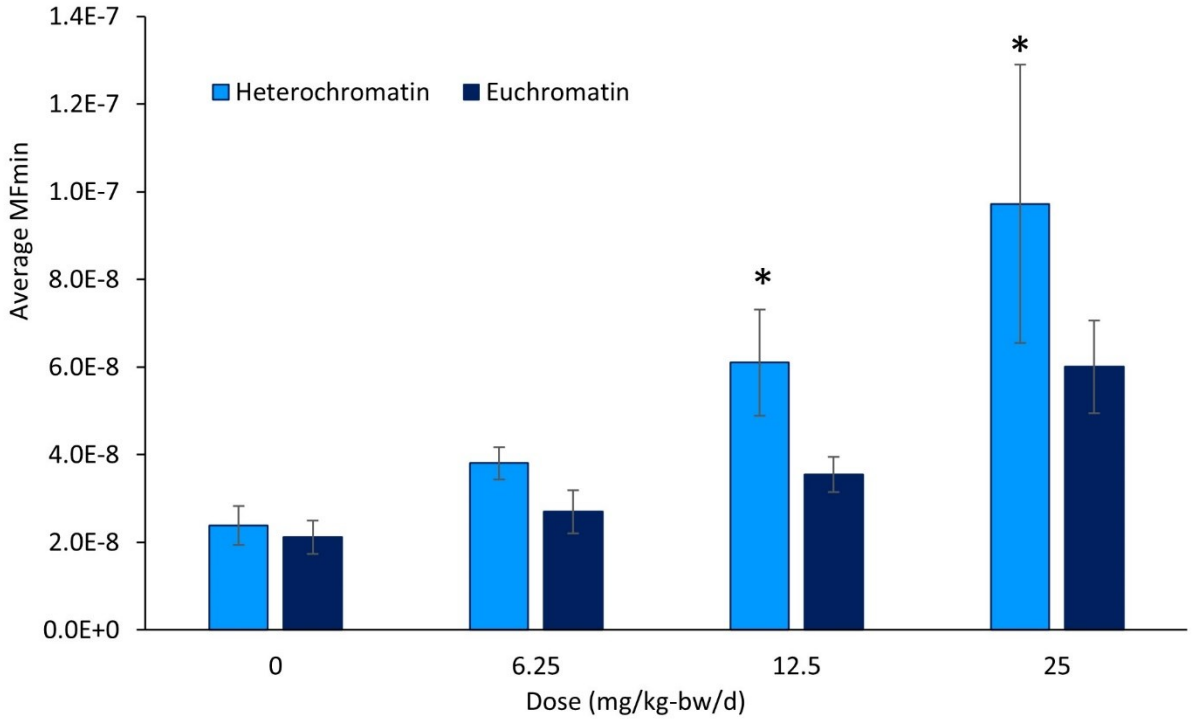

B

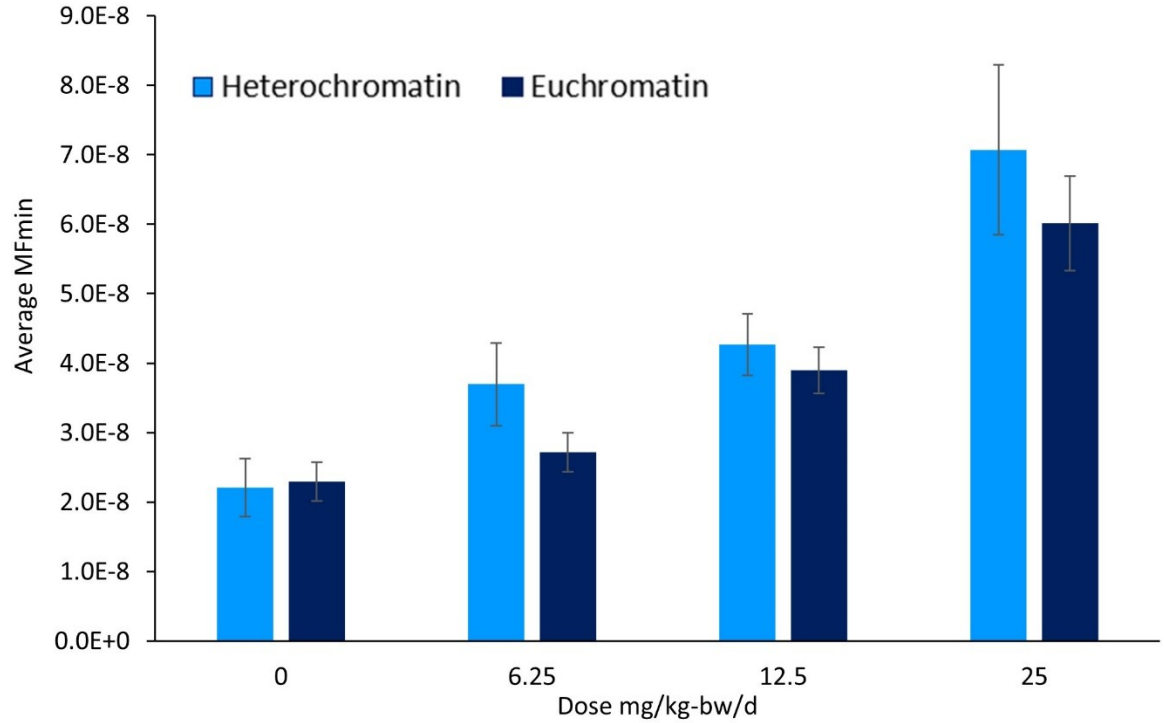

Supplementary Figure 3.5. MF_{Min} of heterochromatic targets compared to euchromatic targets for various doses of PRC using (**A**) all data and (**B**) data without chr2**.** Data are represented as the mean ± SEM (mutations per bp). Asterix indicate a significant difference between heterochromatic and euchromatic targets.

A

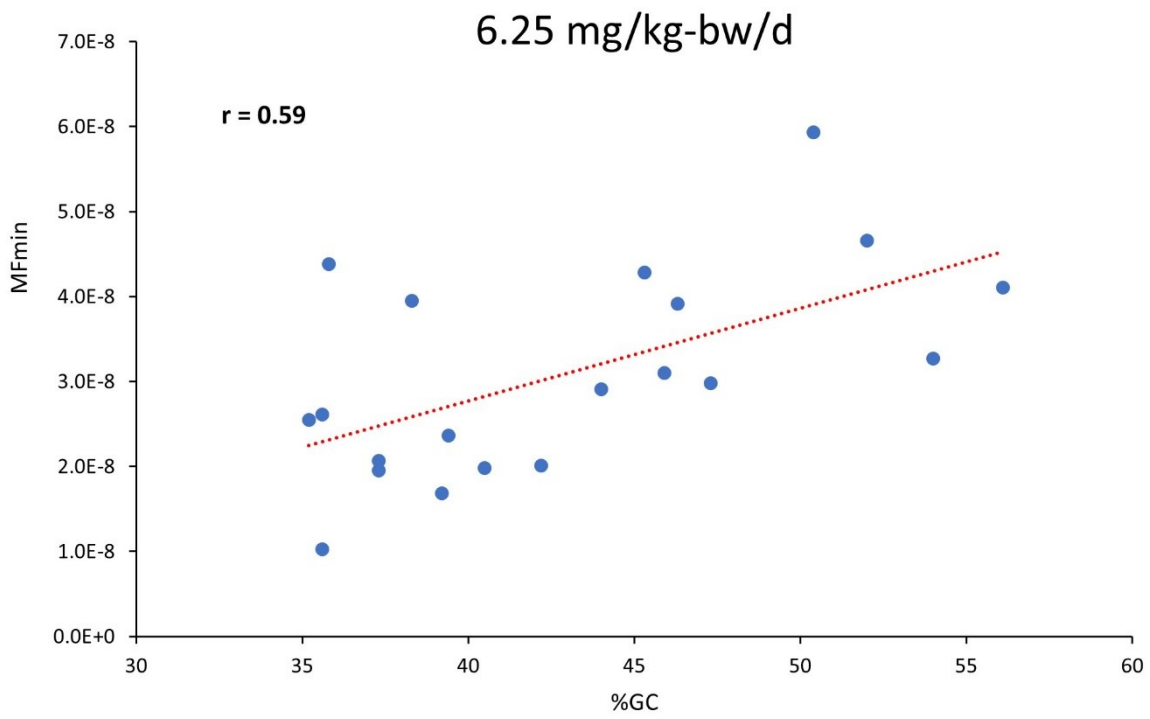
6.25 mg/kg-bw/d
r = 0.59
MFmin
7.0E-8
6.0E-8
5.0E-8
4.0E-8
3.0E-8
2.0E-8
1.0E-8
0.0E+0
30
35
40
45
50
55
60
%GC

B

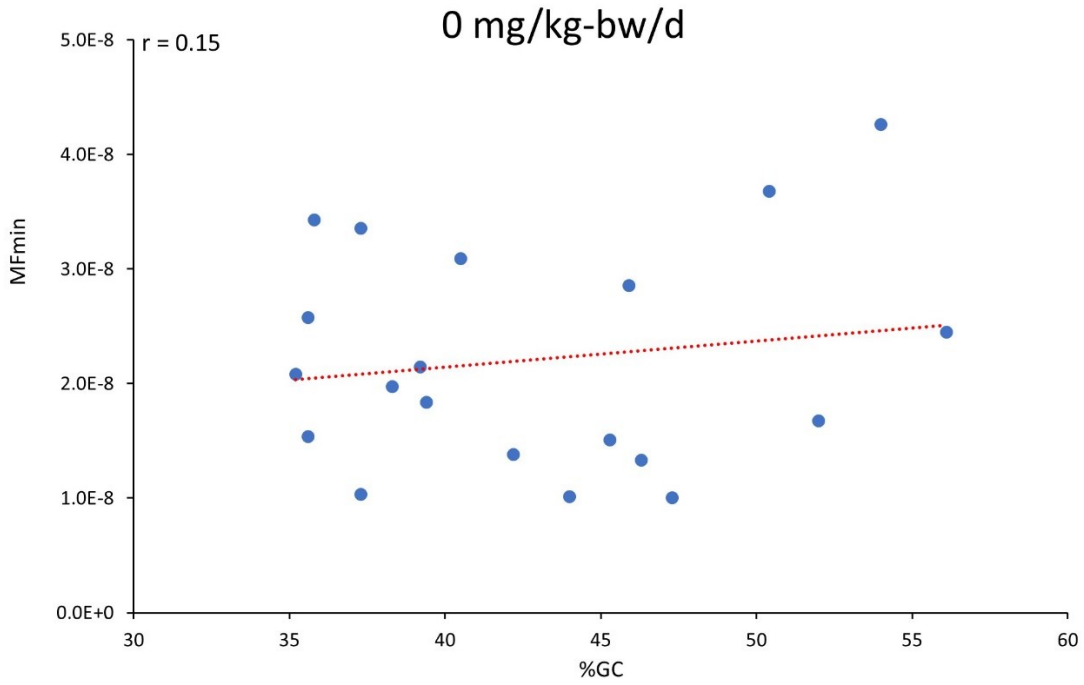
0 mg/kg-bw/d
r = 0.15
MFmin
5.0E-8
4.0E-8
3.0E-8
2.0E-8
1.0E-8
0.0E+0
30
35
40
45
50
55
60
%GC

C

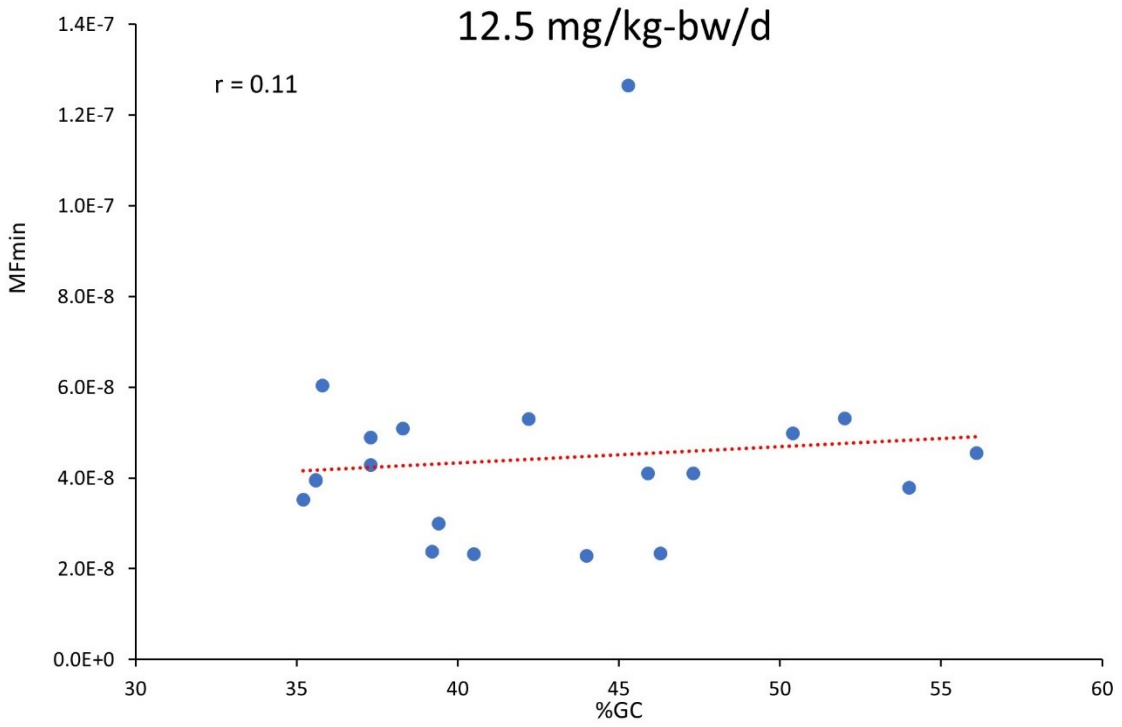

D

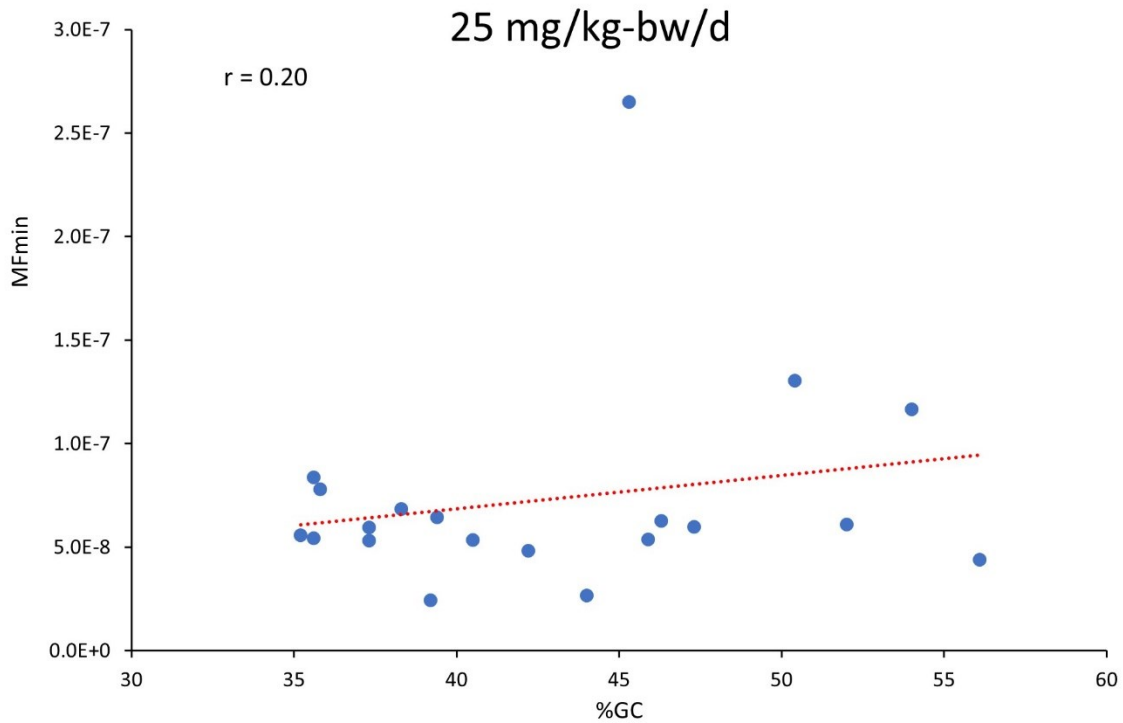

Supplementary Figure 3.6. Pearson's correlation analysis between per target MF_{Min} and the target's GC content (%) for (**A**) 0, (**B**) 6.25, (**C**) 12.5, and (**D**) 25 mg/kg-bw/d PRC. Correlation values (r) in bold are significant P<0.05.

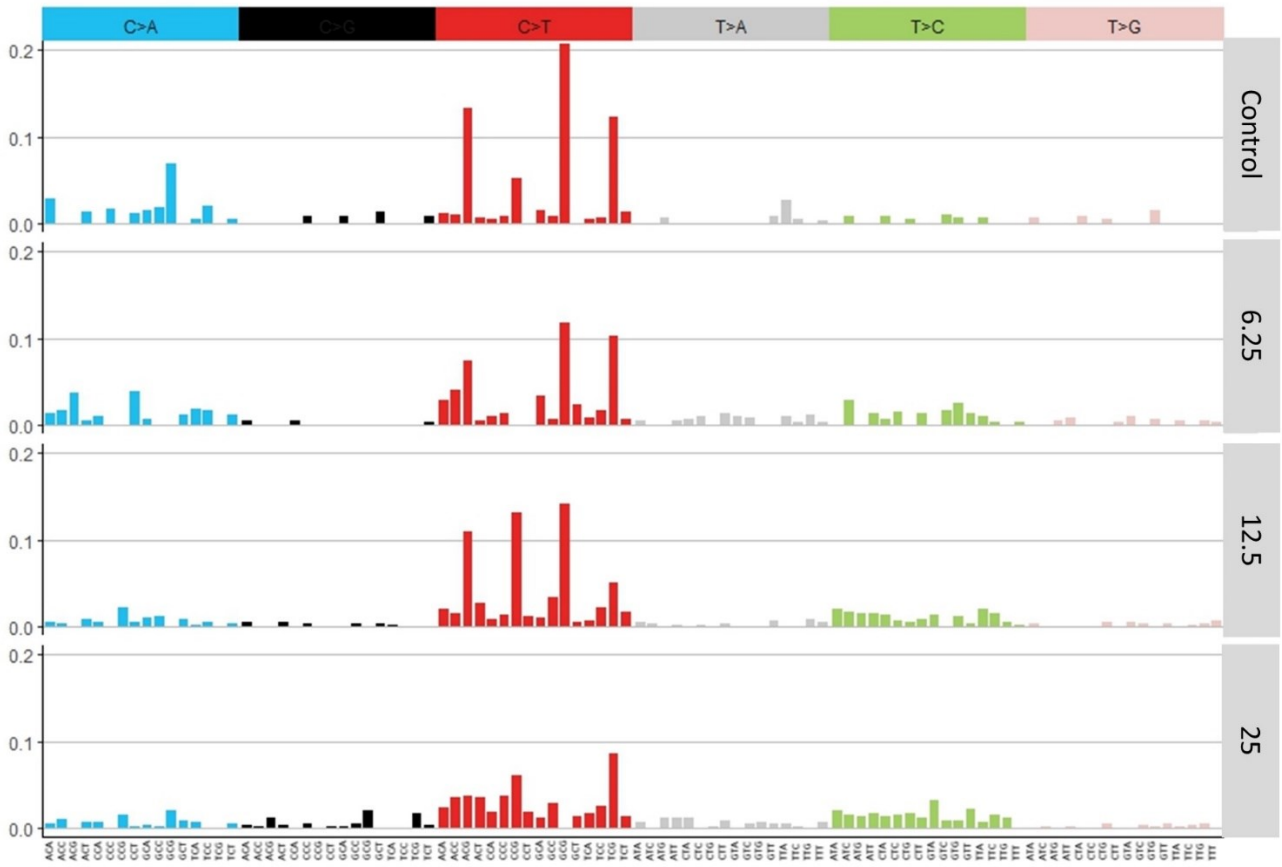

Supplementary Figure 3.7. Mutation spectra with trinucleotide context of controls and PRC dose groups measured by Duplex Sequencing in the germ cells of MutaMouse males. Dose groups (mg/kg-bw/d) are listed along the right. The substitution subtype is listed along the top, and the mutation including the two flanking nucleotides are listed along the bottom. Mutation subtypes are represented by the proportion of total mutations.

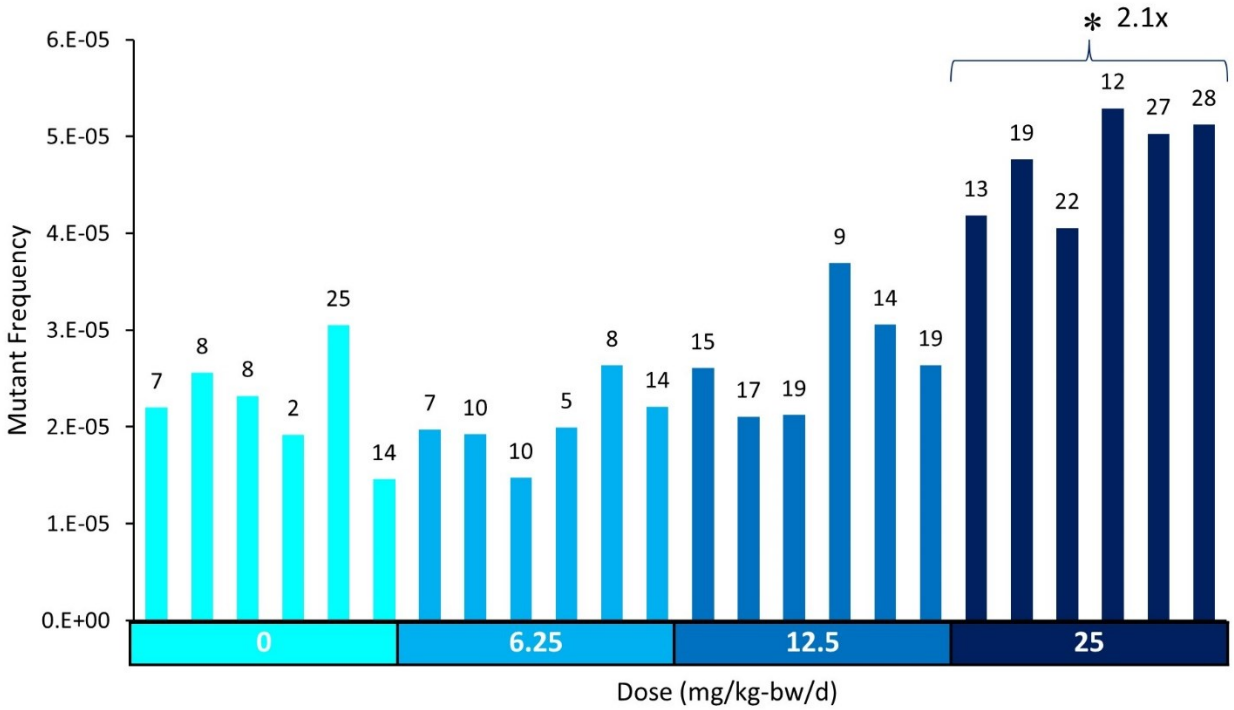

Supplementary Figure 3.8. *LacZ* mutant frequencies in the germ cells of MutaMouse males at various doses of PRC. Bars represent mutant frequency (mutations per locus) for each animal. Data labels indicate the total number of mutant plaques counted for each animal. The X-axis indicates PRC dose group (mg/kg-bw/day). Asterisks indicate a significant difference relative to the controls in the average mutant frequency across animals.

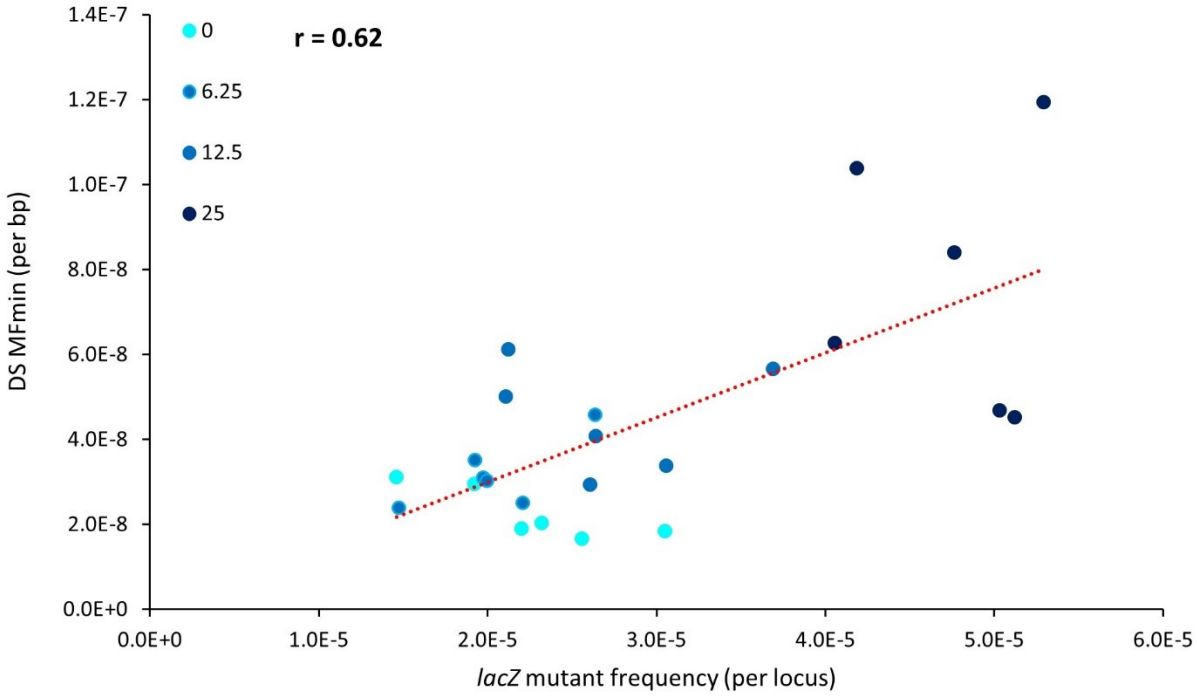

Supplementary Figure 3.9. Pearson's correlation analysis between *lacZ* mutant frequency and Duplex Sequencing (**A**) MF_{Min} for MutaMouse males exposed to PRC. Data are presented as the individual MFs for each animal.

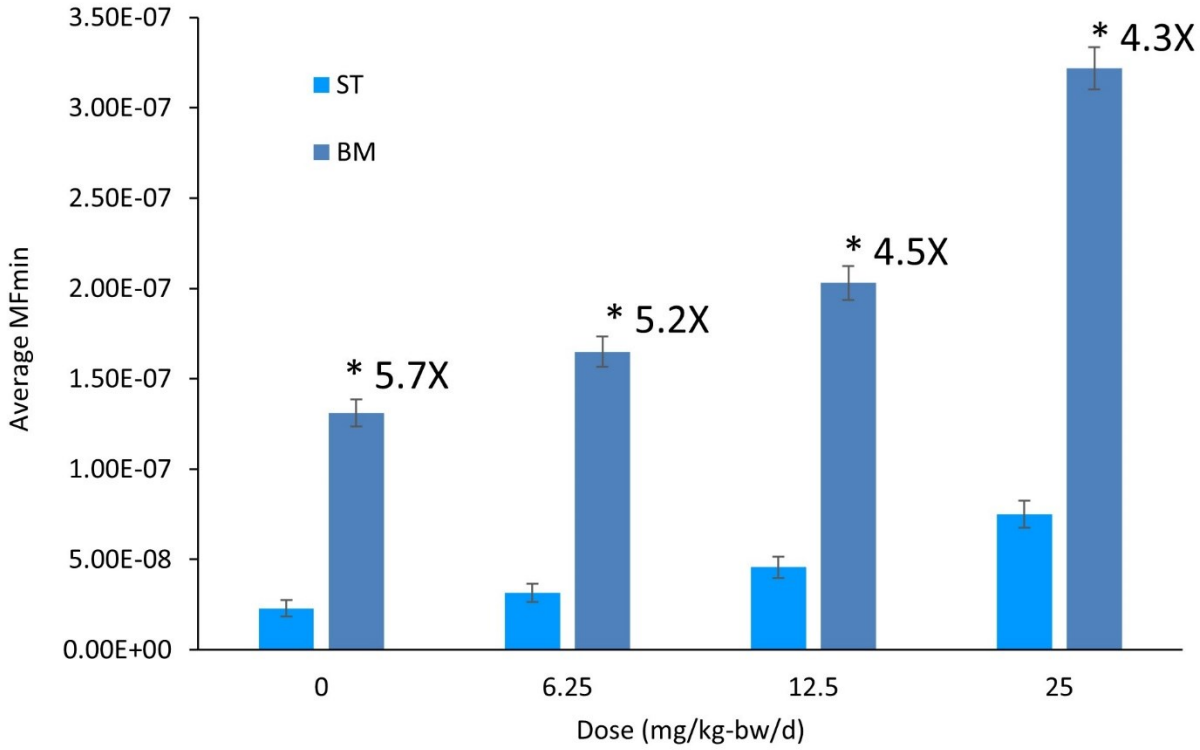

Supplementary Figure 3.10. Average MF_{Min} by dose for MutaMouse male germ cells and bone marrow. Error bars are SEM. Asterisk indicates a significant difference between germ cells and bone marrow.